DOWNHOLE PRESSURE DROP MODELING

By

VENKATARAGHAVAN RAMAN

Bachelor of Technology

Indian Institute of Technology

Madras, INDIA

1994

Submitted to the Faculty of the
Graduate College of the
Oklahoma State University
in partial fulfillment of
the requirements for
the Degree of
MASTER OF SCIENCE
December, 1996

DOWNHOLE PRESSURE DROP MODELING

Thesis Approved:

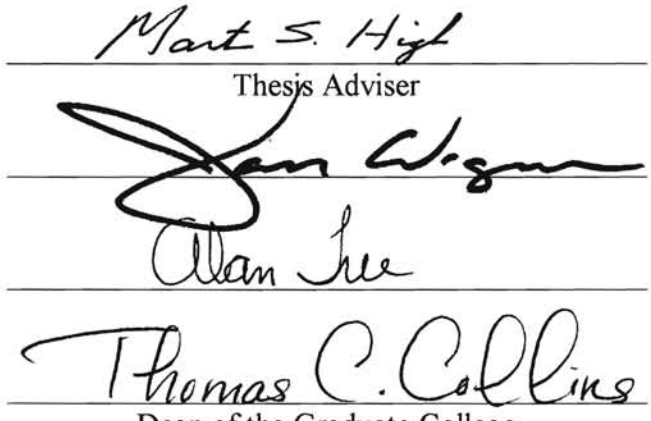

Thesis Adviser

Dean of the Graduate College

ACKNOWLEDGEMENTS

I wish to thank all the people who have helped me, both directly and indirectly, successfully complete this MS program. I would like to thank Dr. Martin S. High, my adviser, for his valuable guidance, constant encouragement, technical assistance and a friendly attitude without which this work might not have been possible. I would also like to thank Dr. Jan Wagner and Dr. D. Alan Tree for their guidance throughout the program.

This project was sponsored by the Downhole Corrosion Consortium whose members are: Amoco, Conoco, GRI, Oryx, and Philips. I would like to thank all the sponsors for their support.

Credit should be given to Mr. Mahesh Sundaram, my colleague in this project for his timely suggestions which have been extremely helpful to me. I would also like to thank my roommates and other friends who have helped me maintain my sanity throughout the last two years.

Finally, I would like to thank my parents, brother, and sister for supporting me emotionally and financially in order to see me complete the MS program successfully.

TABLE OF CONTENTS

LIST OF TABLES

LIST OF FIGURES

NOMENCLATURE

A_C	cross sectional area of the gas core in annular flow, ft^2
A_F	cross sectional area of the annular film in annular flow, ft^2
A_G	cross sectional area available for gas in slug flow, ft^2
A_p	cross sectional area of pipe, ft^2
C_1, C_2	constants used to fit an equation for the Fernandes' void fraction data, dimensionless.
D	pipe internal diameter, ft.
d_{HF}	hydraulic diameter of the annular film in annular flow, ft.
f	friction factor, dimensionless.
F	dimensionless group characterizing two-phase flow
F_E	liquid entrainment fraction in gas core, dimensionless.
f_F	friction factor at the film, dimensionless.
f_i	friction factor at the gas-liquid interface, dimensionless.
f_{LS}	friction factor for superficial liquid velocity, dimensionless.
f_{SC}	friction factor for superficial core velocity, dimensionless.
f_{TB}	friction factor for the Taylor bubble, dimensionless.
f_{tp}	two-phase friction factor, dimensionless.
g	acceleration due to gravity, ft/s^2.
g_c	gravitational constant, $ft.lb_m/lb_f.s^2$.

G	mass flux, $lb_m/(ft^2.s)$.
H_G	gas holdup fraction, dimensionless.
H_{GLS}	gas holdup fraction in the liquid slug, dimensionless.
H_{GTB}	gas holdup fraction in the Taylor bubble, dimensionless.
H_L	liquid holdup fraction, dimensionless.
H_{LF}	liquid film holdup fraction, assuming no entrainment in the gas core, dimensionless.
H_{LLS}	holdup fraction of liquid in the liquid slug, dimensionless.
H_{LTB}	holdup fraction of liquid in Taylor bubble, dimensionless
H_{LTBA}	average liquid fraction in the Taylor bubble diameter, dimensionless.
k	constant used to correlate length of liquid slug with pipe internal, dimensionless.
L_c	cap length of Taylor bubble, ft.
L_{LS}	length of liquid slug, ft.
L_{SU}	length of slug unit, ft.
L_{TB}	length of Taylor bubble, ft.
L_{TB}^*	modified length of Taylor bubble for developing flow, ft.
M_G	mass flow rate of gas, lb_m/s.
M_L	mass flow rate of liquid, lb_m/s.
N	number of case studies, dimensionless.
N_{Re}	Reynolds number, dimensionless.
N_{ReF}, Re_L	Reynolds number for the annular film, dimensionless.
N_{ReSL}	Reynolds number based on superficial liquid velocity, dimensionless.

$(\Delta P)_A$ pressure drop due to acceleration, psia.

$(\Delta P)_f$ pressure drop due to friction, psia.

$(\Delta P)_H$ hydrostatic pressure drop, psia.

$(\Delta P)_T$ total pressure drop, psia.

ΔP pressure drop, lb_f/ft^2.

P pressure, lb_f/ft^2.

P_b linear profile value of pressure at the bottom of section(i), psia.

P_{bnew} estimated value of pressure at the bottom of section(i), psia.

$P_{bottomhole,measured}$ measured bottomhole pressure of a well string, psia.

$P_{bottomhole,model}$ predicted bottomhole pressure of a well string, psia.

P_t pressure at the top of section(i), psia.

$\left(\frac{dP}{dz}\right)_A$ pressure gradient due to acceleration, lb_f/ft^2.

$\left(\frac{dP}{dz}\right)_E$ pressure gradient due to elevation, lb_f/ft^2.

$\left(\frac{dP}{dz}\right)_f$ pressure gradient due to friction, lb_f/ft^2.

$\left(\frac{dP}{dz}\right)_F$ pressure gradient in the annular film, lb_f/ft^2.

$\left(\frac{dP}{dz}\right)_C$ pressure gradient in the gas core, lb_f/ft^2.

$\left(\frac{dP}{dz}\right)_{SC}$ superficial friction pressure gradient, lb_f/ft^2.

$\left(\frac{dP}{dz}\right)_{SL}$ superficial liquid friction pressure gradient, lb_f/ft^2

$\left(\frac{dP}{dz}\right)_{T}$ total pressure gradient, lb_f/ft^2

Q_f volumetric flow rate of the falling film, ft^3/s.

Q_G volumetric flow rate of gas, ft^3/s

Q_L volumetric flow rate of liquid, ft^3/s.

Q_P volumetric flow rate of gas in the plug, ft^3/s.

Re_G gas Reynolds number, dimensionless.

S_F wetted perimeter for the annular film, ft.

S_i wetted perimeter at the interface, ft

v_C velocity of gas core, ft/s.

v_{crit} critical velocity used in the expression for liquid entrainment, ft/s.

v_f specific volume of liquid, ft^3/lb_m.

v_{fg} difference in specific volumes of saturated liquid and vapor, ft^3/lb_m.

v_F film velocity, ft/s.

v_g specific volume of gas, ft^3/lb_m.

v_{GLS} velocity of gas in liquid slug, ft/s.

v_{GTB} velocity of gas in Taylor bubble, ft/s.

v_{LLS} liquid velocity in liquid slug, ft/s.

v_{LTB} liquid velocity in Taylor bubble, ft/s.

v_m mixture velocity, ft/s.

v_P velocity of plug, ft/s.

v_S	slip velocity, ft/s.
v_{SC}	superficial core velocity, ft/s.
v_{SG}	superficial gas velocity, ft/s.
v_{SL}	superficial liquid velocity, ft/s
v_{TB}	Taylor bubble velocity, ft/s.
w	mass flow rate of mixture, lb_m/s.
x	quality, dimensionless.
X_M, Y_M	Lockhart and Martinelli parameters, dimensionless.
Z	correlating factor to estimate interfacial friction, dimensionless.
z	length variable used to represent well depth, ft.

Greek Symbols:

ε	absolute pipe roughness, ft.
θ	angle of inclination of pipe from horizontal, degrees.
$\underline{\delta}$	dimensionless film thickness, ft.
δ	film thickness, ft.
β	ratio of Taylor bubble length to length of slug unit, developed flow, dimensionless.
β^*	ratio of Taylor bubble length to length of slug unit, developing flow, dimensionless.
ρ_c	core density, lb_m/ft^3.
μ_C	core viscosity, $lb_m/(ft.s)$.
τ_F	shear stress in the film, $lb_m/(ft.s^2)$.

ρ_G	gas density, lb_m/ft^3
μ_G	gas viscosity, $lb_m/(ft.s)$
τ_i	interfacial shear stress, $lb_m/(ft.s^2)$
ρ_L	liquid density, lb_m/ft^3
σ_L	liquid surface tension, lb_m/s^2
μ_L	liquid viscosity, $lb_m/(ft.s)$.
λ_L	liquid holdup fraction, dimensionless.
λ_{LC}	liquid holdup fraction in the gas core, dimensionless.
α_{LS}	area average void fraction in liquid slug, dimensionless
μ_{LS}	average viscosity of liquid slug, $lb_m/(ft.s)$.
ρ_{LS}	liquid slug density, lb_m/ft^3.
ρ_m	mixture density, lb_m/ft^3.
μ_m	mixture viscosity, $lb_m/(ft.s)$.
δ_{min}	minimum dimensionless film thickness required to form a slug, dimensionless.
ρ_n	no slip density, lb_m/ft^3.
δ_N	Nusselt film thickness, ft.
ρ_s	slip density, lb_m/ft^3.
α_{SU}	area average void fraction in the slug unit, dimensionless.
α_{TB}	area average void fraction in Taylor bubble, dimensionless.
ρ_{TBA}	average density of the Taylor bubble, lb_m/ft^3.

Chapter I

INTRODUCTION

1.1 Background

Corrosion is a serious problem in gas and oil wells, and the financial loss due to corrosion has always been significant to the oil and gas producing industry (Tuttle, 1987) The increased production costs due to corrosion arise from:

1. replacement of corroded well tubulars,
2. the cost of the application of corrosion inhibitors (substances that prevent corrosion),
3. loss of production during shutdown when the corroded tubulars are replaced, and
4. loss of product (oil or gas) due to leakage from the wells until the corroded tubulars are detected and replaced.

The economic loss has provided the initiative to develop a model to predict the rate of corrosion. The corrosion prediction results could be used to reduce the financial losses by:

1. restricting the application of inhibitor to portions of the well that are more likely to corrode, and
2. preventing the loss of oil or gas through timely detection of corrosion.

Downhole corrosion is a highly complex phenomena that is influenced by the fluid flow and phase behavior. Depending upon the temperature and pressure, it is possible to

have two (water and hydrocarbon gas) phases or three (water, hydrocarbon liquid and hydrocarbon gas) phases. Solids might also be present in the downhole system resulting in erosion action on the pipe wall. However, corrosion occurs only when the pipe wall is in contact with the water phase. If only an aqueous phase and a vapor phase exist, the assumption that the pipe wall is always in contact with a water film can be made (Taitel, 1980). In the case of three phases, the pipe wall can be in contact with either or both of the two liquid phases - oil or water.

A number of factors affect the rate of corrosion: temperature, pressure, flow pattern, flow velocity, liquid and gas composition, concentration of CO_2 and H_2S in the system, amount of water, nature of corrosion product formed and the presence of inhibitors on the pipe wall. The dependence of the corrosion rate on so many factors makes the mathematical modeling of corrosion and the prediction of corrosion rates extremely complicated. A mechanistic model which takes into account all the factors to predict the rate of corrosion would make use of fundamental concepts of chemistry and chemical engineering.

Corrosion is primarily caused by the acidic nature of the oil or gas being extracted from the reservoir. The presence of CO_3^{2-}, HS^-, or other inorganic ions along with water is an ideal environment for corrosion to occur. The CO_2 and H_2S form weak inorganic acids in the presence of water. The inorganic acids thus formed are found to be highly corrosive, making the conditions in the well string conducive for downhole corrosion. The greater the concentration of these ions the more corrosive the well.

Corrosion is not necessarily homogeneous along the well string. Corrosion can be "localized" (pitting) or "uniform." Localized corrosion is characterized by the formation

of pits or grooves at specific sections of the pipe wall. Localized corrosion is caused by the removal of the corrosion product layer from certain sections of the pipe resulting in the exposure of the pipe wall to the corrosive species. The removal of corrosion product may be due to the interaction between the pipe wall and the corrosion product through chemical action or mechanical forces exerted on the wall by the fluid (Joosten et al., 1994). Uniform corrosion, as the name suggests, is corrosion along large sections of pipe resulting in uniform thinning of pipe wall. Corrosion prediction models generally predict uniform corrosion only, due to the extreme difficulty in analytically modeling localized corrosion.

One of the important components of a mechanistic model for downhole corrosion is a method to predict the pressure drop in two-phase or multiphase flow. As the production fluid flows up the well tubular, pressure is reduced due to gravitational head loss, friction losses to the tube wall, and friction losses due to the turbulence in the flow stream. The pressure influences the vapor-liquid equilibrium of the system including the equilibria of the soluble, corrosive species hydrogen sulphide and carbon dioxide. Therefore, predicting the pressure drop in multiphase flow is an extremely complicated, but necessary, calculation in order to predict corrosion rates and sites.

Given the complexity of the downhole corrosion process and the importance of predicting the rate of corrosion as well as the lack of corrosion, a thorough understanding of the basic mechanisms of the various phenomena (electrolyte equilibrium, thermodynamic phase equilibrium, flow pattern, pressure drop, and mass transfer) involved in the prediction of corrosion in natural gas wells becomes important.

1.2 Purpose of this work

Pressure drop estimation for two-phase flow in gas wells depends upon the flow regime which can be bubble, slug, or annular. The primary purpose of this work was to study the various pressure drop correlations available for the slug and annular flow regimes (slug and annular are the most commonly encountered flow regimes in gas wells) and to incorporate the best available correlation into a mechanistic model for corrosion rate prediction. The second goal of this work was to evaluate the overall downhole corrosion prediction model to study the effect of pressure drop on the corrosion rate predictions. A third goal of this work was to make a thorough study of the following modules of computer code in DREAM, a software tool based on a deterministic model to predict corrosion in downhole gas wells, and eliminate any coding errors in the major components of the mechanistic model:

1. mass transfer,
2. corrosion kinetics,
3. annular flow pressure drop (Yao and Sylvester model), and
4. slug flow pressure drop (Sylvester model).

A description of the type of coding errors and the corrections are summarized in Appendix A. The computer code for the pressure drop and flow regime estimation in DREAM 3.1 is listed in Appendix B.

Chapter II

LITERATURE REVIEW

2.1 Overview

This chapter discusses flow regime classification, pressure drop modeling, and corrosion prediction modeling. The different flow regimes encountered in upward vertical two-phase flow are described. The pressure drop models used by previous researchers in the downhole corrosion project at Oklahoma State University and the pressure drop model evaluated in this study are discussed along with the governing equations. The various corrosion prediction models developed by previous researchers (Robertson, 1988; Liu and Erbar, 1990; Liu, 1991; Liu and High, 1993) at Oklahoma State University are also briefly described.

2.2 Description of Flow Regimes

Prediction of the flow pattern in a two-phase flow depends on the relative flow rates of the two phases. When a gas and a liquid flow together in a pipe, they may distribute in a number of different patterns each of which can be classified as a different regime. Since the flow in some regions is chaotic and a generalization of the flow patterns for various two-phase systems is difficult, there are different interpretations of flow pattern classifications in the literature. The flow regimes encountered in upward vertical two-phase flow are described in the subsequent sections. A schematic of the flow patterns occurring in upward, vertical, two-phase flow is given in Figure 1.

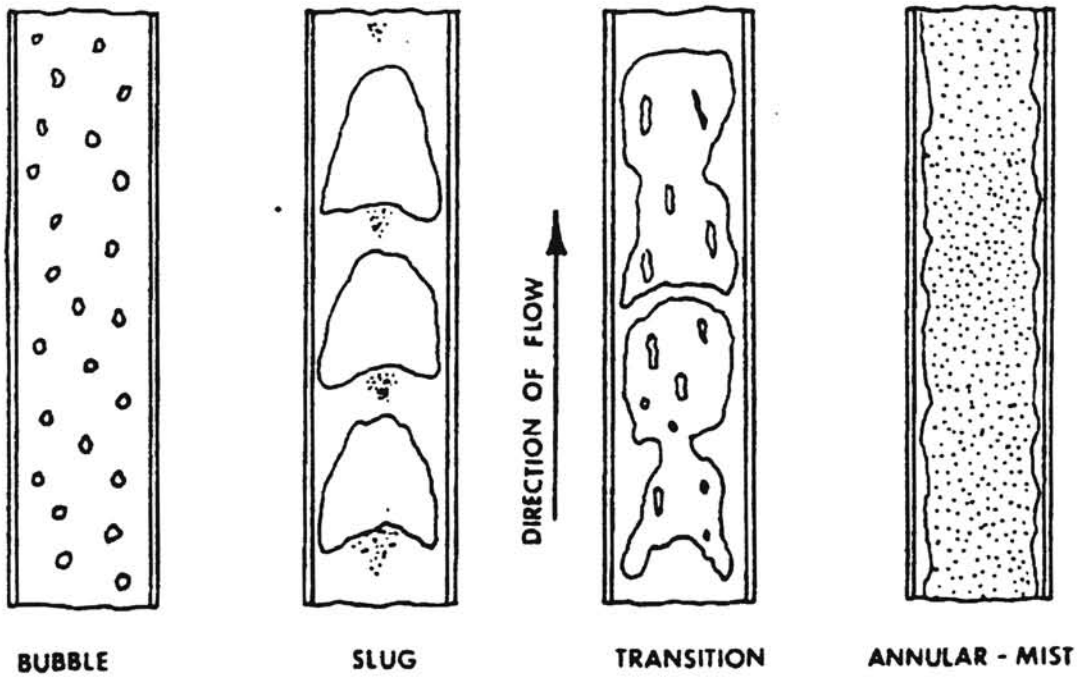

Figure 1. Flow Patterns Encountered in Vertical Upward Two-Phase Flow

(From Orkiszewski, 1967)

2.2.1 Bubble Flow

Two-phase flow is classified as bubble flow (Figure 1) when liquid is the dominant phase with gas distributed as small bubbles in the liquid phase. As the liquid flow rate is increased, the gas bubbles distribute in the liquid as fine bubbles resulting in a dispersed bubble flow. The pipe wall is always contacted by the liquid phase and the pressure gradient is not significantly affected by the gas phase. Bubble flow and dispersed bubble flow are not commonly encountered in gas wells, so no further discussion of these two flow conditions will be presented here.

2.2.2 Slug Flow

The transition from bubble to slug flow will take place if the gas flow rate is higher than that in bubble flow. As the gas flow rate increases, the random motion of the bubbles leads to collisions between bubbles. This bubble-bubble collision results in the coalescence of the bubbles and leads to growth in the size of the bubbles until they become large enough to occupy the entire pipe cross-section, resulting in slug flow.

Slug flow refers to a specific arrangement of the fluid-fluid interface in a two-phase flow. A schematic of slug flow is shown in Figure 1. Slug flow is characterized by the periodic occurrence of large bullet-shaped gas bubbles which are nearly the diameter of the pipe and move uniformly upward. These gas bubbles are referred to as Taylor bubbles. The Taylor bubbles are separated from the pipe wall by a thin liquid film which flows downward. Between two Taylor bubbles, the liquid slugs are present with dispersed gas bubbles. The Taylor bubble along with the liquid slug is generally known as a slug

unit. Since both the liquid and gas phase are present in significant proportions in the two-phase flow, the pressure drop is affected by both phases.

2.2.3 Churn Flow

At gas velocities much higher than that in slug flow, the two-phase flow would be in the annular regime which is described below. Between the slug and the annular flow regimes, the two-phase flow goes through a transition zone classified as churn flow (Figure 1) by Collier (1981). The slugs in slug flow break up and become unstable. The transition between slug and annular flow is smoother (smaller churn flow zone) in narrow tubes than in wider tubes (Taitel et al., 1980). Churn flow is complex and has been included with the slug flow regime for the purposes of this study.

2.2.4 Annular Flow

Annular flow (Figure 1) occurs when the two-phase fluid flows upward with a high gas flow rate and a low liquid flow rate. Under annular flow conditions, the slugs breakup and form a fine mist of dispersed droplets in a continuous gas phase. The pipe wall is wetted by a thin liquid film which may or may not contain gas bubbles. The gas phase controls the pressure gradient in the annular flow regime.

2.3 Determination of Flow Regimes

Two-phase flow can be classified into various flow regimes based on the relative amounts of liquid and gas present, the distribution pattern of the two phases, and the relative velocity of the two phases. Several investigators have classified two-phase flow

into various flow regimes and have discussed the transition from one regime to another (Wallis, 1969; Hewitt and Roberts, 1969; Govier and Aziz, 1972; Duns and Ros, 1963; Taitel et al., 1980). In all of the approaches presented in the literature, two basic types of coordinates have been used to map the different flow patterns: dimensional coordinates and dimensionless coordinates.

2.3.1 Dimensional Coordinates

Dimensional coordinates such as superficial velocities, v_{SG} and v_{SL}, or superficial momentum flux, $\rho_G v_{SG}^2$ and $\rho_L v_{SL}^2$, have been used by some investigators (Wallis, 1969; Hewitt and Roberts, 1969) to map the flow patterns. The use of superficial velocities or the superficial momentum fluxes as coordinates would mean that the fluid properties and pipe size have to be held constant to obtain the flow pattern map. A change in either the fluid properties or the pipe size might result in a different flow pattern map. To include fluids other than air-water system, Govier and Aziz (1972) considered the ratio of fluid properties between the fluids of interest and the air-water system. The model developed by Govier and Aziz (1972) is only an empirical model.

2.3.2 Dimensionless Coordinates

The dimensionless coordinates, gas velocity number $\left(v_{SG}\sqrt[4]{\rho_L/g\sigma_L}\right)$ and liquid velocity number $\left(v_{SL}\sqrt[4]{\rho_L/g\sigma_L}\right)$, were used by another group of investigators (Duns and Ros, 1963). The dimensionless numbers used by the authors (Duns and Ros, 1963) to obtain the flow map are just empirical and a dimensional analysis is not available in the

original reference (Duns and Ros, 1963). The idea of using the gas velocity number and the liquid velocity number as coordinates was to account for the effect of pipe size and fluid properties, so that a generalized flow pattern could be obtained. Since there was no theoretical basis for the selection of these dimensionless coordinates, a generalized flow pattern prediction covering all the flow patterns for different two-phase systems and pipe sizes could not be obtained.

A generalized flow pattern map can be obtained only if the basic flow mechanisms are understood and if equations are developed using theoretical fundamentals. Equations developed from fundamentals would include the effect of pipe size and fluid properties. Taitel et al. (1980) used the four basic flow patterns as classified by Hewitt and Hall-Taylor (1970) and developed equations to show the transition from one regime to another. Barnea (1987) modified the slug-annular transition boundary given by Taitel et al. (1980) and developed a modified flow map (1987) for two-phase vertical upward flow. The Barnea flow map and the Taitel flow map for upward vertical two-phase flow use the superficial velocities, u_{SG} and u_{SL}, as the coordinate system.

2.4 Review of Pressure Drop Models

The estimation of pressure drop in vertical multiphase flow is important for design in the petroleum industry. The estimation of pressure drop in vertical multiphase flow in gas wells involves the prediction of the amounts of liquid and gas flowing in the well. The amount of condensed water in the tubing has a direct bearing on the corrosion rate of the tubing material. The pressure drop in vertical multiphase flow is modeled as a function of the liquid holdup, flow velocity, flow direction, and flow regime.

2.4.1 Different Approaches to Pressure Drop Modeling

Extensive research work has been going on in the field of two-phase pressure drop modeling. Previous researchers have devised a variety of methods to classify two-phase flow regimes and have also developed models to predict the pressure drop in each of these flow regimes. The pressure drop correlations available in literature can be categorized into three modeling approaches (Brill and Beggs, 1977):

a. Approach I: No slip at the gas-liquid interface and no flow regime analysis
b. Approach II: Slip at gas-liquid interface taken into account, but no flow regime analysis
c. Approach III: Slip at gas-liquid interface and flow regime analysis performed

2.4.1.1 Approach I

Pressure drop correlations that belong to Approach I do not perform a flow regime classification and also make an assumption that the gas and liquid at the gas-liquid interface travel at the same velocity in the pipe (no slip condition). The correlations by Poettmann and Carpenter (1952) and Baxendall and Thomas (1961) are examples of correlations belonging to Approach I. The Approach I pressure drop correlations are functions of the two-phase mixture density, friction factor, flow velocity or mass flow rate, and tubing internal diameter. The two-phase mixture density is calculated based on the gas-liquid ratio while the friction factor was empirically correlated as a function of the numerator of the Reynolds number ($Vd\rho$). A typical pressure drop equation belonging to Approach I is given by Brill and Beggs (1977)

$$\left(\frac{dP}{dz}\right)_T = \frac{g}{g_c}\rho_n + \frac{f\rho_n v_m^2}{2g_c D}, \quad (1)$$

where

$$\rho_n = \rho_L \lambda_L + \rho_G\left(1-\lambda_L\right), \quad (2)$$

$$\lambda_L = \frac{Q_L}{Q_L + Q_G}, \quad (3)$$

and

f is the two-phase friction factor obtained from the Moody diagram

Equation (1) is a typical equation belonging to Approach I. The first term on the right hand side in equation (1) represents the elevation component of pressure drop and the second term represents the friction component of pressure drop. The correlations that belong to Approach I correlate the friction factor empirically to arrive at different pressure drop equations.

2.4.1.2 Approach II

Correlations belonging to Approach II account for the effect of the relative velocity between gas and liquid while the effect of flow regime has not been considered. A single pressure drop correlation predicts the pressure drop regardless of the flow regime in Approach II correlations. The Hagedorn and Brown (1965) model is an example of a model belonging to Approach II and is given by

$$\left(\frac{dP}{dz}\right)_T = \left(\frac{dP}{dz}\right)_E + \left(\frac{dP}{dz}\right)_A + \left(\frac{dP}{dz}\right)_f. \quad (4)$$

The pressure drop due to elevation change, $\left(\frac{dP}{dz}\right)_E$, is given by

$$\left(\frac{dP}{dz}\right)_E = \frac{g}{g_c}\left[\rho_L H_L + \rho_G\left(1 - H_L\right)\right]. \tag{5}$$

The acceleration component of pressure drop is given by

$$\left(\frac{dP}{dz}\right)_A = \frac{\rho_s \Delta\left(v_m^2\right)}{2g_c dz}, \tag{6}$$

where

$$\rho_s = \rho_L H_L + \rho_G H_G, \tag{7}$$

and

$$v_m = v_{SL} + v_{SG}. \tag{8}$$

The friction component is given by

$$\left(\frac{dP}{dz}\right)_f = \frac{fw^2}{(2.9652e+11)\rho_s D^5}. \tag{9}$$

The difference between Approach I and Approach II lies in the estimation of the mixture density. The two-phase mixture density is calculated based on the liquid holdup (Equation 7) in Approach II and not the gas-liquid ratio (Equation 2) as in Approach I. The acceleration component is accounted for in Approach II while the acceleration component is neglected in Approach I.

2.4.1.3 Approach III

Approach III correlations account for the relative velocity between gas and liquid and have flow regime dependent pressure drop correlations. Most of the correlations developed in recent times belong to Approach III. The correlations by Duns and Ros

(1963) and Orkiszewski (1967) are examples of correlations belonging to Approach III. Flow regime classification maps have been used to determine the flow regime before proceeding to estimate the pressure drop using correlations specific to that flow regime The Duns and Ros pressure drop equations for the different flow regimes are given by equations (10) and (11).

Bubble and Slug:
$$\left(\frac{dP}{dz}\right)_T = \frac{g}{g_c}\rho_s + \frac{f_m \rho_L v_{SL} v_m}{2Dg_c} \tag{10}$$

where, ρ_s is estimated with different correlations for the bubble and slug flow.

Annular:
$$\left(\frac{dP}{dz}\right)_T = \frac{\left(\frac{g}{g_c}\rho_s + \frac{f\rho_G v_{SG}^2}{2Dg_c}\right)}{1 - E_k}, \tag{11}$$

where

$$E_k = \frac{v_m v_{SG} \rho_n}{g_c P}. \tag{12}$$

The details of derivation of equations (10), (11), and (12) can be obtained from the original reference (Duns and Ros, 1963). Approach III uses a two-phase mixture density based on liquid holdup as in Approach II but has different equations to predict pressure drop for each flow regime.

2.4.2 Homogeneous Flow Method

The Homogeneous Flow method proposed by Collier (1981) was used to predict pressure drop by previous researchers at Oklahoma State University. The Homogeneous Flow method belongs to Approach I and gives a crude estimate of pressure drop. The Homogeneous Flow method assumes that the two-phase flow acts like a single

homogeneous phase. The homogeneous flow method estimates the pressure drop based on average fluid properties. The major assumptions in this approach are:

1. no slip between the two phases
2. thermodynamic equilibrium of the two phases
3. existence of a single phase friction factor for two-phase flow

Robertson (1988) found the homogeneous flow model to be applicable for bubble or annular flow regimes where the two phases consist of high liquid and low gas flow rates or vice versa. The pressure drop as derived by Collier (1981) is given by:

$$\left(\frac{dP}{dz}\right)_T = \frac{\dfrac{2f_{tp}G^2v_f}{D}\left(1+x\dfrac{v_{fg}}{v_f}\right)+G^2v_f\dfrac{v_{fg}}{v_f}\dfrac{dx}{dz}+\dfrac{gSin\theta}{v_f\left(1+x\dfrac{v_{fg}}{v_f}\right)}}{1+xG^2\dfrac{dv_g}{dP}}. \qquad (13)$$

2.4.3 Orkiszewski Model

The model of Orkiszewski (1967) is a flow regime dependent method that belongs to Approach III and employs the Duns and Ros (1963) flow regime map. The Orkiszewski (1967) method classifies vertical upward two-phase flow into the following four flow regimes: bubble, slug, slug-annular transition, and annular-mist. Once the flow regime is determined, the corresponding pressure drop correlation is used to estimate the pressure drop. Since the slug-annular transition zone is highly chaotic and hence complex, separate pressure drop models were not developed for the slug-annular transition zone. Instead, the pressure loss was taken to be a weighted average with respect to slug and annular flow. The details of the model can be obtained from Orkiszewski (1967).

2.4.4 Yao and Sylvester Model for Annular Flow

The Yao and Sylvester (1987) model, developed specifically for the annular-mist flow regime, is an Approach III model. Yao and Sylvester developed a mechanistic model to predict the pressure drop for two-phase annular flow in vertical pipes. The flow pattern map that models the transition between slug and annular regimes was taken from the work of Taitel et al. (1980) as shown in Figure 2. The Yao and Sylvester model uses the equation of Wallis (1969) for the liquid entrainment fraction, the modified Zigrang and Sylvester (1982) equation for friction factor, and the Henstock and Hanratty (1976) equation for roughness factor. The assumptions made in the model are:

1. The flow is fully developed and stable.
2. The fraction of entrained liquid is uniformly dispersed as mist in the continuous gas core at any point in the pipe.
3. The portion of the liquid that is not in the form of dispersed mist forms an annular film of uniform thickness on the pipe wall.
4. The core is considered to be a homogeneous mixture of gas and liquid droplets flowing at the same velocity.

Yao and Sylvester proposed a model for the pressure drop, $\left(\frac{dP}{dz}\right)_T$, in the annular flow regime:

$$\left(\frac{dP}{dz}\right)_T = \left(\frac{dP}{dz}\right)_E + \left(\frac{dP}{dz}\right)_f + \left(\frac{dP}{dz}\right)_A . \tag{14}$$

The pressure gradient due to the elevation change is given by

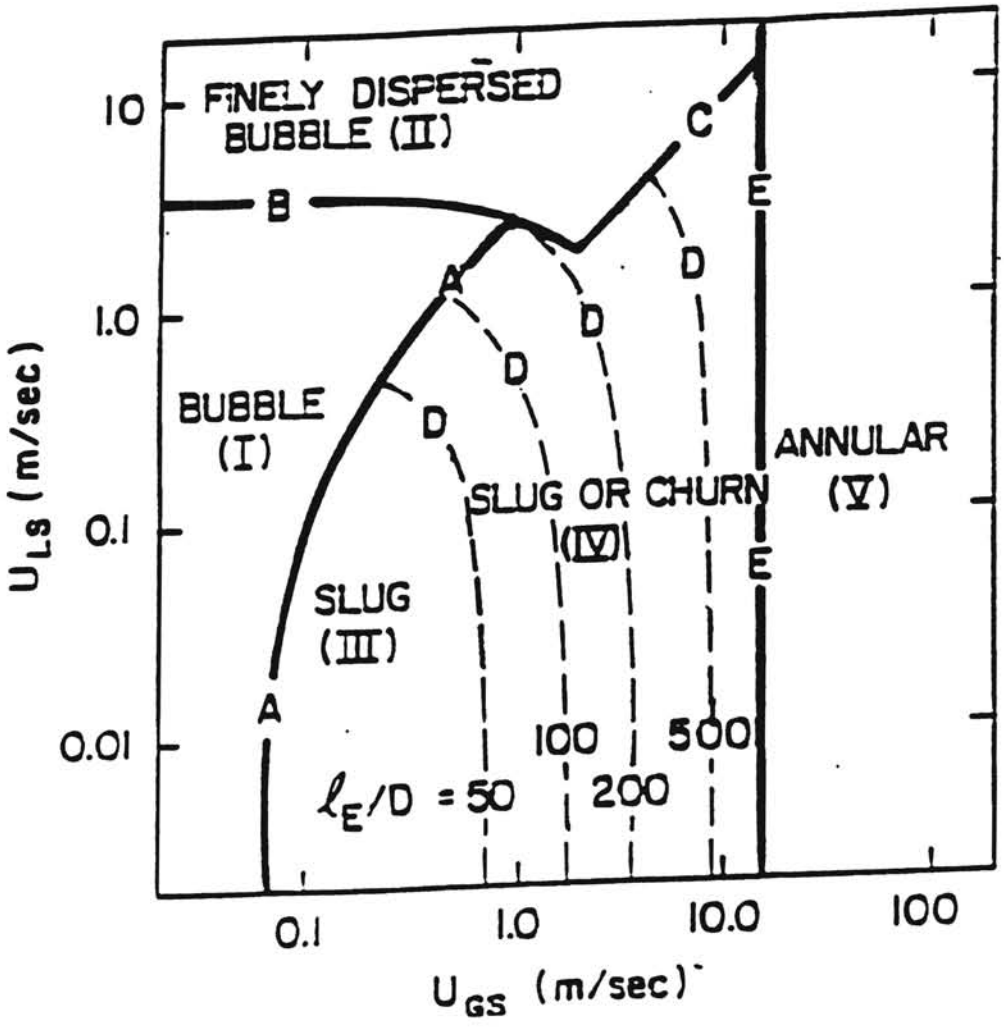

Figure 2. Taitel Flow Map for Air-Water System Flowing Upwards in a 5 cm. Vertical Tube (From Ansari et al., 1994)

$$\left(\frac{dP}{dz}\right)_E = \rho_c \tag{15}$$

where

$$\rho_c = \lambda_{LC}\rho_L + (1-\lambda_{LC})\rho_G, \tag{16}$$

and

$$\lambda_{LC} = \frac{F_E q_L}{(F_E q_L + q_G)}. \tag{17}$$

The liquid entrainment fraction in the gas core is defined by Wallis (1969) as

$$F_E = 1 - \exp\left[-0.125(v_{crit} - 1.5)\right] \tag{18}$$

where

$$v_{crit} = 10000\frac{v_{SG}\mu_G}{\sigma_L}\left(\frac{\rho_G}{\rho_L}\right)^{1/2}. \tag{19}$$

The pressure gradient due to friction losses is given by

$$\left(\frac{dP}{dz}\right)_f = \frac{\rho_c f v_m^2}{2D}. \tag{20}$$

The mixture velocity is defined as

$$v_m = \frac{F_E M_L + M_G}{\rho_c A_C} \tag{21}$$

where

$$A_C = \frac{\pi(D-2\delta)^2}{4}. \tag{22}$$

The friction factor is computed from the modified Zigrang-Sylvester (1982) equation.

$$f = \left[-2\log\left\{ \frac{\varepsilon/D}{3.7} - \left(\frac{5.02}{N_{Re}} \log\left(\frac{\varepsilon/D}{3.7} + \frac{13}{N_{Re}} \right) \right) \right\} \right]^{-2} \tag{23}$$

where

$$N_{Re} = \frac{D\rho_c v_m}{\mu_m}, \text{ and} \tag{24}$$

$$\mu_m = \lambda_L \mu_L + (1-\lambda_L)\mu_L . \tag{25}$$

The effective roughness for annular liquid film was given by Henstock and Hanratty (1976) as

$$\frac{\varepsilon}{D} = \frac{\delta}{D} = \frac{6.59F}{(1+1400F)^{0.5}} \tag{26}$$

where

$$F = \frac{\left\{ \left[0.707(Re_L)^{0.5} \right]^{2.5} + \left[0.0379(Re_G)^{0.9} \right]^{2.5} \right\}^{0.4}}{(Re_G)^{0.9} \left(\frac{\mu_G}{\mu_L} \right) \left(\frac{\rho_L}{\rho_G} \right)^{0.5}}, \tag{27}$$

$$Re_L = \frac{4(1-F_E)M_L}{\mu_L \pi D}, \text{ and} \tag{28}$$

$$Re_G = \frac{\rho_G D v_{SG}}{\mu_G} . \tag{29}$$

The pressure gradient due to acceleration is given by

$$\left(\frac{dP}{dz} \right)_A = \frac{\rho_c v_m dv_m}{dz} . \tag{30}$$

2.4.5 Sylvester Model for Slug Flow

The Sylvester (1987) model, belonging to Approach III, is a modification of the hydrodynamic model of Fernandes et al. (1983). The Taylor bubble velocity and the pressure drop equations have been modified in the Sylvester approach. In the Sylvester approach, the Taitel flow map was used to determine the existence of slug flow. The assumptions made by Sylvester are:

1. the flow is fully developed,
2. the flow is stable which means that the Taylor bubbles and the liquid slug move vertically upwards at the same velocity,
3. the Taylor bubble is surrounded by a layer of thin liquid film which flows downward,
4. the liquid film surrounding the Taylor bubble does not contain any gas bubbles,
5. the ideal Taylor bubble has a spherical nose and a flat tail as shown in Figure 3,
6. the gas bubbles are uniformly distributed throughout the liquid slug, and
7. volume balances can be done instead of mass balances while doing gas phase mass balance, since the gas phase is assumed to be incompressible.

The total pressure drop equation of Sylvester is

$$(\Delta P)_T = (\Delta P)_H + (\Delta P)_f + (\Delta P)_A . \qquad (31)$$

The hydrostatic component of the pressure drop is given by

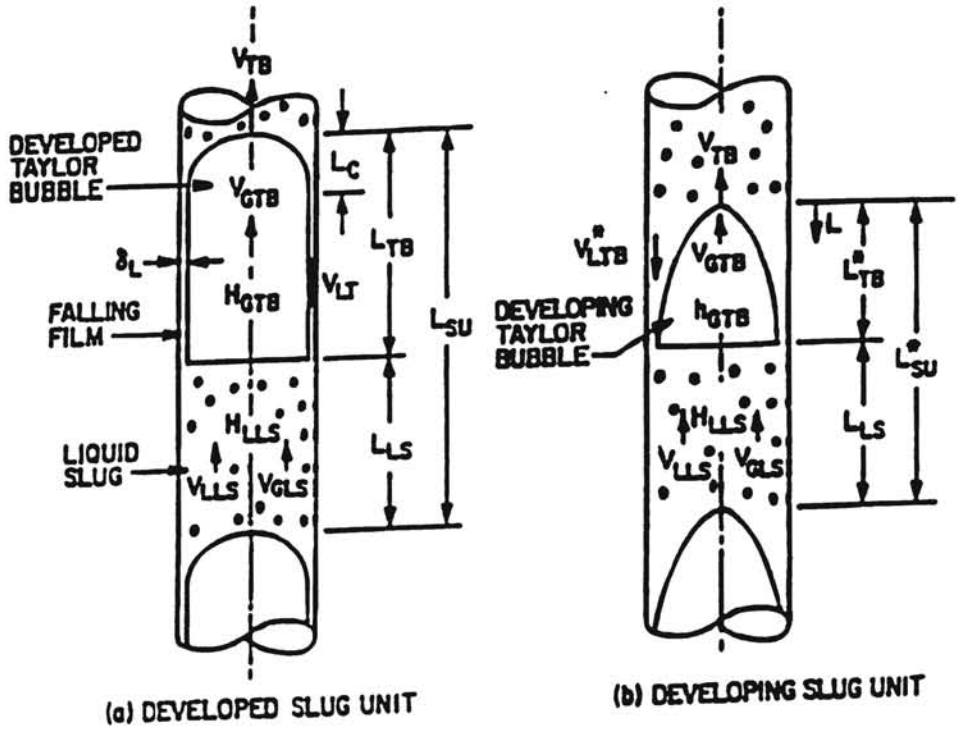

Figure 3. A Schematic of a Developing and a Developed Slug Flow
(From Ansari et al., 1994)

$$(\Delta P)_H = \rho_L(1-\alpha_{LS})gL_{LS} \tag{32}$$

where

$$\alpha_{LS} = \frac{v_{SG}}{1.39 + 2.65(v_{SG} + v_{SL})}, \tag{33}$$

and

$$L_{LS} = 40D. \tag{34}$$

The friction component of pressure drop is given by

$$(\Delta P)_f = \frac{L_{LS}}{2D}\left[\frac{\rho_G \beta f_{TB} v_{TB}^2}{(1-\beta)\left[1-\left(1-\alpha_{TB}^{1/2}\right)\right]} + v_{LLS}\rho_L(1-\alpha_{LS})f_{LS}(1-\beta)\right] \tag{35}$$

where

$$f_{TB} = \frac{1}{\left[-2\log\left\{\frac{1-\sqrt{\alpha_{TB}}}{7.4}\right\}\right]^2}, \tag{36}$$

$$v_{TB} = 1.2v_m + 0.35\sqrt{gD}, \tag{37}$$

$$v_{LLS} = \frac{v_{TB}(\alpha_{TB} - \alpha_{LS}) - (1-\alpha_{TB})v_{LTB}}{(1-\alpha_{LS})}, \tag{38}$$

$$v_{LTB} = 9.916\left[gD(1-\sqrt{\alpha_{TB}})\right]^{1/2}, \tag{39}$$

$$f_{LS} = \left[-2\log\left\{\frac{\varepsilon/D}{3.7} - \left(\frac{5.02}{N_{ReLS}}\log\left(\frac{\varepsilon/D}{3.7} + \frac{13}{N_{ReLS}}\right)\right)\right\}\right]^{-2}, \tag{40}$$

$$N_{ReSL} = \frac{\rho_L(1-\alpha_{LS})v_{LLS}D}{\mu_{LS}}, \tag{41}$$

$$\mu_{LS} = \mu_L(1-\alpha_{LS}) + \mu_G\alpha_{LS}, \tag{42}$$

$$\beta = \frac{v_{SG} - \alpha_{LS}v_{GLS}}{\alpha_{TB}v_{GTB} - \alpha_{LS}v_{GLS}}, \tag{43}$$

and

$$v_{GLS} = v_{LLS} + 1.53\left[\frac{\sigma_L g(\rho_L - \rho_G)}{\rho_L^2}\right]^{1/4}(1-\alpha_{LS})^{0.5}. \tag{44}$$

The pressure drop due to acceleration is given by:

$$(\Delta P)_A = \rho_L(v_{LTB} + v_{TB})(1-\alpha_{TB})(v_{LTB} + v_{TB} + v_{LLS}). \tag{45}$$

The only unknown, α_{TB}, in the above equations is the root of the following equation:

$$9.916\sqrt{gD}(1-\sqrt{\alpha_{TB}})^{0.5}(1-\alpha_{TB}) - v_{TB}\alpha_{TB} + v_{TB}\alpha_{LS} + \tilde{A} = 0 \tag{46}$$

where

$$\tilde{A} = (1-\alpha_{LS})\left[v_m - \alpha_{LS}\left\{1.53\left[\frac{\sigma_L g(\rho_L - \rho_G)}{\rho_L^2}\right]^{0.25}(1-\alpha_{LS})^{0.5}\right\}\right] \tag{47}$$

2.4.6 Ansari et al. Model

Ansari and co-workers (1994) have developed a comprehensive model based on Approach III that predicts the flow regime and the pressure drop in each of the flow regimes. Correlations developed by different investigators have been compiled into one model in the Ansari et al. model. Ansari et al. tested the comprehensive model and compared the model with seven other models in their ability to predict pressure drop. A large data bank consisting of 1712 well cases, covering a wide range of field data, had been used to test the Ansari et al. model.

2.4.6.1 Flow Map

Ansari et al. (1994) used the flow regime map of Barnea (1987), which is a modified Taitel et al. (1980) flow regime map, to include inclined flow. Barnea (1987) compiled the individual models and developed a unified model that would predict the flow patterns for entire range of inclination angles. A typical flow pattern map for well bores (vertical tubes) as predicted by Barnea (1987) is shown in Figure 4.

Figure 4 shows four transition boundaries between the dispersed bubble, bubble, slug or churn, and annular flow regimes. Since most of the gas wells are found to be in the annular or slug flow regimes, the criteria for the existence of annular and slug flow will be discussed here. No distinction is made between dispersed bubble or bubble flow in this thesis.

The line denoting the transition between dispersed bubble and slug flow is:

$$v_{SG} = 0.25v_S + 0.333v_{SL} \tag{48}$$

where, v_S, the slip velocity is given by Harmathy (1960)

$$v_S = 1.53\left[\frac{g\sigma_L(\rho_L - \rho_G)}{\rho_L^2}\right]^{1/4}. \tag{49}$$

The transition from bubble to slug flow is given by:

$$2\left[\frac{0.4\sigma_L}{(\rho_L - \rho_G)g}\right]^{1/2}\left(\frac{\rho_L}{\rho_G}\right)^{3/5}\left[\frac{f}{2D}\right]^{2/5}(v_{SL} + v_{SG})^{1.2} = 0.725 + 4.15\left(\frac{v_{SG}}{v_{SG} + v_{SL}}\right)^{0.5} \tag{50}$$

The transition from dispersed bubble to slug flow is given by:

$$v_{SG} = 3.17v_{SL}. \tag{51}$$

The transition from slug to annular flow is given by:

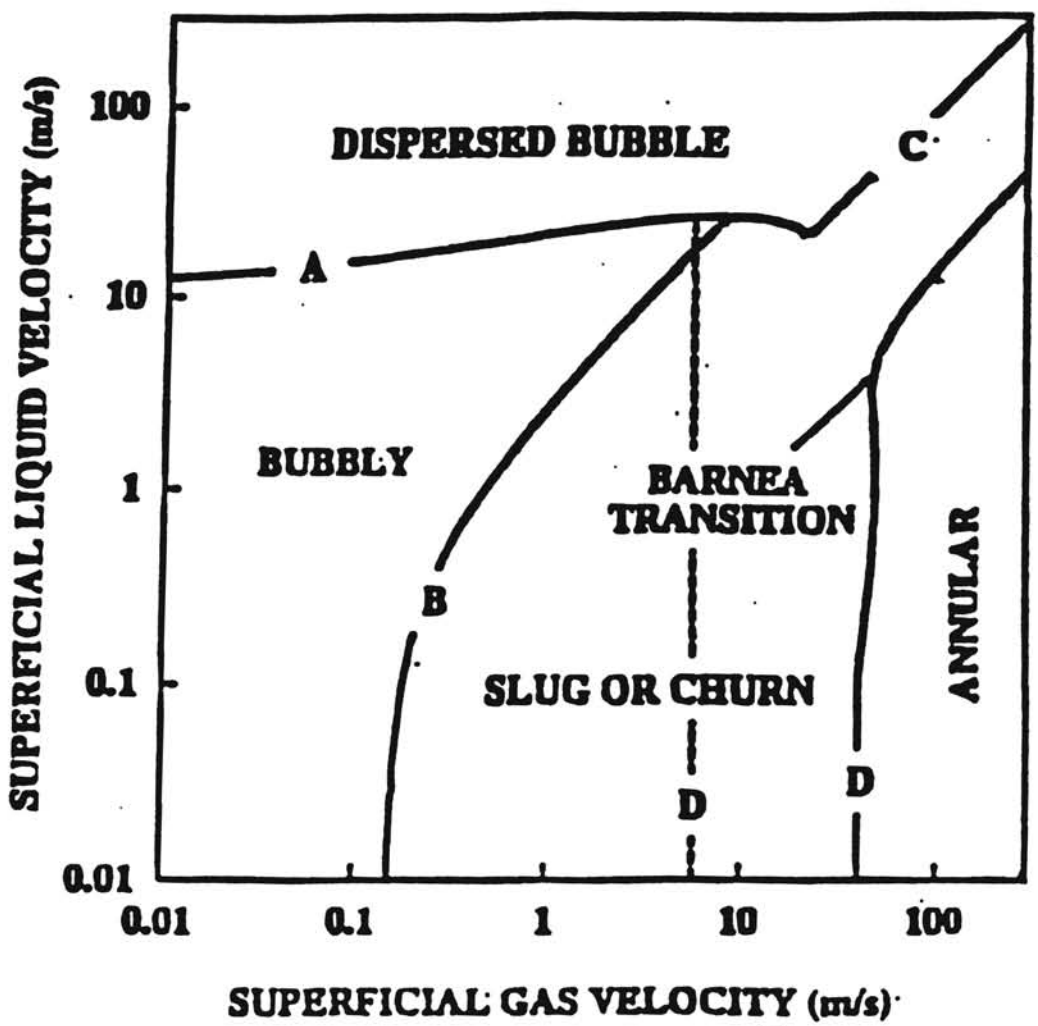

Figure 4 Barnea Flow Map for Vertical Upward Two-Phase Flow
(From Ansari et al., 1994)

$$v_{SG} = 3.1\left[\frac{g\sigma_L(\rho_L - \rho_G)}{\rho_G^2}\right]^{1/4}. \tag{52}$$

The slug-to-annular transition criteria (equation 52), proposed by Taitel et al. (1980) was taken to be valid for the entire range of liquid flow rates. Barnea (1987) modified the criteria (equation 52) for high liquid flow rates. At high liquid flow rates, a thick liquid film bridges the gas core forming a liquid slug. At lower liquid flow rates, the liquid film instability makes the liquid film flow downward. The liquid film instability is expressed by the following equation using the modified Lockhart and Martinelli (1949) parameters

$$Y_M = \frac{2 - 1.5H_{LF}}{H_{LF}^3(1 - 1.5H_{LF})} X_M^2 \tag{53}$$

where

$$X_M = \sqrt{B\frac{\left(\frac{dP}{dz}\right)_{SL}}{\left(\frac{dP}{dz}\right)_{SC}}}, \tag{54}$$

$$Y_M = \frac{gSin\theta(\rho_L - \rho_C)}{\left(\frac{dP}{dz}\right)_{SC}}, \tag{55}$$

$$B = (1 - F_E)^2\left(\frac{f_f}{f_{SL}}\right), \text{ and} \tag{56}$$

$$H_{LF} = 4\underline{\delta}_{min}(1 - \underline{\delta}_{min}). \tag{57}$$

Equation (53) can be solved implicitly using bisection method for the dimensionless minimum film thickness, $\underline{\delta}_{min}$. The transition boundary for high liquid flow rates is given by

$$\left(H_{LF} + \lambda_{LC}\frac{A_C}{A_P}\right) = 0.12 \tag{58}$$

where

$$A_C = \frac{\pi(D-2\delta)^2}{4}, \tag{59}$$

$$A_P = \frac{\pi D^2}{4}, \text{ and} \tag{60}$$

$$\lambda_{LC} = \frac{F_E v_{SL}}{v_{SG} + F_E v_{SL}}. \tag{61}$$

the liquid entrainment fraction F_E is given by Wallis as

$$F_E = 1 - \exp\left[-0.125\left(v_{crit} - 1.5\right)\right] \tag{62}$$

where

$$v_{crit} = 10000\frac{v_{SG}\mu_G}{\sigma_L}\left(\frac{\rho_G}{\rho_L}\right)^{1/2}. \tag{63}$$

2.4.6.2 Bubble Flow

For the bubble flow regime, Ansari et al. used the model proposed by Caetano (1985). Since bubble flow does not occur in gas wells, the Caetano (1985) model has not been incorporated into the final corrosion prediction package. However, the comprehensive corrosion prediction model developed by Liu does have a pressure drop correlation developed by Orkiszewski (1967) for the bubble flow regime. The

Orkiszewski (1967) model was added by Robertson (1988) as part of a comprehensive pressure drop model.

2.4.6.3 Slug Flow

For the slug flow regime, Ansari et al. used the Sylvester model (1987), a modified version of the Fernandes et al. model (1983), without the assumption of fully developed flow. Since a fully developed flow geometry differs from that of a developing flow, the two different flow geometries are treated separately. For fully developed flow, the Sylvester model has been used with some modifications:

1. The pressure gradient due to acceleration has been neglected in the Ansari et al. model.
2. Pressure gradients due to friction are not split into two components (frictional pressure gradient due to Taylor bubble and due to liquid slug) as in the Sylvester model (1987) for a fully developed flow.

For the developing flow, the expressions introduced by McQuillan and Whalley (1985) have been used to estimate the modified Taylor bubble length and the local holdup fraction. A detailed schematic is given in Figure 3 showing a developed slug unit and a developing slug unit. The following derivation is based on the parameters defined in the Figure 3.

Developed Flow

The overall mass balances for gas and liquid are

$$v_{SG} = \beta v_{GTB} (1-H_{LTB}) + (1-\beta) v_{GLS} (1-H_{LLS}), \quad (64)$$

and

$$v_{SL} = (1-\beta) v_{LLS} H_{LLS} + \beta v_{LTB} H_{LTB} \quad (65)$$

where

$$\beta = L_{TB} / L_{SU}. \quad (66)$$

The following two mass balance equations are for the two phases between the liquid slug and the Taylor bubble:

$$(v_{TB} - v_{LLS}) H_{LLS} = [v_{TB} - (-v_{LTB})] H_{LTB}, \quad (67)$$

and

$$(v_{TB} - v_{GLS}) (1 - H_{LLS}) = [v_{TB} - v_{GTB}] (1 - H_{LTB}). \quad (68)$$

The Taylor bubble rise velocity v_{TB} is given by

$$v_{TB} = 1.2v_m + 0.35\left[\frac{gD(\rho_L - \rho_G)}{\rho_L}\right]^{1/2}. \quad (69)$$

The gas bubble velocity in the liquid slug is given by

$$v_{GLS} = 1.2v_m + 1.53\left[\frac{\sigma_L g(\rho_L - \rho_G)}{\rho_L^2}\right]^{1/4} H_{LLS}^{0.5}. \quad (70)$$

The velocity of the liquid film around the Taylor bubble has been correlated with the expression of Brotz (1954):

$$v_{LTB} = \sqrt{196.7g\delta_L}. \quad (71)$$

Substituting for δ_L, we have

$$v_{LTB} = 9.916\left[gD(1-\sqrt{H_{GTB}})\right]^{1/2} \quad (72)$$

The void fraction of liquid slug is obtained by fitting the following expression to the data of Fernandes (1986):

$$H_{GLS} = \frac{v_{SG}}{C_1 + C_2 v_m} \tag{73}$$

where $C_1 = 1.394$ and $C_2 = 2.65$. Equations (64) or (65), (66) through (70), (72), and equation (73) constitute a set of 8 equations which have to be solved for the 8 unknowns (β, v_{GTB}, H_{LTB}, v_{GLS}, H_{LLS}, v_{LLS}, v_{LTB}, v_{TB}) that characterize slug flow. Vo and Shoham (1989) showed that these 8 equations can be reduced to a single algebraic equation with one unknown. This single algebraic equation can be solved using a Newton-Raphson iterative procedure. The system of 8 equations were reduced to give the following equation:

$$9.916\sqrt{gD}(1-\sqrt{1-H_{LTB}})^{0.5} H_{LTB} - v_{TB}(1-H_{LTB}) + \tilde{A} = 0 \tag{74}$$

where

$$\tilde{A} = H_{GLS} v_{TB} + (1-H_{GLS})\left[v_m - H_{GLS}\left\{ 1.53\left[\frac{\sigma_L g(\rho_L - \rho_G)}{\rho_L^2} \right]^{0.25} (1-H_{GLS})^{0.5} \right\} \right]. \tag{75}$$

Let

$$F(H_{LTB}) = 9.916\sqrt{gD}(1-\sqrt{1-H_{LTB}})^{0.5} H_{LTB} - v_{TB}(1-H_{LTB}) + \tilde{A}. \tag{76}$$

Equation (76) can be solved for H_{LTB} and all the eight unknowns can be obtained from the eight equations (64) or (65), (66) - (70), (72), and (73). The expression for the cap length is given by McQuillan and Whalley (1985)

$$L_c = \left\{ \frac{A v_p - (Q_G + Q_L)/(2g)^{0.5}}{A - A_G} \right\}^2 \tag{77}$$

where

$$A_G = \pi (D - 2\delta_N)^2 / 4, \tag{78}$$

$$\delta_N = \left(\frac{3Q_f \mu_L}{\pi g D \rho_L} \right)^{1/3}, \tag{79}$$

$$Q_f = Q_G + Q_L - Q_P, \tag{80}$$

$$Q_P = \left\{ 1 - \frac{4\delta}{D} \right\} \left\{ 1.2(Q_G + Q_L) + 0.35A \left[\frac{gD(\rho_L - \rho_G)}{\rho_L} \right]^{1/2} \right\}, \tag{81}$$

and

$$A = \pi D^2 / 4. \tag{82}$$

The liquid slug length is given by

$$L_{LS} = kD \tag{83}$$

where k can take values from 16 to 45. For the purposes of this study k has been taken as 30. The length of Taylor bubble is then found from the following expression:

$$L_{TB} = \frac{L_{LS}\beta}{1-\beta}. \tag{84}$$

The flow is developed if $L_c < L_{TB}$, and the total pressure drop is given by

$$\left(\frac{dP}{dz} \right)_T = \left(\frac{dP}{dz} \right)_E + \left(\frac{dP}{dz} \right)_A + \left(\frac{dP}{dz} \right)_f. \tag{85}$$

The liquid in the slug decelerates when it goes from the slug to the Taylor bubble and accelerates when it moves from the Taylor bubble to slug. Since both the acceleration and deceleration take place within the same slug unit, the pressure drop due to acceleration is zero in a slug unit.

The pressure drop due to elevation is given by

$$\left(\frac{dP}{dz}\right)_E = \left[(1-\beta)\rho_{LS} + \beta\rho_G\right] g \sin\theta \tag{86}$$

where

$$\rho_{LS} = \rho_L H_{LLS} + \rho_G (1 - H_{LLS}) . \tag{87}$$

The pressure drop due to friction is given by

$$\left(\frac{dP}{dz}\right)_f = \frac{f_{LS}\rho_{LS} v_m^2}{2D}(1-\beta) . \tag{88}$$

The friction factor is given by the modified Zigrang-Sylvester (1982) correlation.

$$f_{LS} = \left[-2\log\left\{ \frac{\varepsilon/D}{3.7} - \left(\frac{5.02}{N_{Re}} \log\left(\frac{\varepsilon/D}{3.7} + \frac{13}{N_{Re}} \right) \right) \right\} \right]^{-2} \tag{89}$$

where

$$N_{Re} = \frac{\rho_{LS} v_m D}{\mu_{LS}}, \tag{90}$$

and

$$\mu_{LS} = \mu_L H_{LLS} + \mu_G H_{GLS} . \tag{91}$$

Developing Flow

If $L_c \geq L_{TB}$, the two-phase flow is not fully developed. When the flow is not fully developed, the Taylor bubble length has to be modified. By equating the Taylor bubble volume in terms of the flow geometry to the actual Taylor bubble volume, the following quadratic equation can be obtained:

$$L_{TB}^{*\,2} + \left(\frac{-2ab - 4c^2}{a^2} \right) L_{TB}^{*} + \left(\frac{b}{a} \right)^2 = 0 \tag{92}$$

where

$$a = 1 - \frac{v_{SG}}{v_{TB}}, \tag{93}$$

$$b = \frac{v_{SG} - v_{GLS}\left(2 - H_{LLS}\right)}{v_{TB}} L_{LS}, \tag{94}$$

and

and $$c = \frac{v_{TB} - v_{LLS}}{\sqrt{2g}} H_{LLS}. \tag{95}$$

The details of the derivation of the quadratic equation can be obtained from Ansari et al. (1994).

The total pressure drop is given by

$$\left(\frac{dP}{dz}\right)_T = \left(\frac{dP}{dz}\right)_E + \left(\frac{dP}{dz}\right)_f. \tag{96}$$

The elevation component is

$$\left(\frac{dP}{dz}\right)_E = \left[\left(1 - \beta^*\right)\rho_{LS} + \beta^* \rho_{TBA}\right] g \, \text{Sin}\, \theta \tag{97}$$

where

$$\beta^* = \frac{L^*_{TB}}{L^*_{TB} + L_{LS}}, \tag{98}$$

$$\rho_{TBA} = \rho_L H_{LTBA} + \rho_G \left(1 - H_{LTBA}\right), \tag{99}$$

and

$$H_{LTBA} = \frac{2\left(v_{TB} - v_{LLS}\right) H_{LLS}}{\sqrt{2gL^*_{TB}}}. \tag{100}$$

Since only vertical well cases are considered for this work, Sin θ takes a value of one and can be dropped from equation (97).

The friction component is given by

$$\left(\frac{dP}{dz}\right)_f = \frac{f_{I,S}\rho_{I,S}v_m^2}{2D}\left(1-\beta^*\right). \tag{101}$$

2.4.6.4 Annular Flow

For the annular flow regime, Ansari and co-workers developed a model that made use of the correlations presented by Wallis (1969) for the liquid entrainment and interfacial friction. The Ansari et al. (1994) approach is based on the annular flow mechanism discussed by Hewitt and Hall-Taylor (1970). All the assumptions made for the Yao and Sylvester model (1987) are assumed to be valid for the Ansari model with the additional assumption of negligible pressure drop due to acceleration. A detailed schematic of a fully developed annular flow is shown in Figure 5. The pipe wall is wetted by a liquid film. A central gas core flows upward with entrained liquid droplets.

Momentum conservation applied to the gas core and the liquid film yields the following two equations:

$$A_C\left(\frac{dP}{dz}\right)_C - \tau_i S_i - \rho_C A_C g\,\mathrm{Sin}\theta = 0, \tag{102}$$

and

$$A_F\left(\frac{dP}{dz}\right)_F + \tau_i S_i - \tau_F S_F - \rho_L A_F g\,\mathrm{Sin}\theta = 0. \tag{103}$$

The gas core is considered to be a homogeneous mixture of gas and entrained liquid droplets flowing at the same velocity (no slip). The core density ρ_C is given by

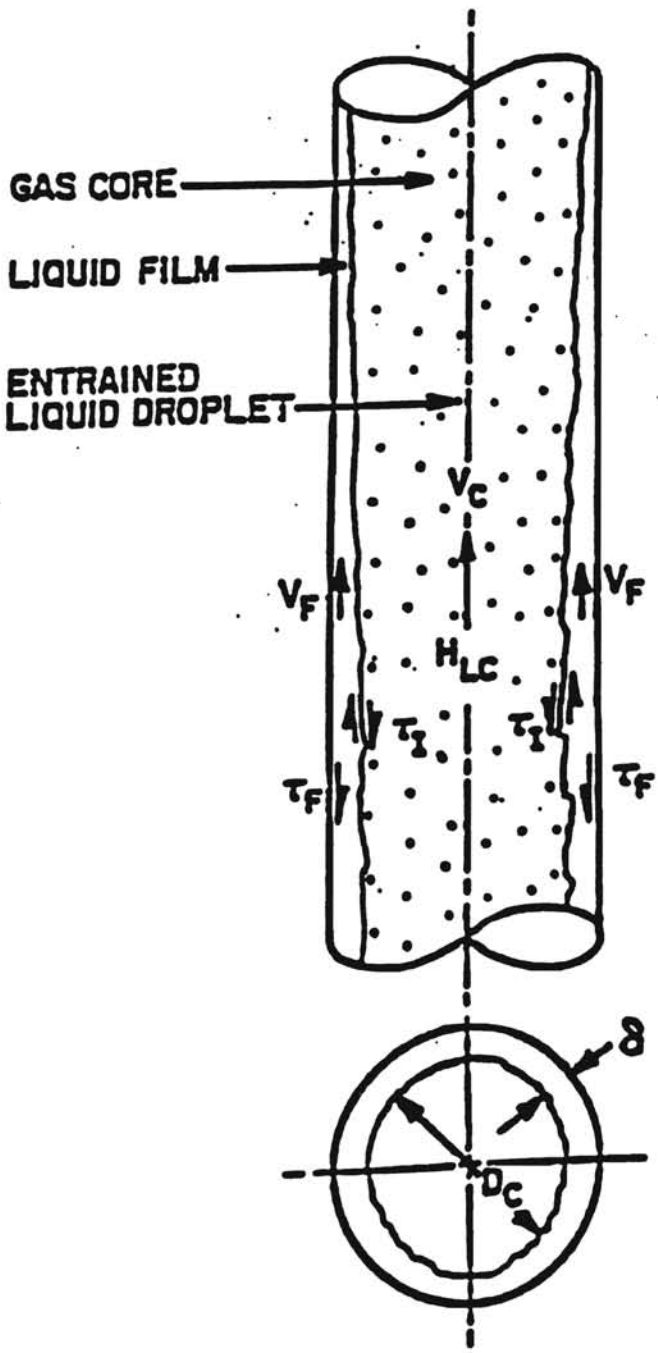

Figure 5. A Schematic of Developed Annular Flow in Vertical Upward Flow (From Ansari et al., 1994)

$$\rho_C = \rho_L \lambda_{LC} + \rho_G (1 - \lambda_{LC}). \tag{104}$$

The superficial friction pressure gradient in the liquid is

$$\left(\frac{dP}{dz}\right)_{SL} = \frac{f_{SL} \rho_L v_{SL}^{\ 2}}{2D} \tag{105}$$

where, f_{SL} can be obtained from the Moody diagram for a Reynolds number defined by

$$N_{ReSL} = \frac{\rho_L v_{SL} d}{\mu_L}. \tag{106}$$

The superficial friction pressure gradient in the core is defined as

$$\left(\frac{dP}{dL}\right)_{SC} = \frac{f_{SC} \rho_c v_{SC}^2}{2D} \tag{107}$$

where, f_{SC} is obtained from the Moody diagram for the following Reynolds number

$$N_{ReSC} = \frac{\rho_C v_{SC} d}{\mu_C}, \tag{108}$$

where

$$v_{SC} = F_E v_{SL} + v_{SG}, \tag{109}$$

and

$$\mu_c = \mu_L \lambda_{LC} + \mu_G \left(1 - \lambda_{LC}\right). \tag{110}$$

The shear stress in the liquid film is given by

$$\tau_F = \frac{f_F \rho_L v_F^2}{8} \tag{111}$$

where f_F is obtained from Moody diagram for a Reynolds number defined by

$$N_{Re_F} = \frac{\rho_L v_F d_{HF}}{\mu_L}, \tag{112}$$

$$v_F = \frac{Q_L(1-F_E)}{A_F} = \frac{v_{SL}(1-F_E)}{4\underline{\delta}(1-\underline{\delta})}, \tag{113}$$

$$\underline{\delta} = \frac{\delta}{D}, \tag{114}$$

and

$$d_{HF} = 4\underline{\delta}(1-\underline{\delta})d. \tag{115}$$

Substituting equation (113) in equation (111) gives

$$\tau_F = \frac{f_F}{8}(1-F_E)^2 \rho_L \left[\frac{v_{SL}}{4\underline{\delta}(1-\underline{\delta})}\right]^2. \tag{116}$$

Equation (116) can be modified to give

$$\tau_F = \frac{D}{4}\frac{(1-F_E)^2}{\left[4\underline{\delta}(1-\underline{\delta})\right]^2}\frac{f_F}{f_{SL}}\left(\frac{dP}{dL}\right)_{SL}. \tag{117}$$

The interfacial shear stress is defined as

$$\tau_i = \frac{f_i \rho_C v_C^2}{8}, \tag{118}$$

where

$$v_C = \frac{v_{SC}}{(1-2\underline{\delta})^2}, \tag{119}$$

and

$$f_i = f_{SC} Z. \tag{120}$$

The correlating factor, Z, for interfacial friction and film thickness is given by Whalley and Hewitt (1978).

$$Z = 1 + 300\underline{\delta}, \qquad F_E > 0.9 \tag{121}$$

$$Z = 1 + 24\left(\frac{\rho_L}{\rho_g}\right)^{1/3}\underline{\delta}, \qquad F_E \le 0.9 \tag{122}$$

Substituting for ρ_C and v_C in equation (118) using equations (107) and (119), respectively,

$$\tau_i = \frac{D}{4}\frac{Z}{(1-2\underline{\delta})^4}\left(\frac{dP}{dz}\right)_{SC}. \tag{123}$$

The wetted perimeter of the core, S_i, is given by

$$S_i = \pi(D - 2\delta), \tag{124}$$

and the wetted perimeter of the liquid film, S_F, is given by

$$S_F = \frac{\pi(D-2\delta) + \pi D}{2} = \pi(D-\delta). \tag{125}$$

The cross-sectional area of the gas core is

$$A_C = \frac{\pi(D-2\delta)^2}{4} \tag{126}$$

and the cross-sectional area of the film is

$$A_F = \pi(D-2\delta)\delta. \tag{127}$$

Substituting equations (116), (122), and (123) - (127) in equations (102) and (103),

$$\left(\frac{dP}{dz}\right)_C = \frac{Z}{(1-2\underline{\delta})^5}\left(\frac{dP}{dz}\right)_{SC} + \rho_C g\,\mathrm{Sin}\theta \tag{128}$$

$$\left(\frac{dP}{dz}\right)_F = \frac{(1-F_E)^2}{64\underline{\delta}^3(1-\underline{\delta})^3}\left(\frac{f_F}{f_{SL}}\right)\left(\frac{dP}{dz}\right)_{SL} - \frac{Z}{4\underline{\delta}(1-\underline{\delta})(1-2\underline{\delta})^3}\left(\frac{dP}{dz}\right)_{SC} + \rho_L g\,\mathrm{Sin}\theta \tag{129}$$

Since the pressure gradient in the core is the same as that in the film, equating equation (128) and (129) gives

$$\frac{Z}{4\underline{\delta}(1-\underline{\delta})(1-2\underline{\delta})^5}\left(\frac{dP}{dz}\right)_{SC} - (\rho_L - \rho_C)g\,\mathrm{Sin}\theta - \frac{(1-F_E)^2}{64\underline{\delta}^3(1-\underline{\delta})^3}\frac{f_F}{f_{SC}}\left(\frac{dP}{dz}\right)_{SL} = 0 \qquad (130)$$

Using the modified Lockhart and Martinelli (1949) parameters X_M and Y_M, equation (130) simplifies to

$$Y_M - \frac{Z}{4\underline{\delta}(1-\underline{\delta})\left[1-4\underline{\delta}(1-\underline{\delta})\right]^{2.5}} + \frac{X_M^2}{\left[4\underline{\delta}(1-\underline{\delta})\right]^3} = 0 \qquad (131)$$

The left side of equation (131) can be considered as a function of $\underline{\delta}$ and solved for $\underline{\delta}$ using the bisection method. The total pressure gradient is given by either of the expressions for the pressure gradient in the core or the film.

$$\left(\frac{dP}{dz}\right)_T = \left(\frac{dP}{dz}\right)_C \qquad (132)$$

or

$$\left(\frac{dP}{dz}\right)_T = \left(\frac{dP}{dz}\right)_F \qquad (133)$$

Since the expression for the pressure gradient in the core is simpler than the expression for the pressure gradient in the film, the total pressure gradient is computed using the following expression:

$$\left(\frac{dP}{dz}\right)_T = \frac{Z}{(1-2\underline{\delta})^5}\left(\frac{dP}{dz}\right)_{SC} + \rho_C g\,\mathrm{Sin}\theta. \qquad (134)$$

Since only vertical well cases were considered for this thesis work, Sin θ takes a value of one and can be dropped from equation (134).

2.5 Corrosion Prediction Models

A number of different mechanisms and models have been proposed to predict the presence or absence of downhole corrosion as well as the rate of corrosion. Different parameters were considered to be indices of corrosion. Some investigators (Smith, 1982, Tuttle, 1987; Tuttle, 1990) believed that the concentration of H_2S and CO_2 were a good index to corrosion prediction, while Bradburn (1977) proposed that the amount of water produced would be a good index. With extensive research in the field of downhole corrosion, corrosion engineers have realized that downhole corrosion is not a simple phenomena that depends upon just one or two factors. Downhole corrosion is highly complex and the need to understand the basic mechanisms led to the development of the following models that predict corrosion in downhole gas wells.

2.5.1 Model of Robertson

The purpose of Robertson's (1988) research was to develop a user friendly computer program that would predict the location of water condensation zone in gas wells, given all the necessary well conditions as input data to the computer program. Robertson's work was based on the idea that corrosion is most likely to occur in that section of the gas well where water condenses. The outcome of Robertson's work was the software tool DOWN*HOLE.

DOWN*HOLE used GPA*SIM (Erbar, 1980) for the thermodynamic phase equilibrium calculations. GPA*SIM uses the Soave-Redlich-Kwong equation of state, modified by Erbar (1972). Modifications were made to GPA*SIM to suit the needs of DOWN*HOLE. Additional subroutines were added to:

1. generate hydrocarbon-rich and water-rich dewpoint curves,
2. perform flash calculations at separator, wellhead, and bottomhole conditions to check for the presence of water,
3. check for existence of two-phase flow conditions,
4. predict pressure drop, and
5. generate a fluid velocity profile for the well string.

2.5.1.1 Prediction of Fluid Properties

Robertson had used different correlations for predicting the fluid properties. The GPA*SIM (Erbar, 1980) program was used to do the thermodynamic phase equilibrium calculation. The vapor phase densities were predicted by GPA*SIM while the liquid phase densities were predicted by the Hankinson-Thomson-COSTALD (1982) procedure. The correlation used to estimate the vapor phase viscosity (for hydrocarbon systems) was developed by Lee et al. (1986). The liquid viscosity and surface tension were taken to be the same as that of water at the desired temperature.

2.5.1.2 Determination of Flow Regime

The work of Taitel et al. (1980) has been used to model the flow pattern transitions. Four main flow regimes were considered by Taitel: bubble, slug, churn and annular. Since the pressure drop models considered include churn flow with slug flow, only bubble-slug and slug-annular transition criteria were considered. A typical flow pattern map for air-water system flowing upward in a vertical 5 cm tube is shown in Figure 2.

The transition from bubble to slug flow occurs when there is an increase in the gas bubble density which would lead to coalescence of bubbles. An increase in the gas bubble density would take place when the gas flow rate is high or if the pipe diameter is small. Taitel et al. have defined the criteria for a pipe with small diameter as one that satisfies the following relation:

$$\left[\frac{\rho_L^2 g D^2}{(\rho_L - \rho_G)\sigma}\right]^{0.25} \leq 4.36. \qquad (135)$$

The transition from slug to annular flow occurs when the gas flow rate is large enough to be able to lift the liquid droplets and is given by:

$$\frac{v_{SG}\rho_G^{1/2}}{\left[\sigma g(\rho_L - \rho_G)\right]^{1/4}} > 3.1. \qquad (136)$$

When both the conditions (135) and (136) are not satisfied, the flow was assumed to be in the bubble flow regime. A detailed derivation of the above mentioned criteria (135 and 136) is given in Robertson (1988).

2.5.1.3 Pressure Drop Correlations Used by Robertson

Robertson's model had seven options to predict the pressure profile along the production string: linear pressure profile, two-phase homogeneous flow method, Orkiszewski's flow regime based method, and Yao-Sylvester's annular-mist flow method. The last three methods could have either a linear temperature or linear enthalpy specified as input. If the linear enthalpy option is used, the temperature profile along the well string is estimated before proceeding to the pressure drop calculation. Once the fluid properties

were estimated, pressure drop was predicted by one of the above mentioned methods, depending upon the preference of the user.

The linear pressure profile assumed the pressure to be linear between the wellhead and the bottomhole. Since the bottomhole pressure drop data obtained from the field are not usually accurate, the linear profile between the measured wellhead and bottomhole conditions can only be approximate. The linear pressure profile assumption was used as a first guess for the other pressure drop estimation methods.

DOWN*HOLE succeeded in predicting the water condensation zone and thereby the presence or absence of corrosion, but could not predict the rate of corrosion. Despite the inability to predict corrosion, Robertson's work is important as it laid the foundation for the subsequently developed models that predict the rate of corrosion in downhole gas wells.

2.5.2 Model of Liu and Erbar

Liu and Erbar (1990) proposed a model to predict downhole corrosion. The Liu and Erbar (1990) model made use of Robertson's work and his computer program DOWN*HOLE. Additional segments were added to DOWN*HOLE to include pH calculations, mass transfer, reaction kinetics, and finally corrosion rate prediction. In this model by Liu and Erbar, the hydrogen ion was considered to be the key corrosive species. The Liu and Erbar (1990) model also made the assumption of no protective film. The assumption of no protective film predicts corrosion rate much higher than the actual corrosion rate in the production strings depending on the location in the string. Even though the approach of Liu and Erbar was oversimplified and does not predict accurate

corrosion rates, it was the first time a comprehensive model taking into account fluid dynamics, phase equilibrium, mass transfer, and reaction kinetics was developed.

2.5.3 Model of Liu

Liu (1991) developed another model which did not make some of the assumptions made in the earlier model (Liu and Erbar, 1990) such as no protective film and diffusion or reaction rate controlled mechanisms. Both the worst case (no protective film) corrosion as well as corrosion rate in the presence of a protective film are predicted by Liu (1991) In the new model (Liu, 1991), the corrosion process was visualized as a three layer model as shown in Figure 6. The three layers were: the turbulent film layer, the diffusion layer, and the corrosion product layer. Corrosive species are first transported through the turbulent film layer. The wall roughness and interfacial shear stress were found to have an effect on the mass transfer in the turbulent layer. The next layer was the diffusion layer where mass transfer is primarily by molecular diffusion and ion migration. When there is no corrosion product, the corrosive species must be transported through only two layers. the turbulent film layer and the diffusion layer. When the corrosion product is present, the corrosive species must diffuse through a third layer, the corrosion product layer while the ferrous ions from the pipe wall (the corrosion product) diffuse in the opposite direction.

2.5.4 Model of Liu and High

Liu made modifications to his earlier model and developed a new software tool to predict downhole corrosion in gas wells, DREAM. The changes have been documented in detail in a report by Liu and High (1993). The following changes were made:

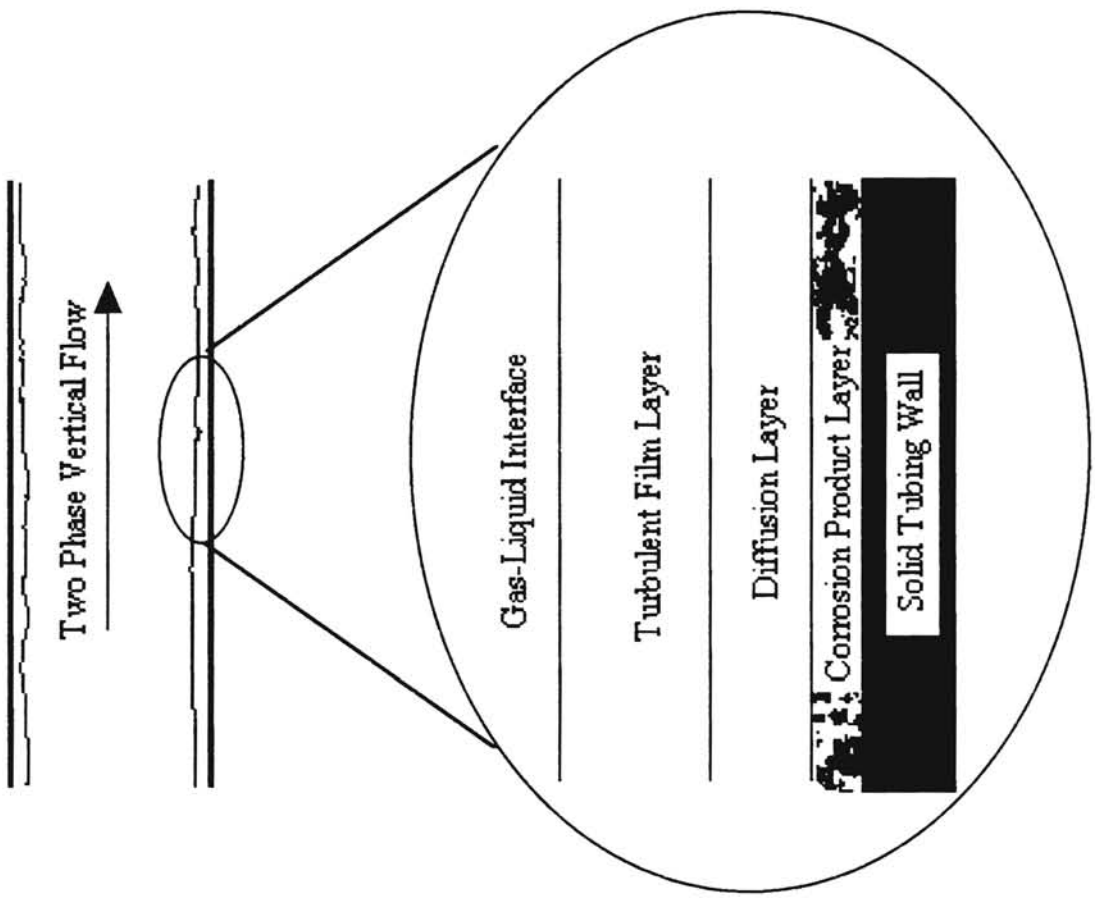

Figure 6. Three Layer Model: an Approach to Model the Downhole System

(From Liu, 1991)

1. The form of the objective function for the three phase thermodynamic flash calculation was changed based on a paper by Bunz et al. (1991). The new objective function gave smoother transitions from three phase to two-phase or single phase.
2. Modifications were made in the pressure drop subroutines to include a new model by Sylvester (1987) for the slug flow regime. The pressure drop in the bubble flow regime was estimated by the Orkiszewski (1967) method. The Yao and Sylvester (1987) model was used for predicting pressure drop in the annular flow regime.
3. The assumption that the net current flow is zero, for a corrosion system, was made in this approach of Liu and High (1993). The zero current assumption replaced the electro-neutrality assumption made in the earlier model by Liu (1991). The above change was made because the electro-neutrality assumption was not valid near the pipe wall.
4. The diffusivity correlation for the species in the $FeCO_3$ film was modified.
5. The assumption made in the earlier model that the corrosion layer behaves like the diffusion layer was not made in this model (Liu and High, 1993).

2.6 Summary

1. The pressure drop predictions were found to deviate from measured pressure drops significantly both in the annular and slug flow regimes.
2. The pressure drop subroutines for the Sylvester (1987) and the Yao and Sylvester (1987) models in DREAM did not match with literature.

3. The computer code crashed in some cases due to some coding errors.
4. The corrosion rate predicted by DREAM did not always match with the caliper survey data.

Chapter III

RESULTS AND DISCUSSION

3.1 Introduction

This study has yielded information regarding the utility of the different pressure drop models under widely varying conditions for water-cut gas wells. The models have been tested against 140 data sets taken from Camacho (1970) and Reinicke et al. (1987) The pressure drop predicted by the models has been compared with water-gas field data only even though the models are applicable to oil wells also. An evaluation of the models is presented in this chapter.

The pressure drop models have also been incorporated into DREAM, a software tool to predict the corrosion rate in downhole gas wells. An evaluation of DREAM has been made and the effect of pressure drop on corrosion rate has been studied.

The computational procedure involved in the flow regime analysis and the pressure drop estimation for upward vertical two-phase flow systems in the annular and slug flow regimes has been explained in Appendix C. In order to verify the accuracy of the computer code, two cases (one each in the slug and the annular flow regimes) were taken and the pressure drop was calculated manually. The results of the manual computation have been attached in Appendix D and Appendix E. The predictions obtained using the FORTRAN code and the manual computations are given below.

Slug Flow:

$(\Delta P)_{manual,\ Sylvester} = 74.04$ psia $\qquad$ $(\Delta P)_{computer,\ Sylvester} = 73.4$ psia

$(\Delta P)_{manual,\ Ansari} = 49.15$ psia $(\Delta P)_{computer,\ Ansari} = 48.1$ psia

Annular Flow:

$(\Delta P)_{manual,\ Yao\ \&\ Sylvester} = 37.8$ psia $(\Delta P)_{computer,\ Yao\ \&\ Sylvester} = 38.6$ psia

$(\Delta P)_{manual,\ Ansari} = 132.05$ psia $(\Delta P)_{computer,\ Ansari} = 132.0$ psia

The pressure drops predicted manually were found to deviate from the pressure drops computed by the FORTRAN code marginally. The difference can be attributed to rounding off errors in the manual computations.

3.2 Analysis of Pressure Drop Predictions for the Air-Water System

The pressure drop subroutines developed in this work were primarily intended for upward vertical two-phase flow in gas wells. Since the applicability of these models could be extended to include other systems such as the air-water two-phase flow system (frequently encountered in the chemical processing industry), the pressure drop predictions were compared against experimental data of the air-water system obtained from Golan (1970). The experimental data taken from Golan (1970) are reported in Table I.

The following formulae have been used in making the statistical analysis:

$$\left(\text{percentage error}\right)_i = \frac{P_{bottomhole,model} - P_{bottomhole,measured}}{P_{bottomhole,measured}} \text{x}100 \qquad (137)$$

$$\text{average absolute error} = \frac{\sum_{i=1}^{N} \left|\left(\text{percentage error}\right)_i\right|}{N} \qquad (138)$$

A comparison of the predicted pressure drop and the experimentally measured pressure drop has been made and the results are presented in Tables II and III. The Yao

TABLE I

Air-Water Experimental Data for Upward Vertical Two-Phase Flow

Run No.	Regime	Gas Flow Rate (scfm)	Water Flow Rate (gpm)	Pressure Bottom (psia)	Pressure Top (psia)	Pressure Gradient psia/ft
40	slug	2	10	4.0	1.3	0.27
50	slug	4.3	10	3.1	1.0	0.21
51	slug	4.8	10	3.2	1.0	0.22
52	slug	5.8	10	3.1	1.1	0.20
53	slug	6.9	10	3.1	1.1	0.20
120	annular	90	10	5.5	4.2	0.13
121	annular	80	10	4.7	3.1	0.16
160	slug	4.4	8	2.8	0.9	0.19
161	slug	5.4	8	2.8	0.9	0.19
162	slug	6.1	8	2.8	0.8	0.20
203	annular	78	8	3.9	2.2	0.17
210	annular	95	8	4.5	3.1	0.14
250	slug	5.8	6	2.5	0.9	0.16
251	slug	6.5	6	2.4	0.9	0.15
294	annular	73	6	2.8	1.6	0.12
300	annular	95	6	3.6	2.2	0.14
310	annular	115	6	4.5	3.0	0.15
350	slug	5	12	3.4	1.0	0.24
351	slug	5.1	12	3.2	1.1	0.21
352	slug	6	12	3.3	1.1	0.22
410	annular	85	12	5.8	4.0	0.18
420	annular	100	12	7.5	5.4	0.21
460	slug	5.5	14	3.4	1.1	0.23
520	annular	100	14	8.5	6.1	0.24
550	slug	1.9	16	2.8	0	0.28
560	slug	3.8	16	4.0	1.1	0.29
610	annular	100	16	9.0	6.0	0.30
612	annular	95	16	9.5	6.4	0.31
620	annular	120	16	10.8	7.7	0.31
650	slug	3.1	18	3.9	1.0	0.29
660	slug	6.2	18	3.8	1.3	0.25
721	annular	93	18	10.0	7.0	0.30
730	annular	115	18	12.0	8.8	0.32
740	annular	125	18	13.2	9.2	0.40
770	slug	2.1	20	3.3	0.1	0.32
830	annular	90	20	11.5	8.4	0.31

TABLE I (cont'd)

Run No.	Regime	Gas Flow Rate (scfm)	Water Flow Rate (gpm)	Pressure Bottom (psia)	Pressure Top (psia)	Pressure Gradient psia/ft.
840	annular	110	20	14.6	10.5	0.40
921	annular	94	22	13.0	9.8	0.32
930	annular	110	22	13.0	9.5	0.35
940	annular	120	22	16.0	11.5	0.44
1410	annular	58	4	1.8	0.9	0.09
1420	annular	65	4	1.9	1.0	0.09

TABLE II

Comparison of Predicted and Experimental Pressure Drop for Upward Vertical Two-Phase Annular Flow (Air-Water System)

Run No.	Experimental Pressure Bottom (psia)	Predicted Pressure Bottom Ansari et al. (psia)	Percentage Error Ansari et al.	Predicted Pressure Bottom Yao and Sylvester (psia)	Percentage Error Yao and Sylvester (psia)
120	5.5	8.66	57.36	4.61	-16.27
121	4.7	6.7	42.65	3.35	-28.66
203	3.9	4.83	23.91	2.37	-39.18
210	4.5	7.28	61.81	3.51	-22.11
294	2.8	3.25	16.19	1.72	-38.52
300	3.6	5.38	49.42	2.5	-30.45
310	4.5	6.3	40.02	3.58	-20.51
410	5.8	6.19	6.67	4.43	-23.70
420	7.5	13.38	78.38	6.25	-16.66
520	8.5	15.58	83.26	7.15	-15.85
610	9	13.19	46.54	7.28	-19.16
612	9.5	12.25	28.97	7.46	-21.44
620	10.8	17.69	63.83	9.96	-7 80
721	10	13.16	31.56	8.16	-18.36
730	12	18.88	57.37	11.19	-6.75
740	13.2	21.87	65.65	12.11	-8.29
830	11.5	15	30.45	9.71	-15.6
840	14.6	21.23	45.43	13.13	-10.05
921	13	19.1	46.96	11.65	-10.36
930	13	21.63	66.38	12.56	-3.40
940	16	27.5	71.86	15.38	-3.89
1410	1.8	2.8	55.75	0.97	-46.06
1420	1.9	2.52	32.57	1.09	-42.57
Average Absolute % Error			47.96		20.25

TABLE III

Comparison of Predicted and Experimental Pressure Drop for Upward Vertical Two-Phase Slug Flow (Air-Water System)

Run No.	Experimental Pressure Bottom (psia)	Predicted Pressure Bottom Ansari et al. (psia)	Percentage Error Ansari et al.	Predicted Pressure Bottom Sylvester (psia)	Percentage Error Sylvester (psia)
40	4	4.04	0.94	4.43	10.72
50	3.1	2.94	-5.23	3.41	9.99
51	3.2	2.8	-12.43	3.3	3.07
52	3.1	2.7	-12.91	3.23	4.07
53	3.1	2.53	-18.46	3.1	-0.01
160	2.8	2.56	-8.55	2.95	5.19
161	2.8	2.36	-15.79	2.77	-0.96
162	2.8	2.14	-23.7	2.57	-8.15
250	2.5	2.13	-15.00	2.47	-1.23
251	2.4	2.03	-15.25	2.39	-0.48
350	3.4	2.93	-13.71	3.49	2.67
351	3.2	3	-6.14	3.56	11.26
352	3.3	2.83	-14.20	3.43	3.9
460	3.4	3.11	-5.30	3.77	10.97
550	2.8	3.22	30.77	3.77	34.52
560	4	3.66	-8.46	4.31	7.82
650	3.9	3.97	1.71	4.65	19.1
660	3.8	3.43	-9.84	4.34	14.14
770	3.3	3.57	8.27	4.25	28.83
Average Absolute % Error			11.93		9.32

and Sylvester (1987) predictions were better on average than the Ansari et al. (1994) predictions in the annular flow regime as seen in Table II. The maximum error in the predictions by Yao and Sylvester (1987) is obtained for two experimental runs (run no. 1410 and 1420) that were found to be in the slug flow regime according to the Barnea flow map even though they were visually observed to be in the annular flow regime. Since the two data points were found to be in the slug-annular transition boundary as predicted by Barnea (1987), they could actually lie in the transition zone or churn flow and not in annular or slug flow regimes. The error might have been lower if churn flow pressure drop equations were available and could have been used to estimate the pressure drop for run numbers 1410 and 1420. The Ansari et al. (1994) model was found to be consistently over predicting the pressure drop and the Yao and Sylvester (1987) was consistently under predicting the pressure drop for the air-water system.

The Ansari et al. (1994) predictions are comparable to the Sylvester (1987) predictions for the slug flow regime, however the Sylvester model is slightly better than the Ansari model on average. The Ansari et al. (1994) model was found to under predict the pressure drop for all but four of the slug flow cases. The four cases for which Ansari et al. (1994) over predicted were found to have the lowest gas-liquid ratio amongst all the cases considered. The pressure drop as given by Ansari et al. (1994) as well as the Sylvester (1987) models is a function of the liquid slug length which was empirically taken to be 30 times the pipe diameter. The constant 30 can be varied from 16 to 45 (Sylvester, 1987) to obtain better pressure drop estimates.

The experimental data of Golan (1970) contained information on the flow regime unlike gas well data where it is not possible to visually observe the flow regime. A

comparison of the experimental data of Golan (1970) with the flow map of Barnea (1987) validated the accuracy of the Barnea transition criteria. Figure 7 shows the Barnea transition boundaries for the air-water upward vertical two-phase flow system and also the experimental data. The experimental data in Figure 7 belong to either slug or annular flow regime and they fall into the respective flow regime zones (with two exceptions) as defined by Barnea in the flow map, thereby validating the accuracy of Barnea transition criteria. The Barnea transition boundaries are theoretical and any minor deviations of the experimental data points from these boundaries can be neglected. The two data points that were found to be close to the slug-annular transition boundary on the slug flow side, but were visually observed to be fully developed annular flow, could have actually been developing annular flow i.e transition or churn flow.

3.3 Analysis of Pressure Drop Predictions for Natural Gas Wells

The data from Camacho (1970) and Reinicke et al. (1987) cover a wide range of field conditions as shown in Table IV. The first 104 cases reported in Table IV were from Camacho (1970) and the remaining cases were taken from Reinicke et al. (1987). The input data contains information on the bottomhole temperature, bottomhole pressure, well head temperature, well head pressure, tubing diameter, well depth, gas and liquid flow rates at the well head, and gas gravity. The gas composition (Table V) was not given for any of the gas wells and hence was assumed arbitrarily based on a typical gas composition such that the calculated gas gravity matched the gas gravity data available in Table IV. The data taken from Reinicke et al. (1987) contain additional information on the angle of

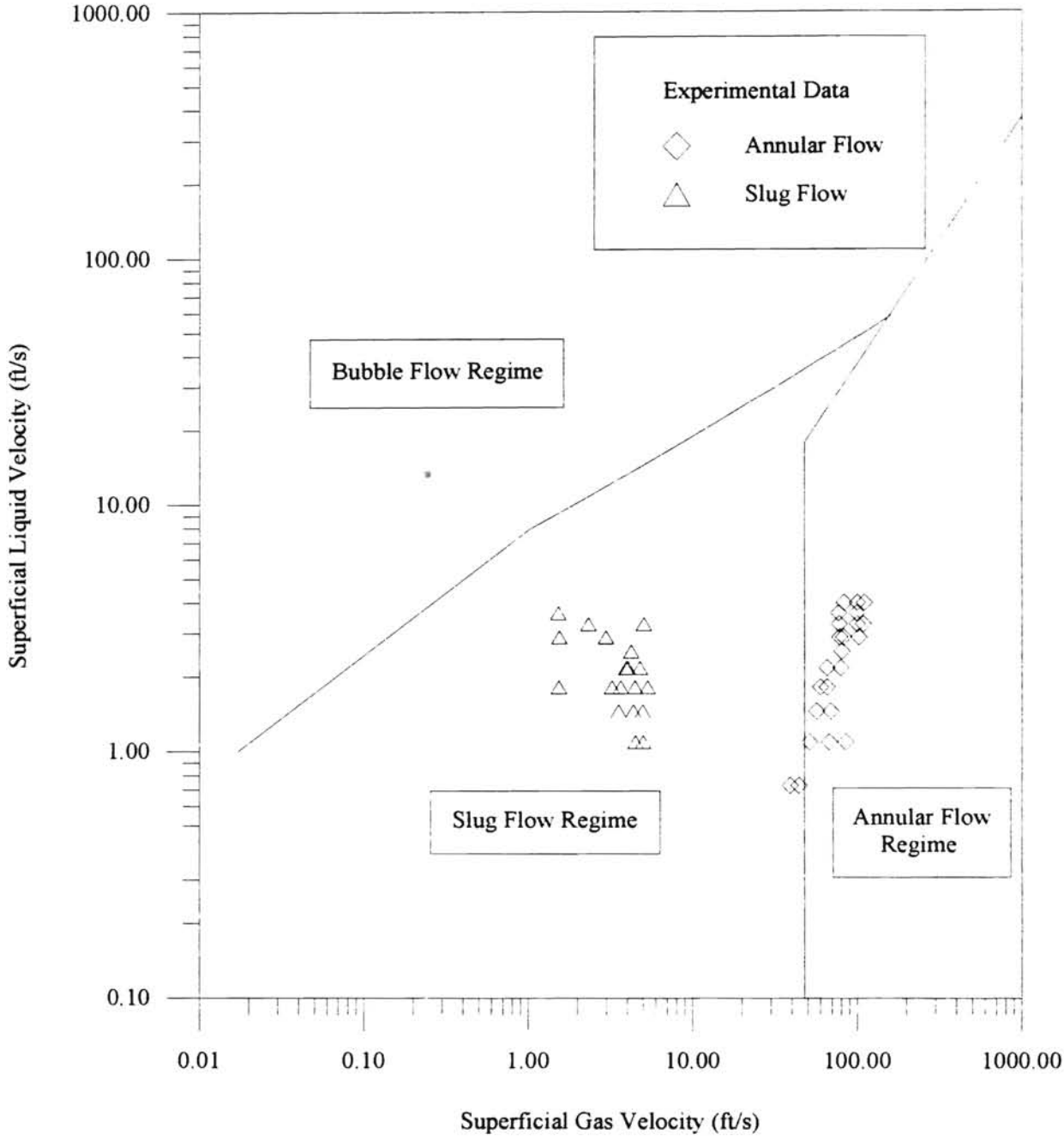

Figure 7

Flow Pattern Map: Experimental Versus Barnea's Predictions

TABLE IV

Downhole Pressure Drop Data for Water-Cut Gas Wells

Well No.	Pipe ID (in.)	Well Depth (ft.)	Gas Flow Rate MSCFD	Water Prodn. bbl/day	G/L scf/bbl	Surface Temp. °F	Bottom Temp. °F	Specific Gas Gravity	Surface Pressure (psia)	Bottom Pressure (psia)
1	1.995	2480	845	192	4400	102	130	0.65	125	340
2	1.995	2500	1416	312	4450	108	138	0.65	325	565
3	1.995	2500	653	144	4533	97	127	0.65	100	260
4	1.995	2500	368	75	4900	93	123	0.65	100	235
5	1.995	2500	613	144	5000	95	125	0.65	95	255
6	1.995	2500	1164	192	6060	100	128	0.65	150	385
7	1.995	2500	766	144	6370	95	125	0.65	100	270
8	1.995	8055	4907	736	6667	126	210	0.64	1699	3197
9	1.995	8055	4324	649	6667	125	210	0.64	1766	3215
10	1.995	8055	3506	526	6667	128	210	0.64	1848	3223
11	1.995	8055	2676	401	6667	121	210	0.64	1907	3229
12	1.995	2500	1049	144	7283	97	127	0.65	115	350
13	1.995	2500	888	144	7400	95	125	0.65	100	350
14	1.995	2500	1358	144	9433	97	127	0.65	115	385
15	1.995	8051	4818	385	12500	111	210	0.64	2097	3198
16	1.995	8051	4062	325	12500	115	210	0.64	2170	3203
17	1.995	8051	3173	254	12500	116	210	0.64	2213	3209
18	1.995	8051	2704	216	12500	119	210	0.64	2235	3213
19	1.995	8055	3688	240	15384	118	210	0.64	2592	3252
20	1.995	8055	4380	285	15384	120	210	0.64	2502	3245
21	1.995	8055	5026	327	15384	129	210	0.64	2313	3241
22	1.995	8055	6308	410	15384	131	210	0.64	2069	3231
23	1.995	8051	5085	183	27777	111	209	0.64	1687	3180

TABLE IV (cont'd)

Well No.	Pipe ID (in.)	Well Depth (ft.)	Gas Flow Rate MSCFD	Water Prodn. bbl/day	G/L scf/bbl	Surface Temp. °F	Bottom Temp. °F	Specific Gas Gravity	Surface Pressure (psia)	Bottom Pressure (psia)
24	1.995	8051	4294	155	27777	110	209	0.64	1913	3190
25	1.995	8051	3811	137	27777	112	209	0.64	2012	3195
26	1.995	8051	2179	78	27777	110	209	0.64	2450	3211
27	1.995	8758	1971	47	41666	102	212	0.64	2221	2924
28	1.995	8758	2473	59	41666	105	212	0.64	2195	2901
29	1.995	8758	2900	70	41666	107	212	0.64	2167	2883
30	1.995	8758	3956	95	41666	98	212	0.64	2080	2830
31	1.995	8051	4710	113	41666	114	205	0.64	2474	3234
32	1.995	8051	5774	139	41666	116	205	0.64	2300	3226
33	1.995	8051	7045	169	41666	114	205	0.64	1892	3215
34	1.995	8051	7288	175	41666	113	205	0.64	1839	3212
35	1.995	8758	1976	36	55555	94	218	0.64	2368	3005
36	1.995	8758	2935	53	55555	99	218	0.64	2314	2969
37	1.995	8758	3482	63	55555	100	218	0.64	2272	2943
38	1.995	8758	3982	72	55555	107	218	0.64	2220	2922
39	1.995	8758	1964	26	76920	104	218	0.64	2451	3120
40	1.995	8758	3003	39	76920	108	218	0.64	2408	3095
41	1.995	8758	3598	47	76920	112	218	0.64	2408	3074
42	1.995	8758	4057	53	76920	113	218	0.64	2379	3060
43	1.995	8051	1826	22	83333	107	208	0.64	2680	3254
44	1.995	8051	3405	41	83333	110	208	0.64	2627	3246
45	1.995	8051	5402	65	83333	114	208	0.64	2498	3232
46	1.995	8051	7400	89	83333	116	208	0.64	2311	3220

TABLE IV (cont'd)

Well No.	Pipe ID (in.)	Well Depth (ft.)	Gas Flow Rate MSCFD	Water Prodn. bbl/day	G/L scf/bbl	Surface Temp. °F	Bottom Temp. °F	Specific Gas Gravity	Surface Pressure (psia)	Bottom Pressure (psia)
47	1.985	7962	4096	934	4386	120	200	0.64	1610	3094
48	1.985	7962	4434	678	6536	120	200	0.64	1965	3105
49	1.985	8713	715	92	7813	100	214	0.64	975	1816
50	1.985	7962	4790	479	10000	120	200	0.64	2065	3112
51	1.985	8050	1782	134	13333	109	206	0.64	2230	3199
52	1.985	8050	2857	214	13333	115	206	0.64	2181	3174
53	1.985	8050	3458	259	13333	120	206	0.64	2165	3156
54	1.985	8050	4212	316	13333	122	206	0.64	2114	3133
55	1.985	7920	4429	266	16666	110	202	0.65	2498	3389
56	1.985	8033	1642	90	18181	104	200	0.64	2285	3218
57	1.985	8033	3094	170	18181	106	200	0.64	2197	3213
58	1.985	8033	3953	217	18181	108	200	0.64	2182	3211
59	1.985	8038	2949	147	20000	115	208	0.64	2262	3264
60	1.985	8038	4779	239	20000	119	208	0.64	2282	3259
61	1.985	8038	5970	298	20000	121	208	0.64	2214	3252
62	1.985	8038	7113	356	20000	120	208	0.64	2100	3244
63	1.985	7890	2924	117	25000	114	200	0.64	2403	3322
64	1.985	7890	5891	236	25000	116	200	0.64	2366	3307
65	1.985	7890	7594	304	25000	116	200	0.64	2245	3287
66	1.985	7890	8993	360	25000	119	200	0.64	2041	3274
67	1.985	8749	3922	106	37030	103	210	0.64	1976	2618
68	1.985	8749	4696	127	37030	106	210	0.64	1667	2495
69	1.985	8749	2408	65	37030	99	210	0.64	2152	2807

TABLE IV (cont'd)

Well No.	Pipe ID (in.)	Well Depth (ft.)	Gas Flow Rate MSCFD	Water Prodn. bbl/day	G/L scf/bbl	Surface Temp. °F	Bottom Temp. °F	Specific Gas Gravity	Surface Pressure (psia)	Bottom Pressure (psia)
70	1.985	8749	1809	49	37030	95	210	0.64	2241	2866
71	1.985	7962	4681	103	45454	116	200	0.64	2155	3118
72	1.985	8665	2500	55	45454	101	214	0.64	1035	1750
73	1.985	8616	2132	47	45454	100	214	0.64	1140	1786
74	1.985	8665	1477	32	45454	98	214	0.64	1323	1863
75	1.985	7920	1051	23	45454	95	214	0.64	1403	1911
76	1.985	8697	4498	90	50000	124	198	0.64	2711	3401
77	1.985	8697	2337	42	55555	96	214	0.64	1621	2239
78	1.985	8697	2042	37	55555	100	214	0.64	1686	2271
79	1.985	8697	710	31	55555	104	214	0.64	1745	2305
80	1.985	7962	1293	23	55555	104	214	0.64	1811	2339
81	1.985	8052	5111	77	66666	110	200	0.64	2155	3114
81	1.985	8052	5111	77	66666	110	200	0.64	2155	3114
82	2.441	8052	3222	116	27777	106	204	0.64	2429	3218
83	2.441	8052	4573	165	27777	115	204	0.64	2418	3211
84	2.441	8052	5587	201	27777	116	204	0.64	2403	3205
85	2.441	8042	6890	248	27777	120	204	0.64	2386	3197
86	2.441	8052	2792	87	32258	116	200	0.64	2520	3262
87	2.441	8052	3830	84	45454	100	208	0.64	2540	3188
88	2.441	8052	5692	125	45454	104	208	0.64	2508	3192
89	2.441	8052	7837	172	45454	115	208	0.64	2451	3179
90	2.441	8052	9754	215	45454	119	208	0.64	2383	3169
91	2.441	8052	4700	66	71428	74	200	0.64	2599	3237

TABLE IV (cont'd)

Well No.	Pipe ID (in.)	Well Depth (ft.)	Gas Flow Rate MSCFD	Water Prodn. bbl/day	G/L scf/bbl	Surface Temp. °F	Bottom Temp. °F	Specific Gas Gravity	Surface Pressure (psia)	Bottom Pressure (psia)
92	2.441	8052	6268	88	71428	79	200	0.64	2578	3230
93	2.441	8052	8389	117	71428	87	200	0.64	2512	3221
94	2.441	8052	10536	148	71428	97	200	0.64	2425	3207
95	2.992	8026	5270	985	5347	120	202	0.64	2140	3148
96	2.992	8026	4570	562	8130	120	202	0.64	2240	3146
97	2.992	8745	4731	435	10869	114	214	0.64	1095	1785
98	2.992	8745	3837	353	10869	120	214	0.64	1135	1805
99	2.992	8745	2948	271	10869	120	214	0.64	1180	1829
100	2.992	8745	2018	186	10869	120	214	0.64	1212	1856
101	2.992	8026	4602	221	20833	120	202	0.64	2505	3123
102	2.992	8745	7798	88	90909	94	214	0.64	1505	1945
103	2.992	8745	5088	56	90909	92	214	0.64	1615	1997
104	2.992	8745	3540	39	90909	89	214	0.64	1658	2021
105	3.98	5413	4860	8	597050	104	302	0.64	5205	6691
106	3.98	5413	9000	18	500000	122	293	0.64	3769	4930
107	3.98	14347	1710	12	142027	79	284	0.64	1779	2602
108	3.98	15079	13590	39	351000	135	288	0.64	5807	7442
109	2.99	15079	17730	45	394000	145	288	0.64	5321	6935
110	2.99	15079	22950	54	425000	163	288	0.64	4733	6315
111	3.98	15735	27000	54	497238	138	286	0.64	6115	8139
112	2.99	15735	17820	66	270000	131	286	0.64	6997	9030
113	2.99	15735	27360	64	427500	147	286	0.64	6784	8930
114	2.99	15735	36270	85	426706	178	286	0.64	6490	8805

TABLE IV (cont'd)

Well No.	Pipe ID (in.)	Well Depth (ft.)	Gas Flow Rate MSCFD	Water Prodn. bbl/day	G/L scf/bbl	Surface Temp. °F	Bottom Temp. °F	Specific Gas Gravity	Surface Pressure (psia)	Bottom Pressure (psia)
115	3.98	15988	21600	43	497238	131	297	0.64	7085	9000
116	2.99	15988	31860	59	540000	156	297	0.64	6953	8952
117	5.98	15988	37890	83	456506	172	297	0.64	6836	8917
118	5.98	15988	45180	76	594474	181	297	0.64	6630	8861
119	3.98	13891	8730	120	72750	190	315	0.64	3388	4564
120	2.99	13891	8550	105	81429	187	315	0.64	3425	4586
121	2.99	13891	14850	147	101020	212	315	0.64	3058	4145
122	2.99	13891	21150	230	91957	223	315	0.64	2234	3418
123	3.98	14006	13500	154	87662	147	284	0.64	5307	7159
124	2.99	14006	21600	246	87805	169	284	0.64	4601	6424
125	3.98	14347	1710	15	110465	77	284	0.64	1793	2631
126	2.44	14347	1710	20	87692	79	284	0.64	1617	2367
127	2.99	13766	2520	56	44840	72	288	0.64	1411	2427
128	2.36	13766	2700	60	45000	72	288	0.64	1448	2427
129	2.36	13766	2430	58	41897	72	288	0.64	1374	2381
130	2.36	13766	630	59	10678	59	288	0.64	1205	2928
131	2.36	13766	450	59	7627	34	288	0.64	1205	2928
132	2.36	13766	540	45	12000	59	288	0.64	1191	2822
133	3.98	14006	9000	377	23866	163	291	0.64	2426	3675
134	2.99	14006	9000	354	25424	162	291	0.64	2352	3455
135	2.99	14006	5400	271	19926	151	291	0.64	4116	5836
136	2.99	14006	5850	294	19898	151	291	0.64	4057	5954
137	2.99	14006	6300	289	21799	151	291	0.64	3822	5380

TABLE IV (cont'd)

Well No.	Pipe ID (in.)	Well Depth (ft.)	Gas Flow Rate MSCFD	Water Prodn. bbl/day	G/L scf/bbl	Surface Temp. °F	Bottom Temp. °F	Specific Gas Gravity	Surface Pressure (psia)	Bottom Pressure (psia)
138	2.99	14006	5400	247	21868	147	291	0.64	4043	5601
139	3.98	5413	2880	71	40563	93	284	0.64	1330	2536
140	3.98	9406	2520	76	33158	93	284	0.64	1617	2955

TABLE V

Assumed Gas Composition
(based on Specific Gas Gravity)

Components	Mole Percent
Methane	88.0
Ethane	5.0
Propane	3.0
I-Butane	2.0
N-Butane	0.5
Nitrogen	1.0
Carbondioxide	0.5

inclination and the liquid density which have not been listed in Table IV. The range of parameters is presented in Table VI.

As the gas flows from the bottomhole to the well head, the flow regime can change depending upon the flow conditions. Out of the 140 data sets considered, 114 cases were found to be in the slug or annular flow regime for more than half the well. A Statistical analysis have been made with these 114 cases (68 slug flow cases and 46 annular flow cases). Within each flow regime, the wells have been sub-divided into three different classes based on the gas-liquid ratios. The wells in each class have been further sub-divided based on the well diameter. The division of the wells into certain categories based on the gas-liquid ratio and the diameter is made to understand how each model performs under varying conditions.

3.4 Error Analysis for the Slug Flow Models

The predictions from the two slug flow models, Sylvester (1987) and Ansari et al. (1994), have been compared against the data reported in Table IV. The Sylvester (1987) model has been used by previous researchers (Robertson, 1988; Liu, 1991; Liu and High, 1993) involved in the Downhole Corrosion project at Oklahoma State University. The Ansari et al. (1994) model is a recent model that has been tested by Ansari and co-workers against some of the well known pressure drop correlations: modified Hagedorn and Brown (1964), Aziz et al. (1972), Duns and Ros (1963), Hasan and Kabir (1988, 1990), Beggs and Brill (1973) with Palmer correction (1975), Orkiszewski (1967) with the Trigia correction (1989), and Mukherjee and Brill (1985). Ansari and co-workers tested the Ansari et al. (1994) model against the Tulsa University Fluid Flow Projects Well

TABLE VI

Range of Parameters for the Gas Wells in this Study

	MIN.	MAX.
Well Depth, ft.	2480	15988
Diameter, in.	1.985	5.98
Gas, MSCFD	368	45180
Water, bbl/day	8	985
Gas/Liquid, scf/bbl	4386	597050
Surface Temperature, °F	34	223
Botttom Temperature, °F	123	315
Surface Pressure, psia	95	7085
Bottom Pressure, psia	235	9030
Specific Gas Gravity	0.64	0.65

data bank for wells producing oil, water and gas and found that the model of Ansari et al. (1994) gives better pressure drop predictions.

In this thesis, pressure drop prediction results from the models of Ansari et al. (1994) and Sylvester (1987) have been compared with field data from wells that produce only gas and water. The results of this comparison have been presented in Table VII. A graph of the percentage error as a function of the gas-liquid ratio is presented in Figure 8 and Figure 9. Figure 8 shows a wider scatter of the error for the Sylvester predictions than the Ansari predictions. For the Sylvester (1987) model, the average absolute error in the estimated bottomhole pressure was 15.7%, the percentage error in the predicted bottomhole pressure was found to vary between -31.9 % and 79.4 %, 62% of the predictions were within an error band of 15%, and a percentage error of 50% or more were encountered in 4 out of the 66 cases studied. For the Ansari et al. (1994) model, the average absolute error in the estimated bottomhole pressure was 11.3%, the percentage error in the predicted bottomhole pressure was found to vary between -31.1 % and 73.1 %, where out of the 66 cases studied 51 were predicted within 15% error, and only 2 cases were predicted with a percentage error of more than 50%.

Table VIII classifies all the slug flow cases on the basis of gas flow rates. The average absolute percentage error in the estimated bottomhole pressure for each range of gas flow rates is listed in Table VIII. The average absolute percentage error for the Ansari et al. (1994) model was 11.3 % while the average absolute percentage error for the Sylvester (1987) model was 15.7 %. The Ansari et al. (1994) model was found to perform better than the Sylvester (1987) model on average for all gas-liquid ratios.

TABLE VII

Predicted Pressure Drop for Upward Vertical Two-Phase Slug Flow Using Sylvester and Ansari et al. Models

Well Number	Bottom Pressure Observed (psia)	Sylvester			Ansari et al.		
		Calc. Press. (psia)	Deviation (psia)	% Error	Calc. Press. (psia)	Deviation (psia)	% Error
1	340.0	487.0	147.0	43.2	312.0	-28.0	-8.2
2	565.0	697.0	132.0	23.4	471.0	-94.0	-16.6
6	385.0	495.0	110.0	28.6	350.0	-35.0	-9.1
8	3197.0	3986.0	789.0	24.7	2503.0	-694.0	-21.7
9	3215.0	3723.0	508.0	15.8	2590.0	-625.0	-19.4
10	3223.0	3386.0	163.0	5.1	2698.0	-525.0	-16.3
11	3229.0	3112.0	-117.0	-3.6	2805.0	-424.0	-13.1
15	3198.0	3729.0	531.0	16.6	2845.0	-353.0	-11.0
16	3203.0	3502.0	299.0	9.3	2945.0	-258.0	-8.1
17	3209.0	3251.0	42.0	1.3	3023.0	-186.0	-5.8
18	3213.0	3148.0	-65.0	-2.0	3067.0	-146.0	-4.5
19	3252.0	3674.0	422.0	13.0	3442.0	190.0	5.8
20	3245.0	3809.0	564.0	17.4	3310.0	65.0	2.0
21	3241.0	3894.0	653.0	20.1	3053.0	-188.0	-5.8
22	3231.0	4265.0	1034.0	32.0	2733.0	-498.0	-15.4
23	3180.0	3238.0	58.0	1.8	2190.0	-990.0	-31.1
24	3190.0	3109.0	-81.0	-2.5	2494.0	-696.0	-21.8
25	3195.0	3034.0	-161.0	-5.0	2629.0	-566.0	-17.7
48	3105.0	3949.0	844.0	27.2	2875.0	-230.0	-7.4
49	1816.0	1698.0	-118.0	-6.5	1764.0	-52.0	-2.9
50	3112.0	3841.0	729.0	23.4	2852.0	-260.0	-8.4

TABLE VII (cont'd)

Well Number	Bottom Pressure Observed (psia)	Sylvester			Ansari et al.		
		Calc. Press. (psia)	Deviation (psia)	% Error	Calc. Press. (psia)	Deviation (psia)	% Error
52	3174.0	3120.0	-54.0	-1.7	2984.0	-190.0	-6.0
53	3156.0	3281.0	125.0	4.0	2935.0	-221.0	-7.0
54	3133.0	3503.0	370.0	11.8	2850.0	-283.0	-9.0
55	3389.0	3776.0	387.0	11.4	3294.0	-95.0	-2.8
57	3213.0	3099.0	-114.0	-3.5	2957.0	-256.0	-8.0
58	3211.0	3333.0	122.0	3.8	2906.0	-305.0	-9.5
59	3264.0	3104.0	-160.0	-4.9	3013.0	-251.0	-7.7
60	3259.0	3680.0	421.0	12.9	2982.0	-277.0	-8.5
61	3252.0	4094.0	842.0	25.9	2881.0	-371.0	-11.4
62	3244.0	4520.0	1276.0	39.3	2733.0	-511.0	-15.8
63	3322.0	3172.0	-150.0	-4.5	3159.0	-163.0	-4.9
64	3307.0	4042.0	735.0	22.2	3038.0	-269.0	-8.1
65	3287.0	4659.0	1372.0	41.7	2877.0	-410.0	-12.5
66	3274.0	5196.0	1922.0	58.7	2920.0	-354.0	-10.8
79	2305.0	2536.0	231.0	10.0	2821.0	516.0	22.4
84	3205.0	3241.0	36.0	1.1	3170.0	-35.0	-1.1
85	3197.0	3444.0	247.0	7.7	3086.0	-111.0	-3.5
95	3148.0	3243.0	95.0	3.0	3246.0	98.0	3.1
96	3146.0	3107.0	-39.0	-1.2	3263.0	117.0	3.7
97	1785.0	1805.0	20.0	1.1	1835.0	50.0	2.8
100	1856.0	1904.0	48.0	2.6	2047.0	191.0	10.3
105	6691.0	5745.0	-946.0	-14.1	6036.0	-655.0	-9.8

TABLE VII (cont'd)

Well Number	Bottom Pressure Observed (psia)	Sylvester			Ansari et al.		
		Calc. Press. (psia)	Deviation (psia)	% Error	Calc. Press. (psia)	Deviation (psia)	% Error
106	4930.0	4116.0	-814.0	-16.5	4313.0	-617.0	-12.5
107	2602.0	3924.0	1322.0	50.8	4503.0	1901.0	73.1
109	6935.0	7367.0	432.0	6.2	7084.0	149.0	2.1
110	6315.0	7822.0	1507.0	23.9	6389.0	74.0	1.2
111	8139.0	7534.0	-605.0	-7.4	8180.0	41.0	0.5
119	4564.0	4258.0	-306.0	-6.7	4909.0	345.0	7.6
120	4586.0	4513.0	-73.0	-1.6	4722.0	136.0	3.0
121	4145.0	5171.0	1026.0	24.8	4095.0	-50.0	-1.2
122	3418.0	6131.0	2713.0	79.4	3484.0	66.0	1.9
123	7159.0	6268.0	-891.0	-12.4	7221.0	62.0	0.9
124	6424.0	7557.0	1133.0	17.6	6059.0	-365.0	-5.7
125	2631.0	3961.0	1330.0	50.6	4543.0	1912.0	72.7
127	2427 0	2290.0	-137.0	-5.6	2662.0	235.0	9.7
130	2928.0	2891.0	-37.0	-1.3	3310.0	382.0	13.0
131	2928.0	3552.0	624.0	21.3	3971.0	1043 0	35.6
132	2822.0	3027.0	205.0	7.3	3448.0	626.0	22.2
136	5954.0	5345.0	-609.0	-10.2	6626.0	672.0	11.3
139	2536.0	1726.0	-810.0	-31.9	1836.0	-700.0	-27.6
140	2955.0	2552.0	-403.0	-13.6	2854.0	-101.0	-3.4
112	9030.0	9004.0	-26.0	-0.3	9228.0	198.0	2.2
113	8930.0	10564.0	1634.0	18.3	8835.0	-95.0	-1.1
115	9000.0	8314.0	-686.0	-7.6	9428.0	428.0	4.8

TABLE VII (cont'd)

Well Number	Bottom Pressure Observed (psia)	Sylvester			Ansari et al.		
		Calc. Press. (psia)	Deviation (psia)	% Error	Calc. Press. (psia)	Deviation (psia)	% Error
118	8861.0	7927.0	-934.0	-10.5	8682.0	-179.0	-2.0

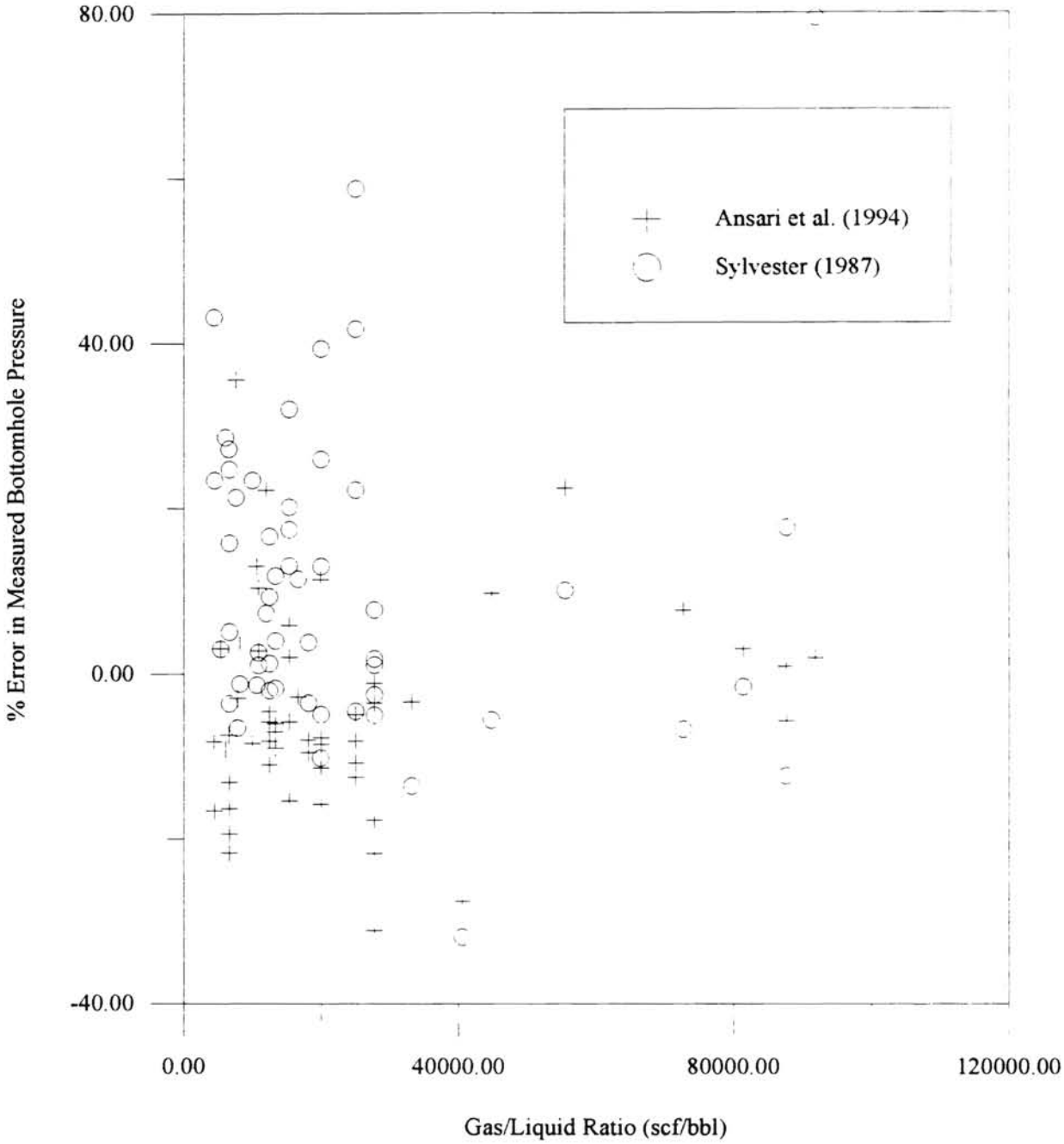

Figure 8

% Error in Measured Bottomhole Pressure as a Function of Gas-Liquid Ratio for the Models of Sylvester and Ansari et al. in the Slug Flow Regime (G/L < 100,000 scf/bbl)

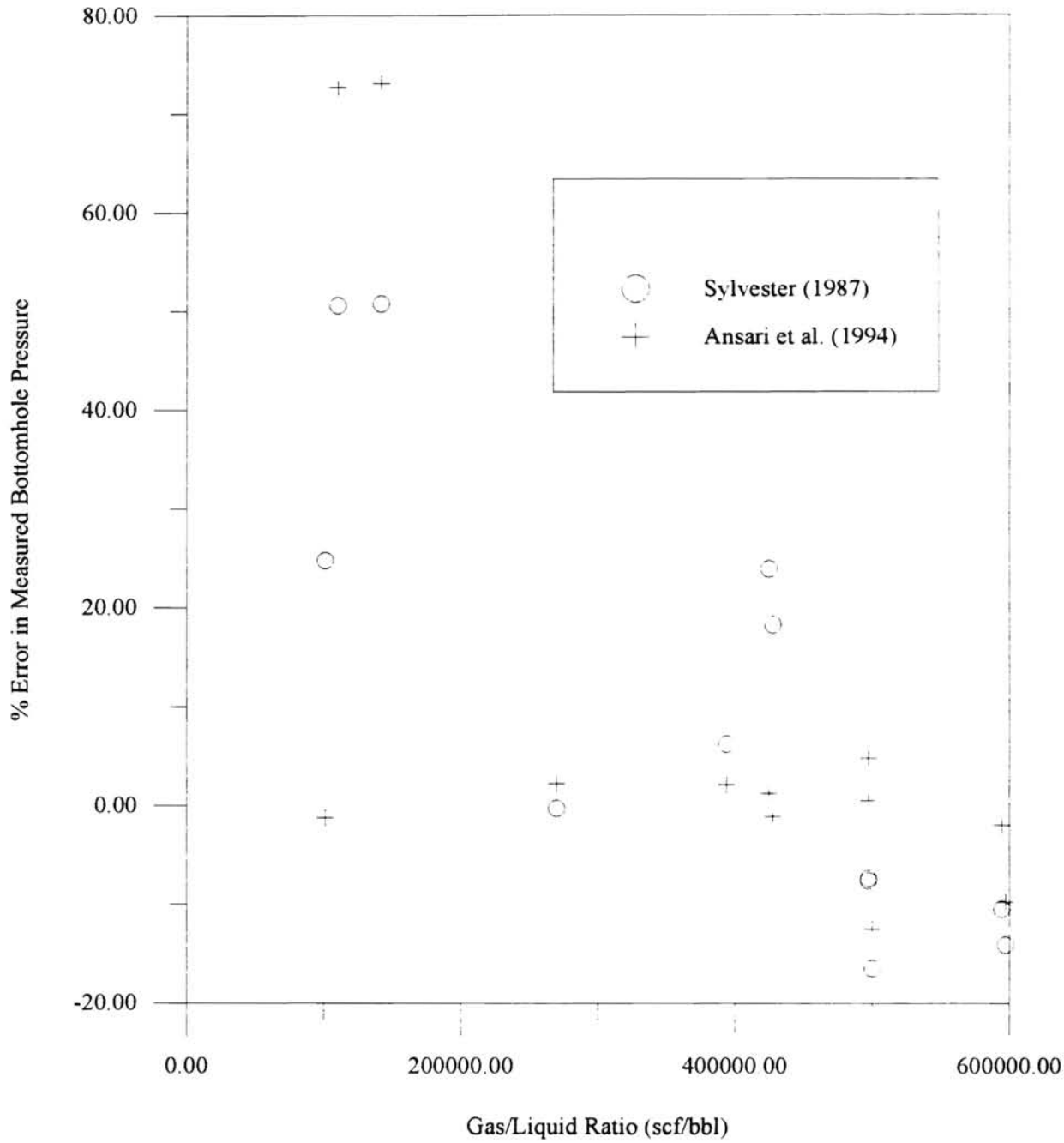

Figure 9

% Error in Measured Bottomhole Pressure as a Function of Gas-Liquid Ratio for the Models of Sylvester and Ansari et al. in the Slug Flow Regime (G/L > 100,000 scf/bbl)

TABLE VIII

Average Absolute % Error in Estimated Bottomhole Pressure: Slug Flow

	No. of Testcases	Sylvester (Avg. Abs. % Error)	Ansari et al. (Avg. Abs. % Error)
All Cases	66	15.7	11.3
G/L<=10000 scf/bbl	13	17.5	12.7
10000<G/L<=100000 scf/bbl	41	14.1	9.7
G/L>100000 scf/bbl	12	19.3	15.3

Tables IX, X and XI classify wells belonging to each range of gas flow rate on the basis of the pipe internal diameter and give the average absolute error in each category. Table IX classifies low (G/L <= 10,000 scf/bbl) gas-liquid ratio wells on the basis of the well diameter. Ansari et al. (1994) was found to perform better than the Sylvester (1987) model on average for smaller diameters at a low gas-liquid ratio. The Sylvester (1987) model was found to perform better than the Ansari et al. (1994) model on average for larger diameters but the sample of wells belonging to high diameters is very low that the result might not have any significance.

Table X classifies medium (10,000 scf/bbl < G/L <= 100,000 scf/bbl) gas-liquid ratio wells on the basis of well diameter. The Ansari et al. (1994) model was found to perform better than or comparable to the Sylvester (1987) model on average for all diameters except one (2.36 in ID). Since the sample space for wells with a 2.36 in. diameter and medium gas-liquid ratio consists of just two wells, the average absolute error might not have any significance.

Table XI classifies high (G/L > 100,000 scf/bbl) gas-liquid ratio wells on the basis of well diameter. The Ansari et al. (1994) model was found to give better or comparable pressure drop predictions on average for the different diameters.

3.5 Error Analysis for the Annular Flow Models

The models evaluated for their ability to accurately predict pressure drops in annular flow are the Yao and Sylvester (1987) model and the Ansari et al. (1994) model. The Yao and Sylvester model was used by the previous downhole corrosion researchers at

TABLE IX

Average Absolute % Error in Estimated Bottomhole Pressure For Each Category of Pipe Diameter: Slug Flow (G/L <= 10000 scf/bbl)

Diameter (in.)	No. of Testcases	Sylvester (Avg. Abs. % Error)	Ansari et al. (Avg. Abs. % Error)
1.985	3	19.0	6.2
1.995	7	20.6	14.9
2.360	1	21.3	35.6
2.992	2	2.1	3.4

TABLE X

Average Absolute % Error in Estimated Bottomhole Pressure For Each Category of Pipe Diameter: Slug Flow (10000 < G/L <= 100000 scf/bbl)

Diameter (in.)	No. of Testcases	Sylvester (Avg. Abs. % Error)	Ansari et al. (Avg. Abs. % Error)
1.985	15	17.1	9.6
1.995	11	11.0	11.7
2.360	2	4.3	17.6
2.441	2	4.4	2.3
2.992	7	16.9	6.4
3.980	4	16.2	9.9

TABLE XI

Average Absolute % Error in Estimated Bottomhole Pressure For Each Category of Pipe Diameter: Slug Flow (G/L > 100000 scf/bbl)

Diameter (in.)	No. of Testcases	Sylvester (Avg. Abs. % Error)	Ansari et al. (Avg. Abs. % Error)
2.992	5	14.7	1.6
3.980	6	24.5	28.9
5.980	1	10.5	2.0

Oklahoma State University (Robertson, 1988; Liu and Erbar, 1990; Liu, 1991; Liu and High, 1993). As mentioned in the previous section, the Ansari et al. (1994) model is a comprehensive model that was found to give good pressure drop predictions by Ansari and co-workers in all the flow regimes and hence has been used in this study.

The results of the comparison between the performance of the Yao and Sylvester model and the Ansari et al. model to accurately predict pressure drop are presented in Table XII. Figure 10 shows the distribution of percentage error with the gas-liquid ratio The predictions by Ansari show a wider scatter than the Sylvester predictions. For the Yao and Sylvester (1987) model, the average absolute error in the estimated bottomhole pressure was found to be 8.7%, the percentage error of the predicted bottomhole pressure was found to vary from -39.1 % to 15.4 %, and 85 % of the cases studied were found to have error less than 15%. For the Ansari et al. (1994) model, the average absolute error in the estimated bottomhole pressure was found to be 34.7%, the predicted bottomhole pressure was found to deviate from estimated values by -13.9 % to 124.6 %, and nearly 42% of the predictions were within 15% of the measured values.

Table XIII gives information on the average absolute percentage error for the annular cases averaged over all the cases within a certain range of gas flow rate. The average absolute percentage error for the Yao and Sylvester (1987) predictions was found to be 8.7 % while the average absolute percentage error for the Ansari et al. (1994) model was found to be 34.7 %. The Yao and Sylvester (1987) predictions were found to be comparable to the predictions of Ansari et al. (1994) on average for gas-liquid ratio less than 10,000 scf/bbl. At higher gas-liquid ratios (G/L > 10,000 scf/bbl), the Yao and

TABLE XII

Predicted Pressure Drop for Upward Vertical Two-Phase Annular Flow Using Yao and Sylvester, and Ansari et al. Models

Well No.	Bottom Pressure Observed (psia)	Yao and Sylvester			Ansari et al.		
		Calc. Pressure (psia)	Deviation (psia)	% Error	Calc. Pressure (psia)	Deviation (psia)	% Error
3	260.0	174.0	-86.0	-33.1	465.0	205.0	78.8
5	255.0	164.0	-91.0	-35.7	471.0	216.0	84.7
12	350.0	248.0	-102.0	-29.1	349.0	-1.0	-0.3
13	350.0	213.0	-137.0	-39.1	339.0	-11.0	-3 1
14	385.0	300.0	-85.0	-22.1	392.0	7.0	1.8
26	3211.0	3057.0	-154.0	-4.8	4552.0	1341.0	41.8
27	2924.0	2814.0	-110.0	-3.8	4578.0	1654.0	56.6
28	2901.0	2839.0	-62.0	-2.1	4142.0	1241.0	42.8
29	2883.0	2865.0	-18.0	-0.6	3785.0	902.0	31.3
30	2830.0	2946.0	116.0	4.1	3016.0	186.0	6.6
31	3234.0	3435.0	201.0	6.2	3475.0	241.0	7.5
32	3226.0	3586.0	360.0	11.2	3111.0	-115.0	-3.6
33	3215.0	3666.0	451.0	14.0	2789.0	-426.0	-13.3
34	3212.0	3706.0	494.0	15.4	2765.0	-447.0	-13.9
35	3005.0	2983.0	-22.0	-0.7	4735.0	1730.0	57.6
36	2969.0	3023.0	54.0	1.8	3977.0	1008.0	34.0
37	2943.0	3050.0	107.0	3.6	3200.0	257.0	8.7
40	3095.0	3117.0	22.0	0.7	4065.0	970.0	31.3
42	3060.0	3222.0	162.0	5.3	3098.0	38.0	1.2
44	3246.0	3347.0	101.0	3.1	3847.0	601.0	18.5
45	3232.0	3472.0	240.0	7.4	3304.0	72.0	2.2

TABLE XII (cont'd)

Well No.	Bottom Pressure Observed (psia)	Yao and Sylvester			Ansari et al.		
		Calc. Pressure (psia)	Deviation (psia)	% Error	Calc. Pressure (psia)	Deviation (psia)	% Error
46	3220.0	3633.0	413.0	12.8	3365.0	145.0	4.5
56	3218.0	2828.0	-390.0	-12.1	4235.0	1017.0	31.6
67	2618.0	2913.0	295.0	11.3	2856.0	238.0	9 1
69	2807.0	2795.0	-12.0	-0.4	4170.0	1363.0	48.6
72	1750.0	1548.0	-202.0	-11.5	1656.0	-94.0	-5.4
73	1786.0	1584.0	-202.0	-11.3	2636.0	850.0	47.6
74	1863.0	1696.0	-167.0	-9.0	3750.0	1887.0	101.3
75	1911.0	1948.0	37.0	1.9	4255.0	2344.0	122.7
76	3401.0	3610.0	209.0	6.1	3681.0	280.0	8.2
77	2239.0	2151.0	-88.0	-3.9	3405.0	1166.0	52.1
78	2271.0	2186.0	-85.0	-3.7	3769.0	1498.0	66.0
81	3114.0	3099.0	-15.0	-0.5	2911.0	-203.0	-6.5
82	3218.0	3016.0	-202.0	-6.3	4714.0	1496.0	46.5
83	3211.0	3111.0	-100.0	-3.1	3779.0	568.0	17 7
86	3262.0	3087.0	-175.0	-5.4	4971.0	1709.0	52 4
87	3188.0	3166.0	-22.0	-0.7	4545.0	1357.0	42.6
88	3192.0	3257.0	65.0	2.0	3740.0	548.0	17.2
90	3169.0	3524.0	355.0	11.2	3259.0	90.0	2.8
91	3237 0	3274.0	37.0	1.1	4456.0	1219.0	37 7
93	3221.0	3461.0	240.0	7 5	3294.0	73.0	2.3
94	3207.0	3576.0	369.0	11.5	3340.0	133.0	4 1
101	3123.0	3077.0	-46.0	-1.5	4920.0	1797.0	57 5
104	2021.0	2174.0	153.0	7.6	4521.0	2500.0	123 7
129	2381.0	2049.0	-332.0	-13.9	5348.0	2967.0	124.6

TABLE XII (cont'd)

Well No.	Bottom Pressure Observed (psia)	Yao and Sylvester			Ansari et al.		
		Calc. Pressure (psia)	Deviation (psia)	% Error	Calc. Pressure (psia)	Deviation (psia)	% Error
133	3675.0	3324.0	-351.0	-9.6	6646.0	2971.0	80.8
134	3455.0	3706.0	251.0	7.3	3897.0	442.0	12.8
138	5601.0	5360.0	-241.0	-4.3	8343.0	2742.0	49.0

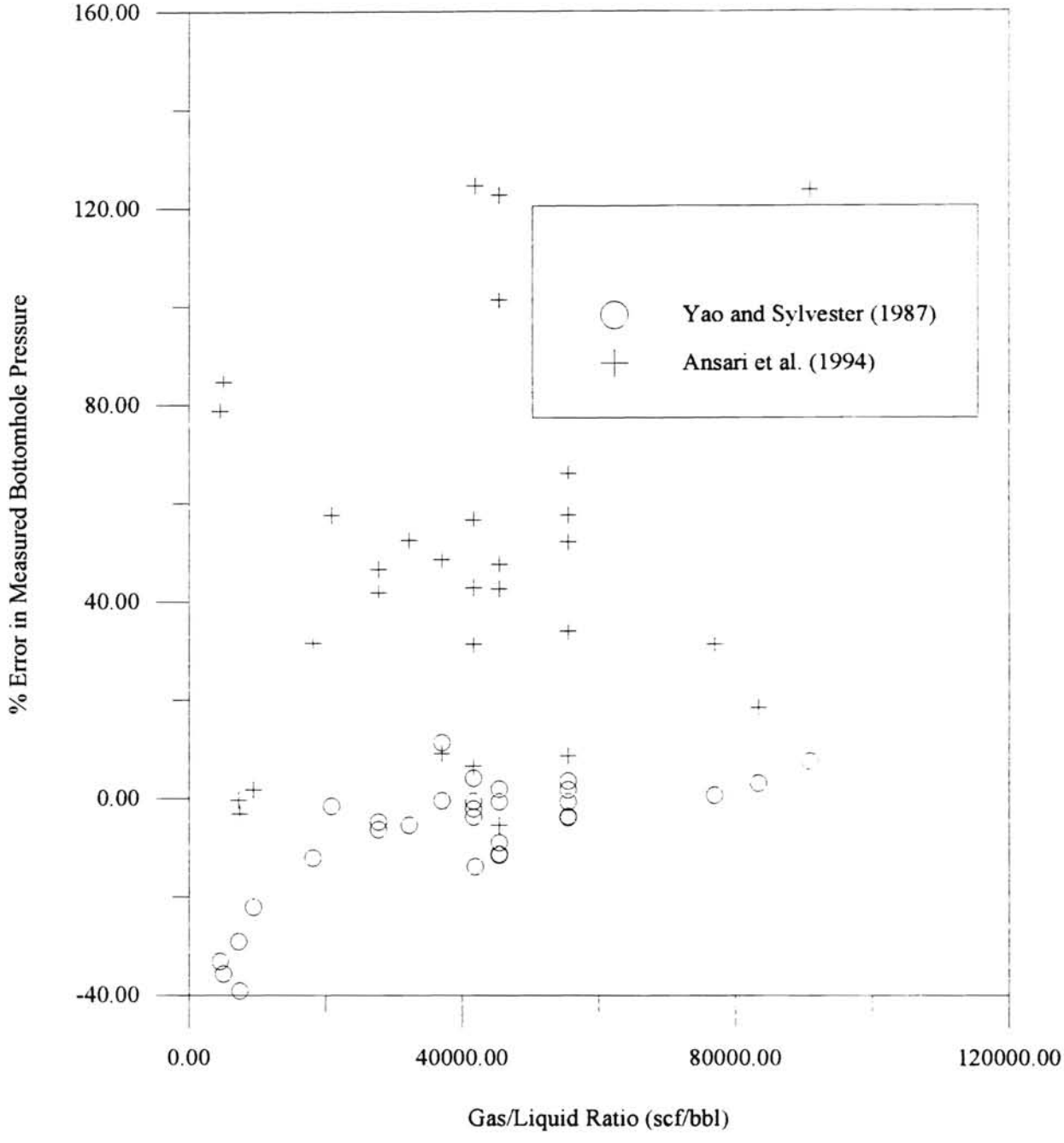

Figure 10

% Error in Measured Bottomhole Pressure as a Function of Gas-Liquid Ratio for the Models of Yao and Sylvester and Ansari et al. in the Annular Flow Regime

TABLE XIII

Average Absolute % Error in Estimated Bottomhole Pressure: Annular Flow

	No. of Testcases	Yao and Sylvester (Avg. Abs. % Error)	Ansari et al. (Avg. Abs. % Error)
All Cases	48	8.7	34.7
G/L<=10000 scf/bbl	5	31.8	33.8
10000<G/L<=100000 scf/bbl	43	6.1	35.9

Sylvester (1987) model performed significantly better than the Ansari et al. (1994) predictions on average.

Table XIV shows that all the wells that have a gas-liquid ratio of less than 10,000 scf/bbl have the same well diameter. The average absolute percentage errors are comparable for both the Yao and Sylvester (1987) as well as the Ansari et al. (1994) model for these wells, with a low gas-liquid ratio, as already mentioned in the previous section.

Table XV classifies the wells with a gas-liquid ratio greater than 10,000 scf/bbl on the basis of the well diameters and gives the average absolute percent error for each class of wells. The Yao and Sylvester (1987) model was found to perform better on average than the Ansari et al. (1994) model irrespective of the well diameter.

The Yao and Sylvester model was found to give better annular flow pressure drop predictions than the Ansari model for all gas-liquid ratios. Most of the bottomhole pressures predicted by the Yao and Sylvester model were found to be within an error of 15%. Since the Yao and Sylvester model gives better pressure drop predictions irrespective of the gas-liquid ratios, it should be used to predict pressure drops in the annular flow regime.

3.6 Evaluation of DREAM:

Based on the results of the research performed on the Ansari et al. model and the Yao and Sylvester model, it has been decided to implement both of these models in the OSU downhole corrosion package, DREAM. The Yao and Sylvester model was implemented to predict the pressure drop in the annular flow regime, and the Ansari et al.

TABLE XIV

Average Absolute % Error in Estimated Bottomhole Pressure For Each Category of Pipe Diameter: Annular Flow (G/L <= 10000 scf/bbl)

Diameter (in.)	No. of Testcases	Yao and Sylvester (Avg. Abs. % Error)	Ansari et al. (Avg. Abs. % Error)
1.995	5	31.8	33.8

TABLE XV

Average Absolute % Error in Estimated Bottomhole Pressure For Each Category of Pipe Diameter: Annular Flow (G/L > 10000 scf/bbl)

Diameter (in.)	No. of Testcases	Yao and Sylvester (Avg. Abs. % Error)	Ansari et al. (Avg. Abs. % Error)
1.985	11	6.5	45.4
1.995	17	5.8	22.0
2.360	1	13.9	124.6
2.441	9	5.4	24.8
2.990	4	5.2	60.7
3.980	1	9.6	80.8

model was implemented to predict the slug flow pressure drops. In addition, the modified flow regime map of Barnea (1987) is used to identify the flow regime given the gas and liquid flow rates.

Three sample case studies were used to evaluate the impact of the modifications made to the pressure drop predictions on the corrosion rate. The three cases considered have high, medium and low corrosion rates. The input data for the three cases are presented in Tables XVI, XVII and XVIII. The corrosion profiles for the three cases along the well depth are shown in Figures 11, 12, and 13 respectively. The pressure drop models do not have a significant impact on the corrosion rates. A first glance at Figure 13 gives the impression that the change in corrosion rates for Case III is significant compared to Case I and Case II (see Figure 11 and 12). However, the ordinate in Figure 13 is an order of magnitude smaller than the ordinate in Figures 11 and 12. The corrosion profiles obtained using the old pressure drop models (Yao and Sylvester, 1987; Sylvester, 1987) as well as the new (Ansari et al., 1994) model do not significantly differ.

The accuracy in the corrosion rate calculations was thought to be a strong function of the accuracy in the pressure drop calculations. The results in Figures 11, 12 and 13 indicate that the corrosion rate is not affected significantly by improving the accuracy in pressure drop predictions.

In this work, the accuracy of the pressure drop models have been established. Even though the new pressure drop models have not significantly affected the corrosion rates, this work has been successful in getting closer to the primary objective of the overall corrosion project: accuracy in every component of the corrosion prediction model. Moreover, the pressure drop subroutines could be used independently to estimate the

TABLE XVI

Well Geometry and Production Data

	Case I	Case II	Case III
ID, in.	2.441	2.441	2.441
Well Depth, ft.	9700	9450	9620
Water Production, bbl/day	28	27	124
Gas Production, MSCFD	2150	1352	2800
Wellhead Temperature, °F	130	130	130
Bottomhole Temperature, °F	290	290	290
Wellhead Pressure, psia	1890	1440	1270
Bottomhole Pressure, psia	4000	4000	4000

TABLE XVII

Gas Analysis (mole %)

	Case I	Case II	Case III
Methane	90.94	91.60	90.10
Ethane	4.37	4.39	6.00
Propane	1.14	1.18	1.68
I-Butane	0.27	0.33	0.45
N-Butane	0.23	0.25	0.34
I-Pentane	0.13	0.14	0.20
N-Pentane	0.08	0.09	0.12
Hexane	0.11	0.13	0.18
Heptane Plus	0.27	0.33	0.40
Nitrogen	0.25	0.30	0.22
Carbon dioxide	2.21	1.26	0.31
Hydrogen Sulphide	0.00	0.00	0.00

TABLE XVIII

Water Analysis (ppm)

	Case I	Case II	Case III
Sodium	6490	6280	127
Calcium	298	454	21
Magnesium	38	50	0
Barium	4	2	3
Strontium	0	0	0
Potassium	0	0	0
Iron	36	0	0
Chloride	10100	10300	195
Sulphate	111	196	0
Carbonate	0	0	0
Bicarbonate	879	313	60

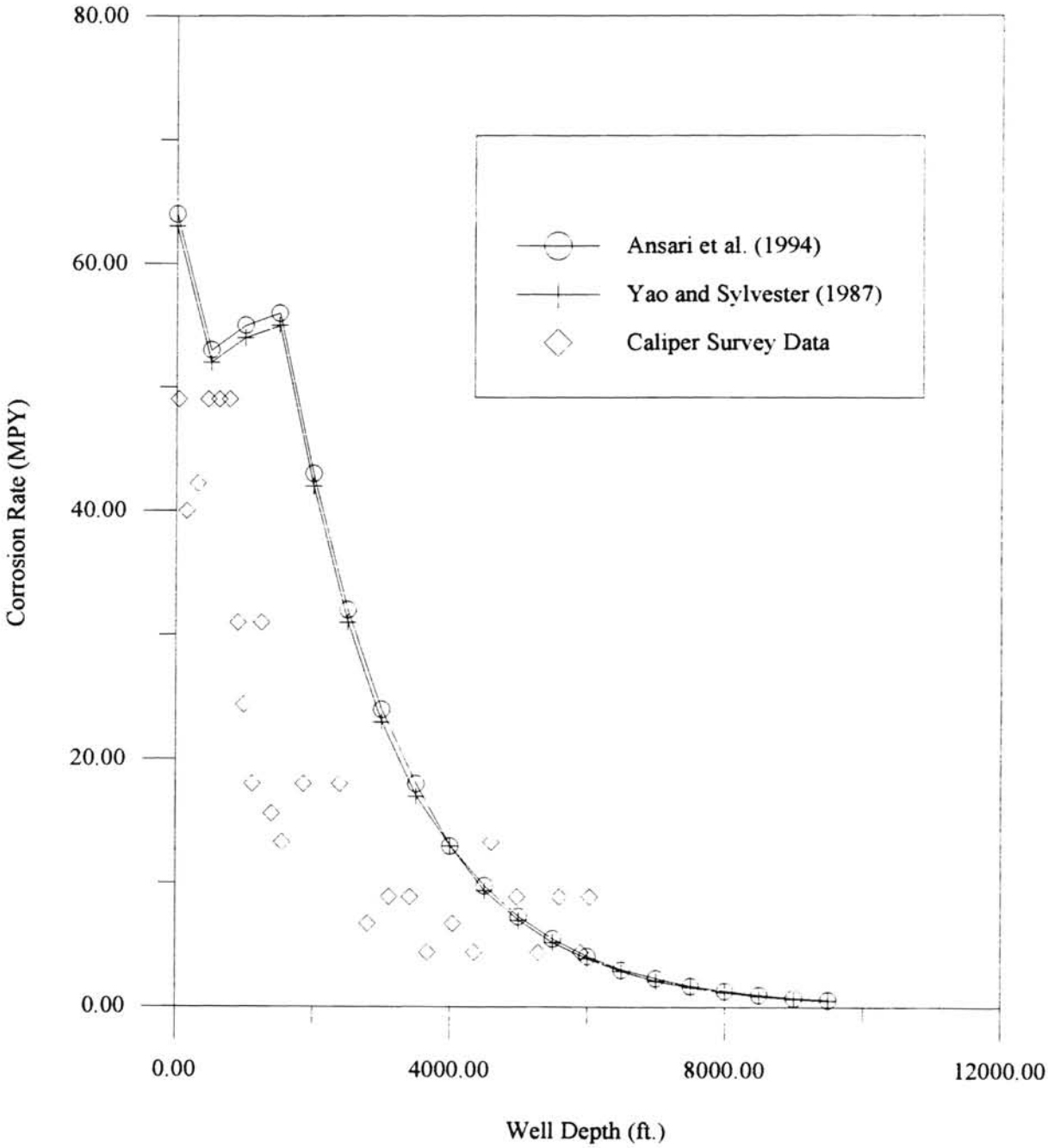

Figure 11

Corrosion Profile Along Well Depth: Case I

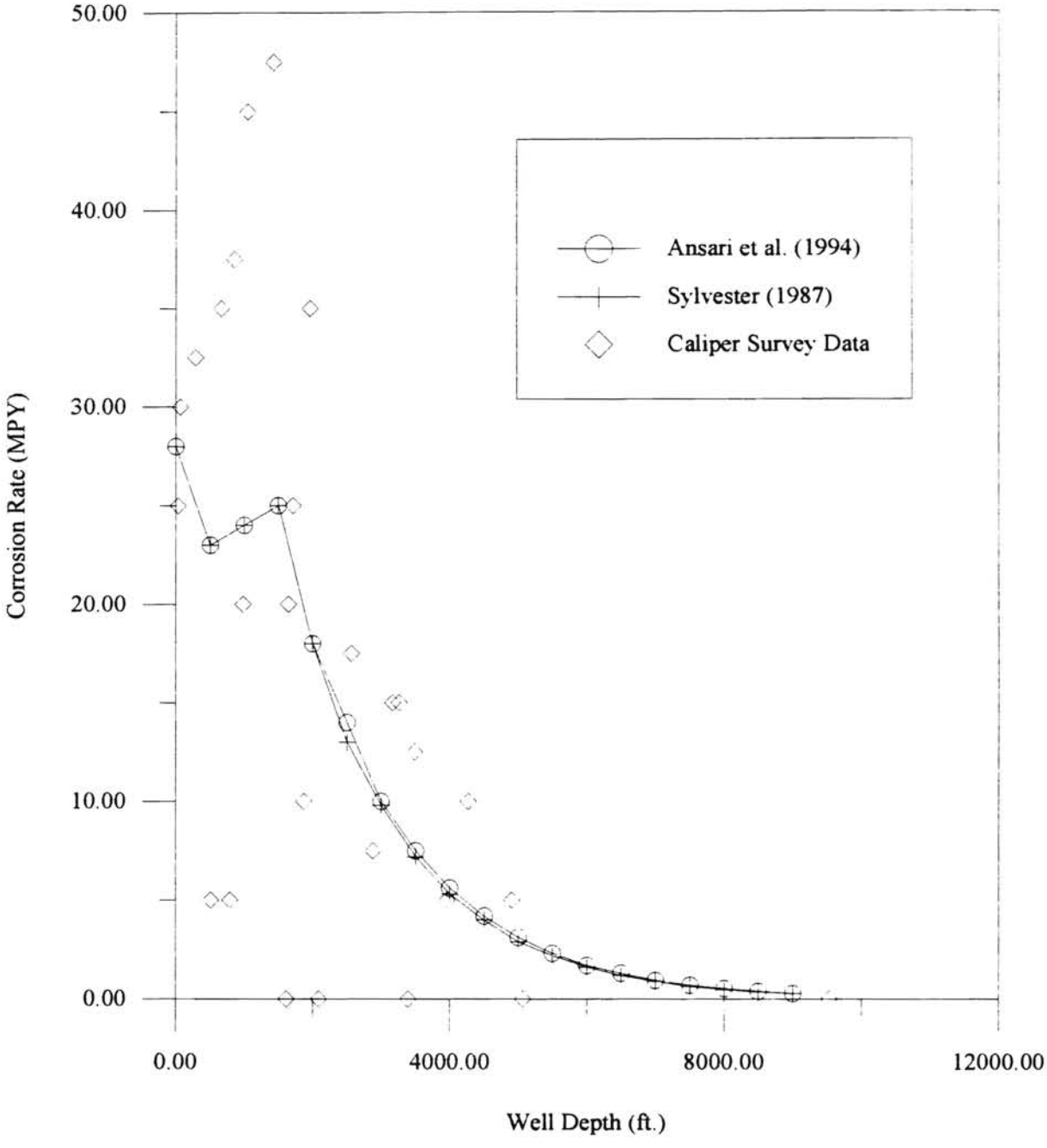

Figure 12

Corrosion Profile Along Well Depth: Case II

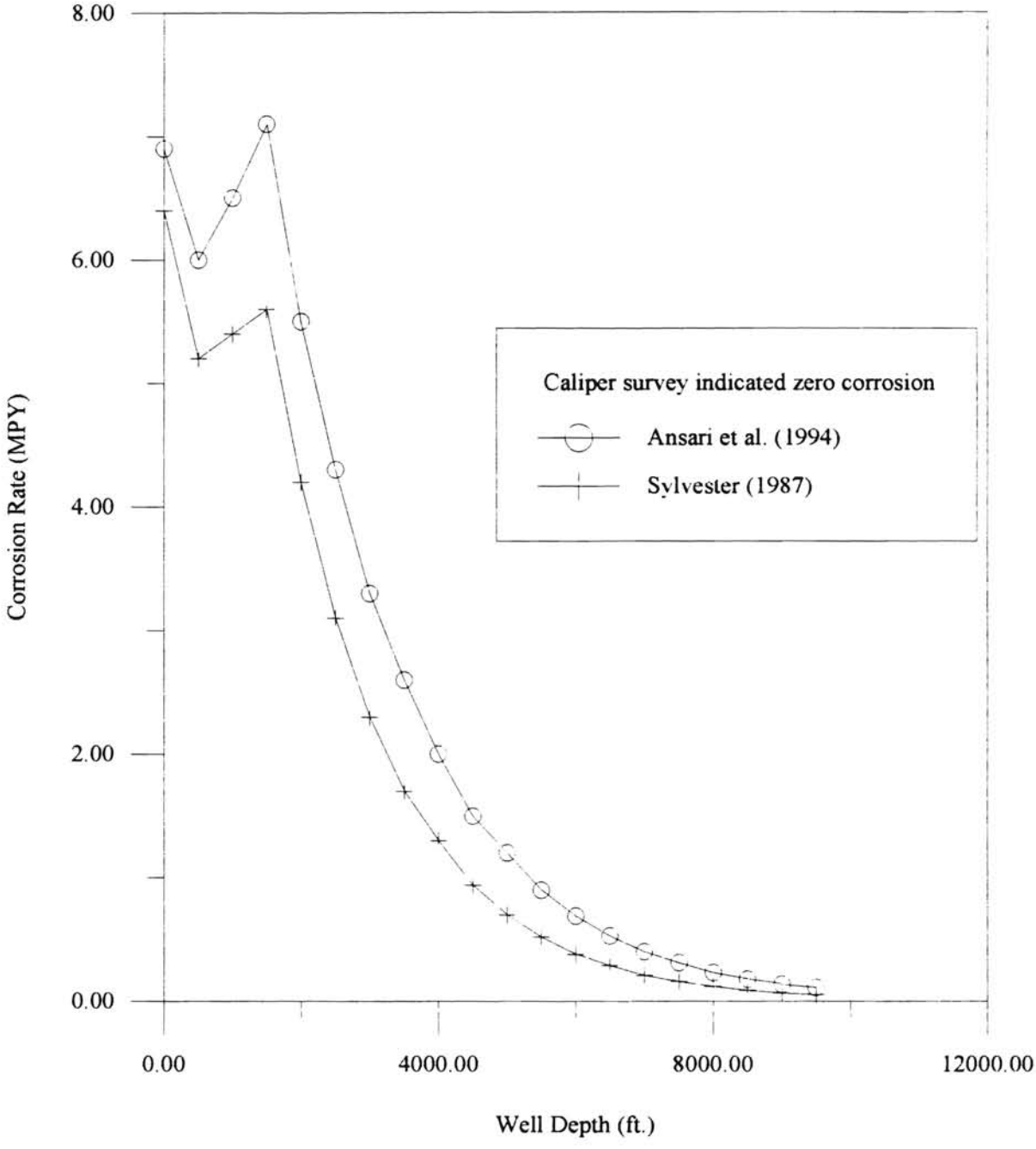

Figure 13

Corrosion Profile Along Well Depth: Case III

pressure drop in upward vertical two-phase flow wells. The pressure drop subroutines developed for this work could also be incorporated into other industrial applications that require the estimation of pressure drop for upward vertical two-phase flow systems.

Chapter IV

CONCLUSIONS AND RECOMMENDATIONS

4.1 Conclusions:

The following conclusions can be made based on this study:

1. The Ansari et al. (1994) model performs better than the Sylvester (1987) model in the slug flow regime for all gas-liquid ratios.
2. In the annular flow regime, the Yao and Sylvester (1987) model gives better results than the Ansari et al. (1994) model for all gas-liquid ratios.
3. The effect of pressure drop models on corrosion rates for the three cases studied is not significant.

4.2 Recommendations:

This study can be extended in the following directions:

1. Well defined pressure drop equations are not available for the transition (or churn flow) zone between the slug and annular flow. In this thesis work, the slug flow pressure drop equations were used to predict pressure drop in the transition zone too. If a pressure drop equation characterizing the transition zone is available, the accuracy in pressure drop estimation might improve. Since theoretical modeling of the transition zone might be difficult, an empirical correlation to predict pressure drop in the transition zone could be developed based on experiments made in the transition zone.

The empirical equation maybe based on the dimensionless parameters used by Duns and Ros (1963).

2. The pressure drop models should be tested for oil-gas systems to extend their applicability to oil wells. Oil-water-gas data can be taken from Govier and Fogarassi (1975). These data are also listed in Tables I through III in Peffer et al. (1988).
3. A parametric study can be made to evaluate the effect of various parameters on the corrosion rate. The results of this parametric study will give a clear picture of the factors that affect corrosion rate. Subsequently, those parameters that affect the corrosion rate can be studied in detail to improve the accuracy of the corrosion rate predictions.
4. The effect of the empirical constant that correlates the length of liquid slug to the pipe diameter in the Sylvester (1987) and the Ansari et al. (1994) model on the slug flow pressure drop can be studied. The empirical constant 'k' can be varied to obtain accurate pressure drop results.

REFERENCES

Ansari, A. M., Sylvester, N. D., Sarica, C., Shoham, O., and Brill, J. P., "A Comprehensive Mechanistic Model for Upward Two-Phase Flow in Wellbores," SPE Production and Facilities, p. 143, 1994.

Aziz, K., Govier, G. W., and Fogarasi, M., "Pressure Drops in Wells Producing Oil and Gas," Journal of Canadian Petroleum Technology, p. 38, 1972.

Barnea, D., "A Unified Model for Predicting Flow-Pattern Transition for the Whole Range of Pipe Inclinations," International Journal of Multiphase Flow, 13, p. 1, 1987.

Barnea, D., Shoham, O., and Taitel, Y., "Flow Pattern Transition for Vertical Downward Two-Phase Flow," Chemical Engineering Science, 37, p. 741, 1982.

Baxendell, P. B., and Thomas, R., "The Calculation of Pressure Gradients in High-Rate Flowing Wells," Journal of Petroleum Technology, p. 1023, 1961.

Beggs, H. D., and Brill, J. P., "A Study of Two-Phase Flow in Inclined Pipes," Journal of Petroleum Technology, p. 607, 1973.

Bradburn, J. B., "Water Production-An Index to Corrosion," South Central NACE Meeting, Houston, Texas, 1977.

Brill, J. P., "Discontinuities in the Orkiszewski Correlation for Predicting Pressure Gradients in Wells," Journal of Energy Resources Technology, 41, p. 34, 1985.

Brill, J. P., and Beggs, H. D., Two-Phase Flow in Pipes,1977.

Brotz, W., "Uber die Vorausberechnung der Absorptionsgesch windig keit von Gasen in Stromenden Flussigkeitsschichten," Chem. Ing. Tech., 26, p. 470, 1954.

Bunz, A. P., Dohrn, R., and Prausnitz, J. M., "Three-phase Flash Calculations for Multi-component Systems," Computers in Chemical Engineering, 15, p. 47, 1991.

Caetano, E. F., "Upward Vertical Two-phase Flow Through an Annulus," Ph.D. Dissertation, University of Tulsa, Tulsa, Oklahoma, 1985.

Camacho, C. A., "Comparison of Correlations for Predicting Pressure Losses in High Gas-Liquid Ratio Vertical Wells," M. S. Thesis, University of Tulsa, 1970.

Collier, J. G., Convective Boiling and Condensation, 2nd Edition, McGraw Hill Book Co., London, England, 1981.

Duns, Jr., H., and Ros, N. C. J., "Vertical Flow of Gas and Liquid Mixtures in Wells," Proceedings of the 6th World Petroleum Congress, Frankfurt, 1963.

Erbar, J. H., "Documentation of the GPA*SIM Program," Gas Processors Association, Tulsa, Oklahoma, 1980.

Fernandes, S. R., and Duckler, A. E., "Hydrodynamic Model for Gas-Liquid Slug Flow in Vertical Tubes," AIChE Journal, 29, p. 981, 1983.

Golan, L. P., "An Air-Water Study of Vertical Upward and Downward Two-Phase Flow," Ph. D Dissertation, Lehigh University, 1970.

Govier, G. W., and Aziz, K., The Flow of Complex Mixtures in Pipes, Van Nostrand Reinhold Co., 1972.

Govier, G. W., and Fogarassi, M., "Pressure Drop in Wells Producing Gas and Condensate," Annual Technical Meeting, Petroleum Society of CIM, Banff, Canada, June 11-13, 1975.

Griffith, P., and Wallis, G. B., "Two-Phase Slug Flow," Journal of Heat Transfer, 83, p. 307, 1961.

Griffith, P., Lau, C. W., Hon, P. C., and Pearson, J. F., "Two Phase Pressure Drop in Inclined and Vertical Pipes," Technical Report No. 80063-81, Heat Transfer laboratory, MIT, Cambridge, Massachusetts, 1973.

Hagedorn, A. R., and Brown, K. E., "Experimental Study of Pressure Gradients Occurring During Continuous Two-Phase Flow in Small-Diameter Vertical Conduits," Journal of Petroleum Technology, p.475, 1965.

Hagedorn, A. R., "Experimental Study of Pressure Gradients Occuring during Continuous Two-Phase Flow in Small Diameter Vertical Conduits," PhD Dissertation, University of Texas, Austin, 1964.

Hankinson, R. W., Coker, T. A., and Thomson, G. H., "Get Accurate LNG Densities with COSTALD," Hydrocarbon Processing, 61(4), p. 207, 1982.

Hasan, A. R., and Kabir, C. S., "A Study of Multiphase Flow Behavior in Vertical Wells," SPE Production Engineering, p. 263, 1988.

Henstock, W. H., and Hanratty, T. J., "The Interfacial Drag and the Height of the Wall Layer in Annular Flows," AIChE Journal, 22, p. 990, 1976.

Harmathy, T. Z., "Velocity of Large Drops and Bubbles in Media of Infinite or Restricted Extent," AIChE Journal, 6, p. 281, 1960.

Hewitt, G. F., and Roberts, D. N., "Studies of Two-Phase Flow Patterns by Simultaneous X-ray and Flash Photography," United Kingdom Atomic Energy Authority Report AERE-M 2159, 1969.

Hewitt, G. F., and Hall-Taylor, N. S., Annular Two-Phase Flow, Pergamon Press, Houston, 1970.

Ishii, M., and Kataoka, I., Advances in Two-Phase Flow and Heat Transfer, Vol. I, p. 93.

Joosten, M. W., Johnsen, T., Dugstad, A., Walmann, T., Jossang, T., Meakin, P., and Feder, J., "In Situ Observation of Localized CO_2 Corrosion," Paper No. 3, Corrosion '94, 1994.

Juswandi, J., "Simulation of the Oil-Water Inversion Process," M. S. Thesis, Oklahoma State University, 1995.

Kabir, C. S., and Hasan, A. R., "Performance of a Two-Phase Gas/Liquid Flow Model in Vertical Wells," Journal of Petroleum Sciences and Engineering, 4, p. 273, 1990.

Lee, A. L., Gonzales, M. H., and Eakin, B. E., "The Viscosity of Natural Gases," Journal of Petroleum Technology, 18(8), p. 997, 1986.

Lesem, L. B., Greytok, F., Marotta, F., McKetta, J. J., Jr., "A Method of Calculating the Distribution of Temperature in Flowing Gas Wells," Petroleum Transactions, AIME, 210, p. 269, 1957.

Liu, G., "A Mathematical Model for Prediction of Downhole Gas Well Uniform Corrosion in CO_2 and H_2S Containing Brines," Ph.D. Dissertation, Oklahoma State University, 1991.

Liu, G., and Erbar, R. C., "Detailed Simulation of Gas Well Downhole Corrosion in Carbon Steel Tubulars," Corrosion/90, Paper No. 30, Las Vegas, Nevada, 1990.

Liu, G., and High, M. S., "Documentation Report for the Downhole Corrosion Model and Computer Program," Downhole Corrosion Consortium, 1993.

Lockhart, R. W. and Martinelli, R. C., "Proposed Correlation of Data for Isothermal Two-Phase, Two-Component Flow in Pipes," Chemical Engineering Progress, 45(1), p. 39, 1949.

McQuillan, K. W., and Whalley, P. B., "Flow Patterns in Vertical Two Phase Flow," International Journal of Multiphase Flow, 11, p. 161, 1985.

Mukherjee, H., and Brill, J. P., "Pressure Drop Correlations for Inclined Two-Phase Flow," Journal of Energy Resources Technology, 1985.

Orkiszewski, J., "Predicting Two-Phase Pressure Drops in Vertical Pipes," Journal of Petroleum technology, 19(6), p. 829, 1967.

Palmer, C. M., "Evaluation of Inclined Pipe Two-Phase Liquid Holdup Correlations Using Experimental Data," M. S. Thesis, University of Tulsa, Tulsa, OK, 1975.

Peffer, J. W., Miller, M. A., and Hill, A. D., "An Improved Method for Calculating Bottomhole Pressures in Flowing Gas Wells With Liquid Present," SPE Production Engineering, p. 643, 1988.

Poettman, F. H., and Carpenter, P. G., "The Multiphase Flow of Gas, Oil and Water Through Vertical Flow Strings with Application to the Design of Gas-Lift Installations," Drilling and Production Practices, API, p. 257, 1952.

Reinicke, K. M., and Remer, R. J., "Comparison of Measured and Predicted Pressure Drops in Tubing for High-Water-Cut Gas Wells," SPE Paper No. 13279, Society of Petroleum Engineering 59th Annual Meeting, Houston, Texas, 1987.

Robertson, C. A., "DOWN*HOLE Phase I: A Computer Model for Predicting the Water Phase Corrosion Zone in Gas and Condensate Wells," M. S. Thesis, Oklahoma State University, Stillwater, Oklahoma, 1988.

Schmidt, Z., "Experimental Study of Two-Phase Slug Flow in a Pipeline-Riser Pipe System," Ph.D. Dissertation, University of Tulsa, 1977.

Smith, F. G., "Controlling Corrosion in Deep South Louisiana Gas Wells," World Oil, 195(6), p. 77, 1982.

Soave, G., "Equilibrium Constants from a Modified Redlich-Kwong Equation of State," Chemical Engineering Science, 27(6), p. 1197, 1972.

Sylvester, N. D., "A Mechanistic Model for Two-Phase Vertical Slug Flow in Pipes," ASME Journal of Energy Resources Technology, 109, p. 206, 1987.

Taitel, Y., Barnea, D., and Dukler, A. E., "Modeling Flow Pattern Transitions for Steady Upward Gas-Liquid Flow in Vertical Tubes," AIChE Journal, 26(3), p. 345, 1980.

Tuttle, R. N., "Corrosion in Oil and Gas Production," Journal of Petroleum Technology, 39(7), p. 756, 1987.

Tuttle, R. N., "What is a Sour Environment?" Journal of Petroleum Technology, 42, p. 260, 1990.

Vo, D. T., and Shoham, O., "A Note on the Existence of a Solution for Two-Phase Slug Flow in Vertical Pipes," ASME Journal of Energy Resources Technology, 111, p. 64, 1989.

Wallis, G. B., One-Dimensional Two-Phase Flow, McGraw-Hill Book Co. Inc., 1969.

Whalley, P. B., and Hewitt, G. F., "The Correlation of Liquid Entrainment Fraction and Entrainment Rate in Annular Two-Phase Flow," UKAEA Report AERE-R9187, Harwell, 1978.

Yao, S. C., and Sylvester, N. D., "A Mechanistic Model for Two-Phase Annular-Mist Flow in Vertical Pipes," AIChE Journal, 33(6), p. 1008, 1987.

Zigrang, D., and Sylvester, N. D., "Explicit Approximation to the Solution of Colebrook's Friction Factor Equation," AIChE Journal, 28, p. 514, 1982.

APPENDIX A

Errors Identified in the DREAM 3.1

Pressure Drop and Mass Transfer FORTRAN Code

Coding errors were identified in the pressure drop and mass transfer subroutines of DREAM 3.1. The coding errors were due to the wrong definition of certain parameters or the use of wrong fluid properties. The coding errors resulted in:

1. erroneous pressure drop predictions,
2. crashing of the computer code for some cases.

These errors were subsequently removed to obtain better pressure drop predictions and also make the computer code robust.

Annular Flow Subroutine (Yao and Sylvester Model):

In the annular flow subroutine, the liquid entrainment fraction of Ishii and Kataoka was used instead of the Wallis (1969) expression used by Yao and Sylvester (1987). The Wallis entrainment fraction expression is given by

$$F_E = 1 - \exp\left[-0.125\left(v_{crit} - 1.5\right)\right]$$

where,

$$v_{crit} = 10000\frac{v_{SG}\mu_G}{\sigma_L}\left(\frac{\rho_G}{\rho_L}\right)^{1/2}.$$

The Ishii and Kataoka entrainment fraction expression is given by

$$F_E = \tanh\left(7.25\text{x}10^{-7}\,We^{1.25}\,Re^{0.25}\right)$$

where,

$$We = \frac{\rho_G v_{SG}^2 D}{\sigma}\left(\frac{\rho_L - \rho_G}{\rho_G}\right)^{1/3},$$

and

$$Re = \frac{\rho_L v_{SL} D}{\mu_L}.$$

The Reynolds number of liquid, Re_{liq}, flowing in pipe was used instead of the Reynolds number of the annular film, Re_{film}, while estimating the film thickness using Henstock and Hanratty (1976). The Reynolds number of liquid and annular film are defined below:

$$Re_{liq} = \frac{4M_L}{\pi D \mu_L}$$

$$Re_{film} = \frac{4M_L(1-F_E)}{\pi D \mu_L}$$

The mean density was defined as

$$\rho_c = \frac{\rho_L \rho_G}{\lambda_{LC}\rho_G + (1-\lambda_{LC})\rho_L},$$

instead of

$$\rho_c = \lambda_{LC}\rho_L + (1-\lambda_{LC})\rho_G.$$

The pressure gradient was taken to be the pressure drop. This was corrected by defining pressure drop as the product of pressure gradient and the well depth.

Slug Flow Subroutine (Sylvester Model):

The acceleration term was neglected in the final pressure drop equation of the slug flow subroutine. The pressure drop due to elevation change and frictional losses were defined as

$$(\Delta P)_H = \rho_L(1-\alpha_{SU}) + \rho_G \alpha_{SU},$$

and

$$(\Delta P)_f = \frac{\left[\rho_L(1-\alpha_{SU}) + \rho_G \alpha_{SU}\right] v_m^2 f_{LS}}{2D}$$

instead of

$$(\Delta P)_H = \rho_L(1-\alpha_{LS})gL_{LS},$$

and

$$(\Delta P)_f = \frac{L_{LS}}{2D}\left[\frac{\rho_G \beta f_{TB} v_{TB}^2}{(1-\beta)\left[1-\left(1-\alpha_{TB}^{1/2}\right)\right]} + v_{LLS}\rho_L(1-\alpha_{LS})f_{LS}(1-\beta)\right].$$

Necessary changes were made in the code to match the code with the equations developed by Sylvester.

Mass Transfer:

In the mass transfer section of the FORTRAN code in DREAM 3.1, incorrect fluid properties and Reynolds number were used. These coding errors have been corrected. The errors identified in the mass transfer section are described below:

1. The mean density and viscosity was used in place of the liquid density.

2. The Reynolds number for the liquid film, gas core and the bulk liquid were interchangeably used.

3. The mass transfer coefficient for the liquid film was defined as

$$K_L = \frac{D_i}{D}Sh$$

instead of

$$K_L = \frac{D_i}{\delta} Sh .$$

APPENDIX B

FORTRAN Code for the Pressure Drop and Flow Regime Analysis

Subroutines in DREAM 3.2

The computer code given in this appendix is part of a software package that predicts corrosion rate for downhole gas wells. The subroutines created or used for evaluation in this thesis work along with the property prediction subroutines have been given below. The flash calculation subroutine has not been included. The subroutines given below can be utilized independently to estimate pressure drop by making minor modifications to the code:

1. Write a master program that reads input information such as wellhead and bottomhole temperature and pressure, gas and liquid flow rates, gas gravity, gas and liquid density, well diameter and well depth.
2. Call the relevant subroutines to estimate the viscosity of gas and liquid and also the liquid surface tension.
3. Call the flow regime estimation subroutine.
4. Depending upon the flow regime, call the relevant pressure drop subroutine.

The parameters that need to be passed in and taken out of each subroutine are described in the computer code as comments at the beginning of each subroutine.

```
      subroutine setup
$include:'common1'
c  Variable declaration
      real yk_mass(20),h_inner,h_total, fdelt(50), film(50)
      entry viscal
c  ***************************************************************
c  Calculate viscosity of gas phase
c   Lee, A. L., Gonzales, M. H., and Eakin, B. E., "The Viscosity of Natural Gases,"
c  Journal of Petroleum Technology, 18(8), p. 997, 1986.
c  ***************************************************************
c  DESCRIPTION OF VARIABLES
c  gden        : gas density
c  cvis        : gas viscosity
c  wvis        : water viscosity
c  rhovap      : gas density
c  ymw         : gas molecular weight
c  ta          : temperature of interest
c  ***************************************************************
c  INPUT       : gas density, gas gravity and temperature of interest.
c  OUTPUT      : gas and water viscosity
c  ***************************************************************
      gden = rhovap * 0.016018
      ckb = 122.4 + 12.9 * ymw + ta
      ckt = (7.77 + 0.0063*ymw)* ta ** 1.5
c  eqn (3) of Lee et al. (1986)
      cka = ckt / ckb
c  eqn (4) of Lee et al. (1986)
      cx = 2.57 + 1914.5/ta +0.0095*ymw
c  eqn (5) of Lee et al. (1986)
      cy = 1.11 + 0.04 * cx
      a = cx *abs(gden) ** cy
      b = exp(a)
c  eqn (2) of Lee et al. (1986)
      cvis = cka * b
c Convert viscosity into lb/ ft- s
      cvis = 0.00024191* cvis  /3600.
c  ***************************************************************
c Correlation for viscosity of water
c  ***************************************************************
      t =((ta - 459.67 - 32.)/1.8) + 273.15
      a = -52.843
      b = 3703.6
      c = 5.866
      d = -5.879e-29
      e = 10
```

```
      wvis_si = exp(a + (b/t) + c*2.303*alog10(t) + d*(t**e))
c Convert from Pa.s to lbm/ft.s
      wvis = wvis_si/1.488
      return


c ***********************************************************************
c Calculate surface tension
      entry stension
c ***********************************************************************
c DESCRIPTION OF VARIABLES
c tempc      : temperature in Celcius
c tempk      : temperature in Kelvin
c tempr      : reduced temperature
c sten_si    : surface tension of water in SI units
c sten       : surface tension in fps units
c ***********************************************************************
c INPUT      : temperature of interest
c OUTPUT     : surface tension of water
c ***********************************************************************
      tempc = (ta - 459.67 - 32.) / 1.8
      tempk = tempc +273.15
      tempr = tempk/647.13
      a = 0.18546
      b = 2.717
      c = -3.554
      d = 2.047
      tem1 =b + c*tempr + d*tempr**2.
      sten_si = a*((1.-tempr)**tem1)
c Convert from N/m to lbm/sec2
      sten = 32.*sten_si/14.6
      return


c ***********************************************************************
c Calculate flow regime using Taitel et al. model
c Taitel. Y., Barnea. d., and Dukler. A. E., "Modeling Flow pattern
c Trasitions for Steady Upward Gas-Liquid Flow in Vertical Tubes," AIChE J.,
c 26(3), 345-354 (May 1980)
c ***********************************************************************
      entry regime(j)
c ***********************************************************************
c DESCRIPTION OF VARIABLES
c rough      : roughness factor
```

```
c asect      : length of the well string
c tubid      : well inside diameter
c area       : cross-sectional area of well string
c gravit     : acceleration due to gravity
c xvapm1     : molar flow rate of gas
c xliqm1     : molar flow rate of hydrocarbon liquid
c xliqm2     : molar flow rate of water
c ymw        : average molecular weight of gas
c almw       : average molecular weight of hydrocarbon liquid
c bmw        : molecular weight of water
c tovap      : mass flow rate of gas
c toliq      : mass flow rate of liquid
c rhovap     : gas density
c rhol1      : hydrocarbon liquid density
c rhol2      : water density
c rholav     : average liquid density
c ugs        : superficial gas velocity
c uls        : superficial liquid velocity
c fe         : liquid entraiment fraction
c alamblc    : liquid holdup fraction in the gas core
c rhoc       : average density of the core in annular flow
c usc        : core velocity
c visc       : core viscosity
c reysl      : reynolds number based on superficial liquid velocity
c reysc      : reynolds number based on superficial core velocity
c fsl        : friction factor based on superficial liquid velocity
c fsc        : frcition factor based on superficial core velocity
c dpdzsl     : superficial liquid friction pressure gradient
c dpdzsc     : superficial friction pressure gradient
c ff         : friction factor at the film
c delt       : minimum film thickness for a stable annular film
c iregim     : 1  Annular flow
c            : 2  Slug flow
c            : 3  Bubble flow
c ac         : cross sectional area of gas core
c vs         : slip velocity
c ulsa,ulsc  : superficial liquid velocity defined by transition A (transition
c            : from dispersed bubble to bubble flow) and transition C
c            : (transition from dispersed bubble to slug flow) respectively,
c            : for the given superficial gas velocity.
c ugsb       : superficial gas velocity defined by transition B (transition
c            : from bubble to slug flow) for the given superficial liquid
c            : velocity.
c veros      : erosional velocity
c vacel      : mixture velocity
```

```
c ymass       : mass fraction of gas in the mixture
c x1mass      : mass fraction of hydrocarbon liquid in mixture
c x2mass      : mass fraction of water in the mixture
c ***************************************************************
c INPUT       : temperature, gas and liquid density, gas and liquid viscosity, liquid
c             : surface tension, well diameter, and gas and liquid flow rates
c OUTPUT      : variable 'iregim'
c ***************************************************************
c Assign variables
c ***************************************************************
      rough = 1.5e-4
      asect = alenth(j +1) - alenth(j)
      tubid = dia(j)/12.
      eond = rough/tubid
      pi = 3.1416
      area = pi * tubid**2 /4.
      small = 1.e-20
      gravit = 32.174
c ***************************************************************
c Estimate gas and liquid superficial velocities, mass flow rates
c ***************************************************************
      b1 = rhol2**2 * gravit * tubid**2
      b2 = (rhol2 - rhovap)*sten
      bubble = (b1 / b2) **0.25
      tovap = xvapm1 *ymw
      ugs = tovap/ rhovap/area
      qg = ugs * area
      ratio = xliqm1 / (xliqm2 + xliqm1)
      if (ratio .gt. 0.1) then
            uls = (xliqm1 * almw / rhol1 + xliqm2 *bmw / rhol2)/area
            rholav = rhol1*rhol2 /(ratio * rhol2 + ( 1. - ratio) * rhol1)
            toliq = xliqm1*almw + xliqm2 * bmw
      else
            uls = (xliqm2 *bmw / rhol2 )/area
            rholav = rhol2
            toliq = xliqm2 * bmw
      end if
      if(uls .le. 1.e-10 .or. xliqm2 .le. 1.e-20) then
            iregim = 0
            go to  310
      end if
      ql = uls * area
c ***************************************************************
c Estimate the parameters required to check for the presence of annular flow
c ***************************************************************
```

```
      s1 = (gravit * b2)**0.25
      uslgtr = (1./3.)*(uls + 1.15*s1)
      annul = ugs * rhovap**0.5 / s1
c *********************************************************************
c Estimate liquid entraiment fraction
c *********************************************************************
c eqn.(72) of Ansari et al. (1994)
      ucrit = 10000*ugs*cvis*((rhovap/rholav)**0.5)/sten
c eqn. (71) of Ansari et al. (1994)
      fe = 1.-exp(-0.125*(ucrit-1.5))
      if (fe.lt.0) fe=0
c *********************************************************************
c Estimate superficial pressure gradients required to calculate
c the Lockhart and Martinelli parameters
c *********************************************************************
c eqn. (70) of Ansari et al. (1994)
      alamblc = fe*uls/(ugs+fe*uls)
c eqn. (69) of Ansari et al. (1994)
      rhoc = rholav*alamblc + rhovap*(1.-alamblc)
c eqn. (89) of Ansari et al. (1994)
      usc = fe*uls + ugs
c eqn. (90) of Ansari et al. (1994)
      visc = wvis*alamblc + cvis*(1.-alamblc)
      eond = 0.00015/tubid
c eqn. (80) of Ansari et al. (1994)
      reysl = rholav*uls*tubid/wvis
      call friclose(eond,reysl,fsl)
c eqn. (79) of Ansari et al. (1994)
      dpdzsl = fsl*rholav*uls**2./(2.*tubid)
c eqn. (88) of Ansari et al. (1994)
      reysc = rhoc*usc*tubid/visc
      call friclose(eond,reysc,fsc)
c eqn. (87) of Ansari et al. (1994)
      dpdzsc = fsc*rhoc*(usc**2.)/(2.*tubid)
      tol = 1.e-5
      ic = 0
      jd = 0
      ie = 0
      call annfilm(rholav,delhen,ff)
      do 47 i = 1,45     !estimation of minimum film thickness
      delt = float(i)/100.
c eqn. (11) of Ansari et al. (1994)
      ahlf = 4.*delt*(1.-delt)
      ahlfd = 4.*(1.-2.*delt)
      b = ((1.-fe)**2.)*(ff/fsl)
```

```
c  eqn. (9) of Ansari et al. (1994)
        xm = (dpdzsl*b/dpdzsc)**0.5
c  eqn. (8) of Ansari et al. (1994)
        ym = gravit*(rholav-rhoc)/dpdzsc
        temp1 = (2.0 - 1.5*ahlf)*xm**2.
        temp2 = 1.0 - 1.5*ahlf
        temp21 = ahlf**3.0
        temp22 = temp2*temp21
c  eqn. (13) of Ansari et al. (1994)
        film(i) = ym - (temp1/temp22)
        if (i.gt.1) then
                temp3 = film(i)*film(1)
                if (temp3.le.0) then
                        iflag = 1
                        goto 19
                endif
        endif
47      continue
19      continue
c  ********************************************************************
c  Depending upon the superficial velocities of the two phases and using the
c  Barnea flow map, identify the flow regime.
c  ********************************************************************
        if ((film(1).le.0).and.(iflag.ne.1)) then
                iregim = 2
                goto 310
        elseif (film(1).gt.0) then
                iregim = 2
                goto 310
        endif
        ac = 3.1415*(tubid*(1. - 2.*delt))**2./4.
        ap = 3.1415*tubid**2./4.
c  eqn. (12) of Ansari et al. (1994)
        barn = ahlf + alamblc*ac/ap
c  ********************************************************************
c  Check for existence of annular flow
c  ********************************************************************
        if( annul .gt. 3.1) then
                if (delt.le.0) then
                        if (alamblc.le.0.12) then
                                iregim = 1
                                goto 310
                        endif
                elseif (delt.ge.0.45) then
                        iregim = 2
```

```
                goto 310
            else
                if (barn .le. 0.12) then
                    iregim = 1
                    goto 310
                endif
            endif
        endif
c ***********************************************************************
c Check for existence of slug flow
c ***********************************************************************
c Transition A: Transition from dispersed bubble to bubble flow.
c ***********************************************************************
c eqn. (3) of Ansari et al. (1994)
        vs = 1.53*(s1/rholav**0.5)
c eqn. (2) of Ansari et al. (1994)
        ulsa = 3.*(ugs - 0.25*vs)
c ***********************************************************************
c Transition C: Transition from dispersed bubble to slug flow.
c ***********************************************************************
c eqn. (5) of Ansari et al. (1994)
        ulsc = ugs/3.17
c ***********************************************************************
c Transition B: Transition from bubble to slug flow (eqn. (4) of Ansari et al. (1994)).
c ***********************************************************************
        ie = 0
        temp1 = (0.4*sten/((rholav-rhovap)*gravit))**0.5
        temp2 = ((rholav/sten)**0.6)*((ff/(2.*tubid))**0.4)
        ugsb = ugs
 21     temp3 = (2.*temp1*temp2)*((uls+ugsb)**1.2)
        temp4 = ((temp3 - 0.725)/4.15)**2.
        ugsbn = (uls*temp4)/(1.-temp4)
        check = abs(ugsbn - ugsb)
        ie = ie + 1
        if ((check .gt. tol) .and. (ie.lt.25)) then
            if (ugsbn.ge.0) then
                ugsb = ugsbn
                goto 21
            else
                ugsb = 0
            endif
        endif
        if (ugsbn.ge.0) then
            ugsb = ugsbn
        else
```

```
            ugsb = 0
        endif
        ugs_ac = 0.279*vs
        call ugsab(rholav,ugs_ab)
        if (ugs_ab.le.0) then
            ugs_ab = ugs_ac
            iflag9 = 1
        endif
        if (ugs.lt.ugs_ab) then
            if(ugs.gt.ugsb) then
                iregim = 2
                goto 310
            endif
        elseif ((iflag9.ne.1).and.(ugs.lt.ugs_ac)) then
            if(uls.lt.ulsa)then
                iregim = 2
                goto 310
            endif
        else
            if (uls.lt.ulsc) then
                iregim = 2
                goto 310
            endif
        endif
c ***********************************************************************
c If the condition of annular flow and slug flow are not satified, assume
c bubble flow.
c ***********************************************************************
        iregim = 3
 310  continue
        rhmxl = (tovap*rhovap + toliq*rholav)/(tovap+toliq)
        ireg(j) = iregim
        veros(j+1) = 100./(abs(rhmxl)**0.5)
        vacel(j+1) = uls + ugs
        eofov(j+1) = veros(j+1)/(vacel(j+1) + 1.e-12)
        ymass(j+1) = tovap/(toliq + tovap)*100.
        x1mass(j+1) = xliqm1*almw/(toliq + tovap)*100.
        x2mass(j+1) = xliqm2*bmw/(toliq + tovap)*100.
        return


c ***********************************************************************
c Yao and Sylvester model for pressure drop estimation in the annular flow
c ***********************************************************************
c Yao, S. C., and Sylvester, N. D., "A Mechanistic Model for Two-Phase
```

```
c Annular-Mist Flow in Vertical Pipes," AIChE Journal, 33(6),p.1008, 1987
c ******************************************************************
      entry alfilm(j)
c ******************************************************************
c Estimate liquid entrainment fraction using the expression proposed by Wallis.
c Wallis, G. B., One-Dimensional Two Phase Flow, McGraw-Hill Book Co. Inc.,
c New York City, 1969.

c ******************************************************************
c DESCRIPTION OF VARIABLES
c fre        liquid entrainment fraction
c ymlf       mass flow rate of liquid in the annular film
c re_film    Reynolds number for the annular film
c reliq      liquid reynolds number
c regas      gas reynolds number
c deta_t     film thickness
c dpdza      acceleration component of pressure drop
c dpdze      elevation component of pressure drop
c dpdzf      friction component of pressure drop
c dpdzt      total pressure drop
c ******************************************************************
c INPUT      : gas and liquid density, gas and liquid viscosity, liquid , well diameter,
c            : surface tension, and gas and liquid superficial velocities
c OUTPUT     : pressure drop
c ******************************************************************
c eqn. (3) of Yao and Sylvester (1987)
      beta = 10000.0*ugs*cvis*((rhovap/rholav)**0.5)/sten
c eqn. (2) of Yao and Sylvester (1987)
      fre =1.0 - exp((1.5 - beta)*0.125)
      if (fre.lt.0) fre = 0
c eqn. (5) of Yao and Sylvester (1987)
      volfr = fre * ql /(fre *ql + qg)
c eqn. (4) of Yao and Sylvester (1987)
      rhomen = volfr*rholav + (1.0 - volfr)*rhovap
c eqn. (12) of Yao and Sylvester (1987)
      vis_mean = volfr*wvis + (1.0 - volfr)*cvis
c ******************************************************************
c Estimate annular film thickness using the expression given by Henstock and
c Hanratty.
c Henstock, William H., and Hanratty, Thomas J., "The Interfacial Drag and the
c Height of the Wall Layer in Annular Flows," AIChE Journal, 22, (6), p. 990, 1976
c ******************************************************************
      ymlf = (1.0 - fre)*toliq
      reliq = 4. * toliq /(pi*tubid*wvis)
c eqn. (15) of Yao and Sylvester (1987)
```

```
      re_film = 4. *ymlf/(pi*tubid*wvis)
      if(re_film .le. 0)re_film = 1.e-6
c  eqn. (16) of Yao and Sylvester (1987)
      regas = rhovap * tubid * ugs / cvis
c  eqn. (14) of Yao and Sylvester (1987)
      fnum1 = (0.707*re_film**0.5)**2.5
      fnum2 = (0.0379 * re_film**0.9)**2.5
      fnum = (fnum1 + fnum2)**0.4
      fdemon = regas**0.9*(cvis/wvis)*(rholav/rhovap)**0.5
      rhocor = rholav*rhovap /( volfr * rhovap + (1. -volfr)*rholav)
      viscor = volfr*wvis + (1. - volfr)*cvis
      ffact = fnum/fdemon
c  eqn. (13) of Yao and Sylvester (1987)
       a = 6.59*ffact*tubid
       b = sqrt( 1. + 1400. *ffact)
       deta_t = a/b
c  ********************************************************************
c  Estimate slug flow film thickness
c  ********************************************************************
      if(iregim .ne. 1) then
            tol = 1.e-5
            vis_k_mean = vis_mean/rhomen
            reynold_mean = vacel(j)*tubid/vis_k_mean
            deta_t = 46.1*tubid*(diffus_cef(7)/vis_k_mean)**0.3333*
     #      reynold_mean**(-0.9)
      end if
      if (deta_t .le. 1.e-6) deta_t = 1.0e-6
      deta_film = deta_t*3.048   !deta_film has a unit dm
c  ********************************************************************
c  Calculate core mean velocity, renolds number, and friction factor
c  ********************************************************************
c  eqn. (8) of Yao and Sylvester (1987)
      cormlg = fre* toliq + xvapm1 * ymw
c  eqn. (9) of Yao and Sylvester (1987)
      corare = pi*(tubid - 2. * deta_t)**2/4.
c  eqn. (7) of Yao and Sylvester (1987)
      corv = cormlg / rhomen /corare
c  eqn. (11) of Yao and Sylvester (1987)
      corre = tubid *rhomen*corv/vis_mean
      detaod = deta_t / tubid
      call friclose(detaod,corre,fricf)
c  ********************************************************************
c  Calculate pressure gradient
c  ********************************************************************
c  eqn. (6) of Yao and Sylvester (1987)
```

```
      dpdzf = rhomen* fricf* corv**2/(4633.06*tubid) /2.
c eqn. (18) of Yao and Sylvester (1987)
      dpdze = rhomen / 144.
c eqn. (19) of Yao and Sylvester (1987)
      dpdza = rhomen* corv *(vacel(j) - vacel(j+1))/asect/4633.06
c eqn. (17) of Yao and Sylvester (1987)
      dpdzt = (dpdzf + dpdze + dpdza)*asect



      entry annular(j)
c ***************************************************************
c Ansari, A. M., Sylvester, N. D., Sarica, C., Shoham, O., Brill, J. P., "A
c Comprehensive Mechanistic Model For Upward Two-Phase Flow in Well Bores,"
c SPE Production & Facilities, May 1994, p.143
c ***************************************************************
c DESCRIPTION OF VARIABLES
c tubid      : well inside diameter
c gravit     : acceleration due to gravity
c rhovap     : gas density
c rholav     : average liquid density
c ugs        : superficial gas velocity
c uls        : superficial liquid velocity
c fe         : liquid entraiment fraction
c alamblc    : liquid holdup fraction in the gas core
c rhoc       : average density of the core in annular flow
c usc        : core velocity
c visc       : core viscosity
c reysl      : reynolds number based on superficial liquid velocity
c reysc      : reynolds number based on superficial core velocity
c fsl        : friction factor based on superficial liquid velocity
c fsc        : frcition factor based on superficial core velocity
c dpdzsl     : superficial liquid friction pressure gradient
c dpdzsc     : superficial friction pressure gradient
c ff         : friction factor at the film
c delt       : annular film thickness
c z          : empirical factor defining interfacial friction
c phicsq     : dimensionless group
c dpdzt      : total pressure drop
c ***************************************************************
c INPUT      : gas and liquid density, gas and liquid viscosity, liquid, well diameter,
c            : surface tension, and gas and liquid superficial velocities
c OUTPUT     : total pressure drop
c ***************************************************************
c Estimate friction factor
```

```
c ***********************************************************************
c  eqn. (72) of Ansari et al. (1994)
      ucrit = 10000*ugs*cvis*((rhovap/rholav)**0.5)/sten
c  eqn. (71) of Ansari et al. (1994)
      fe = 1.-exp(-0.125*(ucrit-1.5))
      if (fe.lt.0) fe=0
c ***********************************************************************
c  Estimate Lockhart and Martinelli parameters
c ***********************************************************************
c  eqn. (70) of Ansari et al. (1994)
      alamblc = fe*uls/(ugs+fe*uls)
c  eqn. (69) of Ansari et al. (1994)
      rhoc = rholav*alamblc + rhovap*(1.-alamblc)
c  eqn. (89) of Ansari et al. (1994)
      usc = fe*uls + ugs
c  eqn. (90) of Ansari et al. (1994)
      visc = wvis*alamblc + cvis*(1.-alamblc)
      delt = 0.001
      eond = 0.00015/tubid
c  eqn. (80) of Ansari et al. (1994)
      reysl = rholav*uls*tubid/wvis
      call friclose(eond,reysl,fsl)
c  eqn. (79) of Ansari et al. (1994)
      dpdzsl = fsl*rholav*uls**2./(2.*tubid)
c  eqn. (88) of Ansari et al. (1994)
      reysc = rhoc*usc*tubid/visc
      call friclose(eond,reysc,fsc)
c  eqn. (87) of Ansari et al. (1994)
      dpdzsc = fsc*rhoc*(usc**2.)/(2.*tubid)
      tol = 1.e-2
      call annfilm(rholav,delhen,ff)
      ic = 0
      b = ((1.-fe)**2.)*(ff/fsl)
c  eqn. (9) of Ansari et al. (1994)
      xm = (dpdzsl*b/dpdzsc)**0.5
c  eqn. (10) of Ansari et al. (1994)
      ym = gravit*(rholav-rhoc)/dpdzsc
c ***********************************************************************
c  Estimate annular film thickness
c ***********************************************************************
      do 22 i = 1,49
            delt = float(i)/100.
            temp1 = 4*delt*(1.-delt)
            temp2 = temp1*((1.-temp1)**2.5)
            if (fe.gt.0.9) then
```

```
c  eqn. (84) of Ansari et al. (1994)
                        z = 1.+ 300.*delt
                        zd = 300.
                endif
c  eqn. (85) of Ansari et al. (1994)
                        z = 1. + 24.*delt*(rholav/rhovap)**0.3333
                        zd = 24.*(rholav/rhovap)**0.3333
                endif
c  eqn. (96) of Ansari et al. (1994)
                fdelt(i) = ym - (z/temp2) + (xm**2./temp1**3.)
                if (i.gt.1) then
                        check = fdelt(i)*fdelt(1)
                        if (check.lt.0) then
                                iflag2 = 1
                                goto 23
                        endif
                endif
22      continue
23      if (iflag2.ne.1) then
                delt = delhen
        endif
        if (fe.gt.0.9) then
                z = 1.+ 300.*delt
        else
                z = 1. + 24.*delt*(rholav/rhovap)**0.3333
        endif
c  ***********************************************************************
c  Estimate pressure drop
c  ***********************************************************************
c  eqn. (99) of Ansari et al. (1994)
        phicsq = z/((1.-2.*delt)**5.)
c  eqn. (102) of Ansari et al. (1994)
        dpdzt = (phicsq*dpdzsc + gravit*rhoc)*asect/4633.06
        return




        entry slugpt(j)
c  ***********************************************************************
c  Ansari, A. M., Sylvester, N. D., Sarica, C., Shoham, O., Brill, J. P., "A
c  Comprehensive Mechanistic Model For Upward Two-Phase Flow in Well Bores,"
c  SPE Production & Facilities, May 1994, p.143
c  ***********************************************************************
```

```
c DESCRIPTION OF VARIABLES
c alc          : Taylor bubble cap length
c alls         : length of liquid slug
c alsu         : length of slug unit
c altb         : length of Taylor bubble
c altbstar     : modified Taylor bubble length
c beta         : ratio of length of Taylor bubble to length of slug unit
c betastar     : modified ratio of length of Taylor bubble to length of slug unit for
c              : developing flow
c dpdze        : pressure gradient due to elevation change
c dpdzf        : pressure gradient due to friction
c dpdzt        : total pressure drop
c fls          : friction factor for the liquid slug
c gravit       : acceleration due to gravity
c hgls         : average holdup fraction of gas in the liquid slug
c hlls         : average holdup fraction of liquid in the liquid slug
c hltb         : average holdup fraction of liquid in the Taylor bubble
c qf           : falling film volumetric flow rate
c qp           : gas volumetric in the Taylor bubble
c rels         : reynolds number for the liquid slug
c rholav       : average liquid density
c rhols        : average density of the mixture in the liquid slug
c rhovap       : gas density
c tdn          : Nusselt film thickness
c tubid        : well inside diameter
c ugls         : velocity of the gas bubbles in the liquid slug
c ugs          : superficial gas velocity
c ugtb         : velocity of gas in Taylor bubble
c ulls         : velocity of liquid in the liquid slug
c uls          : superficial liquid velocity
c ultb         : velocity of the falling film
c utb          : Taylor bubble rise velocity
c xmuls        : average viscosity of the mixture in the liquid slug
c ***************************************************************
c INPUT        : gas and liquid density, gas and liquid viscosity, liquid, well diameter,
c              : surface tension, and gas and liquid superficial velocities
c OUTPUT       : total pressure drop
c ***************************************************************
      tol = 1.e-5
      gravit = 32.174
      ustotl = ugs + uls
      rhodef = rholav - rhovap
c ***************************************************************
c Solve for the eight unknowns that define slug flow: beta, hltb, hgls, ugtb, ultb, ugls,
c ulls, and utb.  Solution procedure is given by
```

```
c  Vo, D. T., Shoham, O., "A Note on the Existence of a Solution for two-Phase Slug
c  Flow in Vertical Pipes," ASME Journal of Energy Resources Technology, 64,
c  p.111, 1989.
c  ***************************************************************
c  eqn. (38) of Ansari et al. (1994)
        hgls = (0.3048*ugs)/(0.425+2.65*0.3048*ustotl)
        hlls = 1. - hgls
        st1 = gravit*tubid*rhodef/rholav
c  eqn. (34) of Ansari et al. (1994)
        utb = 1.2*ustotl + 0.35*st1**0.5
        st2 = sten*gravit*rhodef/rholav**2.
        st3 = hgls*utb + hlls*(ustotl - hgls*1.53*st2**0.25*hlls**0.5)
        hltb = 0.5
        st4 = 9.916*(gravit*tubid)**0.5
        ic = 0
   51   continue
        st5 = 1.-(1.-hltb)**0.5
c  eqn. (41) of Ansari et al. (1994)
        fhltb = st4*(st5**0.5)*hltb-utb*(1.-hltb)+st3
c  eqn. (42) of Ansari et al. (1994)
        fhltbd = utb + st4*(st5**0.5+hltb/(4*((1.-hltb)*st5)**0.5))
c  eqn. (43) of Ansari et al. (1994)
        hltbn = hltb - fhltb/fhltbd
        test = abs(hltb - hltbn)
        if (test.le.tol) goto 520
        hltb = hltbn
        goto 51
        520 continue
        hltb = hltbn
c  ***************************************************************
c  Estimate all the unknown parameters
c  ***************************************************************
c  eqn. (37) of Ansari et al. (1994)
        ultb = st4*(st5**0.5)
c  eqn. (32) of Ansari et al. (1994)
        ulls = utb - (utb+ultb)*hltb/hlls
c  eqn. (35) of Ansari et al. (1994)
        ugls = ulls + 1.53*st2**0.25*hlls**0.5
c  eqn. (33) of Ansari et al. (1994)
        ugtb = utb - (utb-ugls)*(1.-hlls)/(1.-hltb)
c  eqn. (30) of Ansari et al. (1994)
        beta = (ulls*hlls-uls)/(ulls*hlls+ultb*hltb)
c  ***************************************************************
c  Estimate the friction factor
c  ***************************************************************
```

```
c  eqn. (61) of Ansari et al. (1994)
        rhols = rholav*hlls + rhovap*(1.-hlls)
        xmuls = wvis*hlls + cvis*hgls
c  eqn. (66) of Ansari et al. (1994)
        rels = rhols*ustotl*tubid/xmuls
        eond = 0.00015/tubid
        call friclose(eond,rels,fls)
c  ***********************************************************************
c  Estimate the pressure gradient for developed flow
c  ***********************************************************************
c  eqn. (60) of Ansari et al. (1994)
        dpdze = ((1.-beta)*rhols+beta*rhovap)/144.
C  eqn. (65) of Ansari et al. (1994)
        dpdzf = fls*rhols*ustotl**2.*(1.-beta)/(2*tubid*4633.06)
c  ***********************************************************************
c  Check if the slug flow is fully developed.  If the slug flow is not fully developed,
c  modify the Taylor bubble length.
c  ***********************************************************************
c  eqn. (48) of Ansari et al. (1994)
        alls = 30.*tubid
c  eqn. (49) of Ansari et al. (1994)
        altb = alls*beta/(1.-beta)
        alsu = alls + altb
        area = 3.1415*(tubid**2.)/4.
        check = 0.1
        i = 0
        qf = 0.1
        do while ((i.le.50).and.(check.gt.0.0001))
                temp4 = 3.1415*gravit*tubid*rholav
                temp5 = 3.*qf*wvis
c  eqn. (8) of McQuillan and Whalley (1984)
                tdn= ((temp5/temp4)**2.)**0.167
                temp1 = utb*area
c  eqn. (7) of McQuillan and Whalley (1984)
                qp = (1-4.*tdn/tubid)*temp1
c  eqn. (9) of McQuillan and Whalley (1984)
                qfnew = qp - (uls + ugs)*area
                check = abs(qfnew - qf)
                qf = qfnew
                i = i + 1
        end do
        temp2 = (utb - ugs - uls)*area/((2.*gravit)**0.5)
        temp3 = area - 3.1415*(tubid - (2.*tdn))**2./4.
C  eqn. (18) of McQuillan and Whalley (1984)
        alc = (temp2/temp3)**2.
```

```
      if (alc.lt.altb) goto 595
c ***********************************************************************
c Developing Flow
c ***********************************************************************
c
c eqn. (55) of Ansari et al. (1994)
      a = 1.- ugs/utb
c eqn. (56) of Ansari et al. (1994)
      b = (ugs-ugls*(2.-hlls))*alls/utb
c eqn. (57) of Ansari et al. (1994)
      c = (utb-ulls)*hlls/((2.*gravit)**0.5)
      x2 = -(2.*a*b+4.*c*c)/(a**2.)
      x3 = (b/a)**2.
      d = x2**2.-4.*x3
c ***********************************************************************
c If the quadratic does not have a real solution, assume developed flow
c ***********************************************************************
      if (d.lt.0) then
            goto 595
      endif
      ltbstar1 = (-x2 + d**0.5)/2.
      ltbstar2 = (-x2 - d**0.5)/2.
c ***********************************************************************
c If the quadratic does not have a sensible solution(positive number), assume
c developed flow
c ***********************************************************************
      if (ltbstar1.lt.0) then
            goto 595
      elseif (ltbstar2.le.0) then
            ltbstar = ltbstar1
      elseif (ltbstar1.lt.ltbstar2) then
            ltbstar = ltbstar1
      else
            ltbstar = ltbstar2
      endif
c ***********************************************************************
c Estimate modified pressure gradient based on the modified parameters
c ***********************************************************************
      betastar = ltbstar/(ltbstar+alls)
      alsu = alls/(1.-betastar)
c eqn. (64) of Ansari et al. (1994)
      hltba = 2.*(utb-ulls)*hlls/((2.*gravit*ltbstar)**0.5)
c eqn. (63) of Ansari et al. (1994)
      rhotba = rholav*hltba+rhovap*(1.-hltba)
c eqn. (62) of Ansari et al. (1994)
      dpdze = ((1.-betastar)*rhols+betastar*rhotba)/144.
```

```
C  eqn. (65) of Ansari et al. (1994)
        dpdzf = fls*rhols*ustotl**2.*(1 -betastar)/(2*tubid*4633.06)
c ***************************************************************
c  Estimate the total pressure drop
c ***************************************************************
595     dpdzt = (dpdze*alsu + dpdzf*alls)*asect/alsu
        return



        entry olslugpt(j)
c ***************************************************************
c  Sylvester, N. D., "A Mechanistic Model for two-Phase Vertical Slug Flow in
c  Pipes," ASME Journal of Energy Resources Technology, 109, p.206, 1987
c ***************************************************************
c  DESCRIPTION OF VARIABLES
c  alphls      : average holdup fraction of gas in the liquid slug
c  altb        : average void fraction in Taylor bubble
c  beta        : ratio of length of Taylor bubble to length of slug unit
c  detal       : liquid film thickness
c  dpa         : acceleration pressure drop of slug unit
c  dpdzt       : total pressure drop
c  dpfls       : friction pressure drop of liquid slug
c  dpftb       : friction pressure drop of Taylor bubble
c  dph         : hydrostatic pressure drop of slug unit
c  fls         : friction factor for the liquid slug
c  gravit      : acceleration due to gravity
c  slugls      : length of liquid slug
c  slugsu      : length of slug unit
c  rels        : reynolds number for the liquid slug
c  rholav      : average liquid density
c  rhovap      : gas density
c  tubid       : well inside diameter
c  ugls        : velocity of the gas bubbles in the liquid slug
c  ugs         : superficial gas velocity
c  ugtb        : velocity of gas in Taylor bubble
c  ulls        : velocity of liquid in the liquid slug
c  uls         : superficial liquid velocity
c  ultb        : velocity of the falling film
c  utb         : Taylor bubble rise velocity
```

```
c ***************************************************************
c INPUT     : gas and liquid density, gas and liquid viscosity, liquid, well diameter,
c           : surface tension, and gas and liquid superficial velocities
c OUTPUT    : total pressure drop
c ***************************************************************
c Solve for the eight unknowns that define slug flow: beta, altb, alphls, ugtb, ultb, ugls,
c ulls, and utb.  Solution procedure is given by
c Vo, D. T., Shoham, O., "A Note on the Existence of a Solution for two-Phase Slug
c Flow in Vertical Pipes," ASME Journal of Energy Resources Technology, 64,
c p.111, 1989.
c ***************************************************************
      gama = 40.
      tol = 1.e -5
      ustotl = ugs + uls
      rhodef = rhol2 - rhovap
c eqn. (15) of Sylvester (1987)
      alphls = 0.3048*ugs/(0.425 +2.65*0.3048*ustotl)
      allsm1 = 1. - alphls
      st1 = gravit *tubid *(rhodef) / rhol2
c eqn. (7) of Sylvester (1987)
      utb = 1.2 * ( ugs + uls) + 0.35 * st1**0.5
      st2 = sten* gravit * rhodef / rhol2**2
      st3 = allsm1 * (ustotl - alphls * 1.53 * st2**0.25*allsm1**0.5)
      altb = 0.5
      st4 = 9.916 * (gravit *tubid)**0.5
      ic = 0
510   continue
c eqn. (18) of Vo and Shoham (1989)
      faltb = st4 * (1. - altb**0.5)**0.5*(1.-altb) -
     #  utb * (altb-alphls) + st3
c eqn. (19) of Vo and Shoham (1989)
      faltbd = -st4 *(( 1. - altb**0.5)**0.5 + ( 1. -altb)/(4.*(altb*
     #  (1. -altb**0.5))**0.5)) - utb
      alnew = altb - faltb/faltbd
      test = abs(altb - alnew)
      if(test .le. tol) go to 521
      altb = alnew
      go to 510
521   continue
      altb = alnew
c ***************************************************************
c Estimate all the unknown parameters
c ***************************************************************
c eqn. (7) of Vo and Shoham (1989)
      ultb = st4 * ( 1. - altb**0.5)**0.5
```

```
c  eqn. (4) of Vo and Shoham (1989)
        ulls = utb -(utb + ultb)*(1. - altb)/allsm1
c  eqn. (6) of Vo and Shoham (1989)
        ugls = ulls + 1.53*st2**0.25*allsm1**0.5
c  eqn. (3) of Vo and Shoham (1989)
        ugtb = utb - (utb - ugls)*alphls /altb
c  eqn. (2) of Vo and Shoham (1989)
        beta = (allsm1*ulls - uls)/(allsm1*ulls + (1-altb)*ultb)
c  eqn. (32) of Sylvester (1987)
        slugls = gama * tubid
        slugsu = slugls/(1. - beta)
        detal = (tubid /2.)*(1. - altb ** 0.5)
c  eqn. (20) of Sylvester (1987)
        dhrol = tubid - 2.*detal
c  ***********************************************************************
c  Friction factor for Taylor bubble
c  ***********************************************************************
c  eqn. (22) of Sylvester (1987)
        ftb = 1./(-2.*alog10((1.-altb**0.5)/7.4))**2
c  ***********************************************************************
c  Friction factor for liquid slug
c  ***********************************************************************
c  eqn. (27) of Sylvester (1987)
        xmuls = wvis*allsm1 + alphls*cvis
c  eqn. (26) of Sylvester (1987)
        rels = rholav*ulls*allsm1*tubid/xmuls
        eond = 0.00015/tubid
        call friclose(eond,rels,fls)
c  ***********************************************************************
c  Estimate the pressure drop components
c  ***********************************************************************
c  eqn. (17) of Sylvester (1987)
        dpa = rholav*(ultb + utb)*(1.0 - altb)*(ultb + utb + ulls)/
     #    4633.06
c  eqn. (18) of Sylvester (1987)
        dph = rholav*(1.0 - alphls)*slugls/144
c  eqn. (23) of Sylvester (1987)
        dpftb = rhovap*(ugtb**2.0)*ftb*beta*slugsu/(2.0*dhrol)
     #    /4633.06
c  eqn. (24) of Sylvester (1987)
        dpfls = rholav*(1.0 - alphls)*(ustotl**2.0)*fls*(1.-beta)*slugsu/
     #    (2.0*tubid*4633.06)
c  ***********************************************************************
c  Estimate the total pressure drop
c  ***********************************************************************
```

```
c  eqn. (16) of Sylvester (1987)
        dpdzt = (dpa+dph+dpftb+dpfls)*asect/slugsu
        return


c  ***************************************************************
c  Subroutine to estimate the friction factor based on the Zigrang-Sylvester correlation
c  Zigrang, D., and Sylvester, N. D., "Explicit Approximation to the Solution of
c  Colebrook's friction factor equation," AIChE Journal, 28, p.514, 1982.
c  ***************************************************************
        subroutine friclose(rough, reynod, fricfc)
        term1 = rough /3.7
        term2 = 5.02/reynod
        term3 = 13./reynod
        term4 = term2 * alog10(term1 +term3)
        if(term1 .le. term4) go to 10
        term5 = -2.*alog10(term1 - term4)
c  eqn. (12) of Zigrang and Sylvester (1982)
        fricfc = 1. / term5**2
        go to 20
 10     continue
        fricfc = 16./reynod
 20     continue
        if(reynod .le. 2000) fricfc = 16./reynod
        return
      end


c  ***************************************************************
c  Subroutine to calculate the friction factor in the annular film
c  ***************************************************************
        subroutine annfilm(rholav,delhen,ff)
$include:'common1'
c  eqn. (72) of Ansari et al. (1994)
        ucrit = 10000.0*ugs*cvis*((rhovap/rholav)**0.5)/sten
c  eqn. (71) of Ansari et al. (1994)
        fe = 1.0 - exp(-0.125*(ucrit-1.5))
        if (fe.lt.0) fe=0
        ymlf = (1.0 -fe)*toliq
c  eqn. (15) of Yao and Sylvester (1987)
        re_film = 4.*ymlf/(3.1415*tubid*wvis)
c  eqn. (16) of Yao and Sylvester (1987)
        regas = rhovap*tubid*ugs/cvis
c  eqn. (14) of Yao and Sylvester (1987)
        fnum1 = (0.707*re_film**0.5)**2.5
```

```
      fnum2 = (0.0379*re_film**0.9)**2.5
      fnum = (fnum1 + fnum2)**0.4
      fdenom = regas**0 9*(cvis/wvis)*(rholav/rhovap)**0.5
      ffact = fnum/fdenom
c  eqn. (13) of Yao and Sylvester (1987)
      ai = 6.59*ffact*tubid
      bi = sqrt(1. + 1400.*ffact)
      delhen = ai/bi
c  eqn. (76) of Ansari et al. (1994)
      dhf = 4.*delhen*tubid*(1.-delhen)
c eqn. (75) of Ansari et al. (1994)
      uf = uls*(1.-fe)/(4.*delhen*(1.-delhen))
      area_c = (3.1415*((1.-2.*delhen)*tubid)**2.)/4.
      area = 3.1415*tubid**2./4.
      ql = uls*area
      ul = fe *ql/area_c
c  eqn. (74) of Ansari et al. (1994)
      reyf = rholav*uf*dhf/wvis
      call friclose(delhen, reyf, ff)
      return
      end



c ***************************************************************
c  Identify the point of intersection of the transition curves (A and B) in the Barnea
c  flow map
c ***************************************************************
      Subroutine ugsab(rholav, ugs_ab)
$include:'common1'
      ugsb=10.
      b2 = (rhol2 - rhovap)*sten
      s1 = (gravit * b2)**0.25
c  eqn. (3) of Ansari et al. (1994)
      vs = 1.53*(s1/rholav**0 5)
c  eqn. (2) of Ansari et al. (1994)
211   ulsa = 3.*(ugsb - 0.25*vs)
      ie = 0
      gravit = 32.0
      call annfilm(rholav,delhen,ff)
c  eqn. (4) of Ansari et al. (1994)
```

```
temp1 = (0.4*sten/((rholav-rhovap)*gravit))**0.5
temp2 = ((rholav/sten)**0.6)*((ff/(2.*tubid))**0.4)
temp3 = (2.*temp1*temp2)*((ulsa+ugsb)**1.2)
temp4 = ((temp3 - 0.725)/4.15)**2.
ugsbn = (ulsa*temp4)/(1.-temp4)
check = abs(ugsbn - ugsb)
ie = ie + 1
if ((check .gt. 0.0001) .and. (ie.lt.25)) then
        if (ugsbn.ge.0) then
                ugsb = ugsbn
                goto 211
        else
                ugsb = 0
        endif
endif
if (ugsbn.ge.0) then
        ugs_ab = ugsbn
else
        ugs_ab = 0
endif
return
end
```

APPENDIX C

Computational Procedure for the Estimation of Pressure Drop

for Upward Vertical Two-Phase Flow Systems

The pressure drop and phase equilibrium calculations are coupled and hence the overall calculational procedure is iterative. The steps to calculate the pressure drop for all the models can be summarized as follows:

1. Determine the necessary input data for the calculations: pipe internal diameter, well depth, bottomhole temperature, bottomhole pressure, well head temperature, well head pressure, separator temperature and pressure, gas composition and water analysis at the well head.
2. Assume a linear temperature profile between the top and the bottom of the well.
3. Assume a linear pressure profile between the top and bottom of the well for an initial guess to the subsequent calculation.
4. Divide the gas well into sections of 500 ft. so that each section can be treated as a single entity where all fluid properties can be assumed to be constant. (No variations were found in the pressure drop results as the length of well string was varied from 500 to 50 ft. Hence the well strings were divided into 500 ft sections for this work.)
5. Calculate the average temperature using the temperatures at the top, T_t, and bottom, T_b, of the i^{th} section of the well. Similarly, estimate the average pressure from the pressure at the top, P_t, and bottom, P_b, of the i^{th} section of the well.
6. Perform the flash calculations at the average temperature and pressure, and calculate the relative amounts of gas and liquid along with their compositions.

7. Estimate all the properties of the fluids: density, viscosity, and surface tension at the average temperature and pressure.
8. Use the Barnea flow map and identify the flow regime present in the i^{th} section of the well.
9. Estimate the pressure drop, ΔP, using the appropriate equations (Yao and Sylvester (1987) or the Ansari et al. (1994) models for the annular flow regime; Sylvester (1987) or the Ansari et al. (1994) models for the slug flow regime).
10. Evaluate the new pressure P_{bnew} at the bottom of the i^{th} section by adding ΔP to P_t.
11. Compare P_{bnew} with P_b. If the values are not within a specified tolerance limit, assign P_{bnew} to P_b and return to step 5.
12. Once P_{bnew} converges to P_b within a tolerance, assign P_{bnew} to P_b.
13. Go to the $(i+1)^{th}$ section. Assign P_b of i^{th} section to P_t of $(i+1)^{th}$ section. Take the linear profile value for P_b of the $(i+1)^{th}$ section.
14. Repeat the entire procedure from step 5 until bottomhole is reached.

APPENDIX D

Example Calculation of Pressure Drop: Slug Flow

A hand calculation should be performed to validate the calculations being performed in the FORTRAN code. As an example calculation, assume the following well data:

Well head temperature (T_w)	: 121 °F
Bottom hole temperature (T_{BH})	: 210 °F
Well head pressure (P_w)	: 1907 psia
Bottom hole pressure (P_{BH})	: 3229 psia
Well Depth	: 8055 ft.
Pipe Diameter	: 1.995 in
Gas production	: 2676 MSCFD
Water production	: 401 B/D

Estimate temperature and pressure:

$$\frac{dT}{dz} = \frac{T_{BH} - T_w}{WD} = \frac{210 - 121}{8055} = 0.011^\circ F / ft.$$

$$T_1 = T_w + \left(\frac{dT}{dz}\right) WD$$

$$= 121 + 0.011(500) = 126.52^\circ F$$

$$T_a = \frac{T_w + T_1}{2} = 583.76\ R$$

$$\frac{dP}{dz} = \frac{P_{BH} - P_w}{WD} = \frac{3229 - 1907}{8055} = 0.164\ psia / ft.$$

$$P_1 = P_w + \left(\frac{dP}{dz}\right) WD = 1989.06\ psia$$

Gas Viscosity (μ_g):

Gas density (ρ_g) : 5.91 lbm/ft^3 = 0.094 gm/cc

Molecular weight (M) : 16.8 lbm/lb mole

Temperature (T) : 583.76 R

$$K = \frac{[7.77 + 0.0063M]T^{1.5}}{122.4 + 12.9M + T} = 120.37$$

$$X = 2.57 + \frac{1914.5}{T} + 0.0095M = 6.01$$

$$Y = 1.11 + 0.04X = 1.35$$

$$\mu_g = K\exp\left(X\rho^Y\right) = 1.03e-5 \text{ lbm / ft.s}$$

Water Viscosity (μ_l):

Temperature (T) : 324.13 K

a = -52.843 b = 3703.6 c = 5.866 d = 5.879e-29 e = 10

$$\mu_l = \exp\left(a + \frac{b}{T} + c\ln T + dT^e\right) = 3.7e-4 \text{ lbm / ft.s}$$

Surface Tension (σ_L):

Temperature (T) : 324.13 K

Critical Temperature (T_c) . 647.13 K

a = 0.18546 b = 2.717 c = -3.554 d = 2.047

$$T_r = \frac{T}{T_c} = 0.501$$

$$\sigma_L = a\left[1 - T_r\right]^{b+cT_r+dT_r^2} = 0.1481 \text{ lbm / s}^2$$

Flow Regime Analysis:

Check for existence of annular flow.

Condition I : $$v_{SG} \geq 3.1\left[\frac{g\sigma_L(\rho_L - \rho_G)}{\rho_g^2}\right]^{0.25}$$

Condition II : $$\left(H_{I.F} + \lambda_{I.C}\frac{A_c}{A_p}\right) \leq 0.12$$

Check for condition I:

Liquid Density (ρ_L) : 61.45 lbm/ft^3

Gas Density (ρ_G) : 5.91 lbm/ft^3

Gravity (g) : 32 ft/s^2

Surface Tension (σ_L) : 0.148 lbm/s^2

Convert standard volume to actual volume

$V_{std} = q_{G\text{-}std} = 2676000$ ft^3/day

$T_{std} = 298$ K $T_{ac} = 324.13$ K

$P_{std} = 1$ atm $P_{ac} = 132.52$ atm

$$q_{g-ac} = V_{ac} = \frac{P_{std}V_{std}}{T_{std}}\frac{T_{ac}}{P_{ac}} = 21963.97 \text{ ft}^3/\text{day} = 0.254 \text{ ft}^3/\text{s}$$

$$v_{SG} = \frac{q_{g-ac}}{A_p} = 11.71 \text{ ft./s}$$

The computer code does flash calculations to estimate the amount of gas flow. Hence, the superficial gas velocity estimated by the computer code will vary from the above calculated value, though marginally. The superficial gas velocity, computed by the code as 11.304 ft./s, will be taken for subsequent calculations to avoid accumulating the effect of this error.

$$3.1\left[\frac{g\sigma_L(\rho_L-\rho_G)}{\rho_g^2}\right]^{0.25} = 0.357 < v_{SG}$$

Condition I is satisfied.

Check for condition II.

Holdup fraction (λ_{LC}) estimation:

Superficial liquid velocity (v_{LS}): 1.22 ft/s

$$v_{crit} = 10000\frac{v_{SG}\mu_G}{\sigma_L}\left(\frac{\rho_G}{\rho_L}\right)^{0.5} = 2.438$$

$$F_E = 1-\exp\left[-0.125(v_{crit}-1.5)\right] = 0.111$$

$$\lambda_{LC} = \frac{F_E v_{LS}}{v_{SG}+F_E v_{LS}} = 0.0118$$

Estimation of Lockhart-Martinelli parameters:

$$X_M = \sqrt{\frac{B\left(\frac{dP}{dz}\right)_{SL}}{\left(\frac{dP}{dz}\right)_{SC}}}$$

Estimate $\left(\frac{dP}{dz}\right)_{SL}$:

$$N_{ReSL} = \frac{\rho_L v_{SL} D}{\mu_L} = 33685.4$$

$$\frac{\varepsilon}{D} = 0.0009$$

$$f_{SL} = \left[-2\log\left\{ \frac{\varepsilon/D}{3.7} - \left(\frac{5.02}{N_{ReSL}} \log\left(\frac{\varepsilon/D}{3.7} + \frac{13}{N_{ReSL}} \right) \right) \right\} \right]^{-2} = 0.0253$$

$$\left(\frac{dP}{dz}\right)_{SL} = \frac{f_{SL}\rho_L v_{SL}^2}{2D} = 6.96$$

Estimate $\left(\frac{dP}{dz}\right)_{SC}$:

$$v_{SC} = F_E v_{SL} + v_{SG} = 11.439 \text{ ft/s}$$

$$\mu_C = \mu_L \lambda_{LC} + \mu_G (1 - \lambda_{LC}) = 1.454e-5 \text{ lbm/ft.s}$$

$$\rho_C = \rho_L \lambda_{LC} + \rho_G (1 - \lambda_{LC}) = 6.565 \text{ lbm/ft}^3$$

$$N_{ReSC} = \frac{\rho_C v_{SC} d}{\mu_C} = 858706.3$$

$$f_{SC} = \left[-2\log\left\{ \frac{\varepsilon/D}{3.7} - \left(\frac{5.02}{N_{ReSC}} \log\left(\frac{\varepsilon/D}{3.7} + \frac{13}{N_{ReSC}} \right) \right) \right\} \right]^{-2} = 0.017$$

$$\left(\frac{dP}{dL}\right)_{SC} = \frac{f_{SC}\rho_C v_{SC}^2}{2D} = 50.451$$

Estimate f_F:

Mass flow rate of liquid (M_{TL}) : 1.629 lbm/s

$$N_{Re\,Film} = \frac{4(1 - F_E)M_{TL}}{\mu_L \pi D} = 299759$$

$$N_{ReG} = \frac{\rho_G D v_{SG}}{\mu_G} = 1078311$$

$$F = \frac{\left\{\left[0.707\sqrt{N_{ReFilm}}\right]^{2.5} + \left[0.0379\left(N_{ReG}\right)^{0.9}\right]^{2.5}\right\}^{0.4}}{\left(N_{ReG}\right)^{0.9}\left(\frac{\mu_G}{\mu_L}\right)\left(\frac{\rho_L}{\rho_G}\right)^{0.5}} = 0.017$$

$$\underline{\delta} = \frac{\varepsilon}{D} = \frac{6.59F}{(1+1400F)^{0.5}} = 0.0226$$

$$d_{HF} = 4\underline{\delta}(1-\underline{\delta})D = 0.0147$$

$$v_F = \frac{v_{SL}(1-F_E)}{4\underline{\delta}(1-\underline{\delta})} = 12.284$$

$$N_{ReF} = \frac{\rho_L v_F d_{HF}}{\mu_L} = 29990.3$$

$$f_F = \left[-2\log\left\{\frac{\varepsilon/D}{3.7} - \left(\frac{5.02}{N_{ReF}}\log\left(\frac{\varepsilon/D}{3.7} + \frac{13}{N_{ReF}}\right)\right)\right\}\right]^{-2} = 0.0522$$

$$B = \left(1-F_E\right)^2 \frac{f_F}{f_{SL}} = 1.63$$

$$X_M = \sqrt{\frac{B\left(\frac{dP}{dz}\right)_{SL}}{\left(\frac{dP}{dz}\right)_{SC}}} = 0.4743$$

$$Y_M = \frac{gSin\theta(\rho_L - \rho_C)}{\left(\frac{dP}{dz}\right)_{SC}} = 34.81$$

Estimate minimum dimension-less film thickness required for stability of liquid film by solving the following equation by the "bisection method".

$$Y_M = \frac{2 - 1.5H_{LF}}{H_{LF}^3(1 - 1.5H_{LF})} X_M^2$$

where, $H_{LF} = 4\underline{\delta}_{min}(1 - \underline{\delta}_{min})$

The minimum dimension-less film thickness ($\underline{\delta}_{min}$) was found to be 0.07.

$$H_{LF} = 4\underline{\delta}_{min}(1 - \underline{\delta}_{min}) = 0.2604$$

$$A_C = \frac{\pi(D - 2D\underline{\delta}_{min})^2}{4} = 0.016$$

$$\left(H_{I.F} + \lambda_{I.C}\frac{A_c}{A_p}\right) = 0.269 > 0.12$$

Condition II is not satisfied. Therefore, the flow cannot be in the annular regime.

Pressure drop estimation by Sylvester (1987) method:

Estimation of α_{TB}:

$$v_m = v_{SL} + v_{SG}$$

$$v_{TB} = 1.2v_m + 0.35\sqrt{gD} = 15.84 \text{ ft/s}$$

$$\alpha_{LS} = \frac{v_{SG}}{(0.425/0.3048) + 2.65v_m} = 0.33$$

$$\tilde{A} = (1 - \alpha_{LS})\left[v_m - \alpha_{LS}\left\{1.53\left[\frac{\sigma_L g(\rho_L - \rho_G)}{\rho_L^2}\right]^{0.25}(1 - \alpha_{LS})^{0.5}\right\}\right] = 8.17$$

Solve the following equation for α_{TB}, using the Newton-Raphson technique.

$$9.916\sqrt{gD}(1 - \sqrt{\alpha_{TB}})^{0.5}(1 - \alpha_{TB}) - v_{TB}\alpha_{TB} + v_{TB}\alpha_{LS} + \tilde{A} = 0$$

α_{TB} was found to be 0.8899.

$$v_{LTB} = 9.916\left[gD(1-\sqrt{\alpha_{TB}})\right]^{1/2} = 5.444 \text{ ft / s}$$

$$v_{LLS} = \frac{v_{TB}(\alpha_{TB}-\alpha_{LS})-(1-\alpha_{TB})v_{LTB}}{(1-\alpha_{LS})} = 12.31 \text{ ft / s}$$

$$v_{GLS} = v_{LLS} + 1.53\left[\frac{\sigma_L g(\rho_L-\rho_G)}{\rho_L^2}\right]^{1/4}(1-\alpha_{LS})^{0.5} = 12.95 \text{ ft / s}$$

Estimate pressure drop due to acceleration:

$$(\Delta P)_A = \frac{\rho_L(v_{LTB}+v_{TB})(1-\alpha_{TB})(v_{LTB}+v_{TB}+v_{LLS})}{4633.06} = 1.044 \text{ psia / slug unit}$$

Estimate the hydrostatic pressure drop:

$$L_{LS} = 40D = 6.65 \text{ ft}$$

$$(\Delta P)_H = \frac{\rho_L(1-\alpha_{LS})gL_{LS}}{4633.06} = 1.883 \text{ psia / slug unit}$$

Estimate the frictional pressure drop:

$$f_{TB} = \frac{1}{\left[-2\log\left\{\frac{1-\sqrt{\alpha_{TB}}}{7.4}\right\}\right]^2} = 0.056$$

$$D_H = D\left[1-(1-\sqrt{\alpha_{TB}})\right] = 0.1568 \text{ ft}$$

$$\beta = \frac{v_{SG}-\alpha_{LS}v_{GLS}}{\alpha_{TB}v_{GTB}-\alpha_{LS}v_{GLS}} = 0.792$$

$$(\Delta P)_{FTB} = \frac{\rho_G v_{GTB}^2 f_{TB}\beta L_{LS}}{2D_H(1-\beta)(4633.06)} = 1.255 \text{ psia / slug unit}$$

$$\mu_{LS} = \mu_L(1-\alpha_{LS})+\mu_G\alpha_{LS} = 2.49e-4 \text{ lbm / ft.s}$$

$$N_{Re\,LS} = \frac{\rho_L(1-\alpha_{LS})v_{LLS}D}{\mu_{LS}} = 335207.8$$

$$f_{LS} = \left[-2\log\left\{\frac{\varepsilon/D}{3.7} - \left(\frac{5.02}{N_{Re\,LS}}\log\left(\frac{\varepsilon/D}{3.7} + \frac{13}{N_{Re\,LS}}\right)\right)\right\}\right]^{-2} = 0.02$$

$$(\Delta P)_{FLS} = \frac{\rho_L(1-\alpha_{LS})v_m^2 f_{LS} L_{LS}}{2D(4633.06)} = 0.552 \text{ psia / slug unit}$$

$$\text{No. of slug units} = \frac{500(1-\beta)}{L_{LS}} = 15.64$$

The overall pressure drop is given by

$$(\Delta P)_T = \left[(\Delta P)_A + (\Delta P)_H + (\Delta P)_{FTB} + (\Delta P)_{FLS}\right](\text{no. of slug units}) = 74.04 \text{ psia}$$

The pressure drop estimated by the FORTRAN code was found to be 73 4 psia.

Pressure drop estimation using Ansari et. al (1994) model:

$\alpha_{TB} = 0.8899$

$v_{LTB} = 5.44$ ft/s

$v_{LLS} = 12.31$ ft/s

$v_{GLS} = 12.95$ ft/s

$v_{GTB} = 14.75$ ft/s

$\beta = 0.79$

$H_{GLS} = 1 - H_{LLS} = \alpha_{LS} = 0.33$

All the above parameters have been computed in the earlier section for the Sylvester (1987) method. Since the Ansari et. al (1994) approach follows the same

framework as Sylvester, the computation for the above mentioned parameters can be avoided.

Check for developing flow.

$$L_{LS} = 30D = 4.9875 \text{ ft}$$

$$L_{TB} = \frac{L_{LS}\beta}{1-\beta} = 18.99 \text{ ft}$$

The following three equations have to be solved iteratively for the three unknowns (Q_P, δ_N, and Q_f).

$$Q_P = \left(1 - \frac{4\delta_N}{D}\right) v_{TB} A_P$$

$$\delta_N = \left(\frac{3Q_F \mu_L}{\pi g D \rho_L}\right)^{1/3}$$

$$Q_f = Q_P - \left(Q_G + Q_L\right)$$

Solving the above three equations, the three parameters were estimated to be

$Q_P = 0.3081 \text{ ft}^3/\text{s}$

$\delta_N = 0.0034 \text{ ft}$

$Q_f = 0.0363 \text{ ft}^3/\text{s}$

The cap length was estimated as follows:

$$A_G = \pi (D - 2\delta_N)^2 / 4 = 0.02 \text{ ft}^2$$

$$L_c = \left\{\frac{A_P v_{TB} - (Q_G + Q_L)/(2g)^{0.5}}{A_P - A_G}\right\}^2 = 26.98 \text{ ft}$$

Since the cap length (L_C) is greater than the length of Taylor bubble (L_{TB}), the slug flow is not fully developed. The length of Taylor bubble has to be modified. The modified Taylor

bubble length is obtained by solving the following quadratic equation, a function of the modified Taylor bubble length.

$$L_{TB}^{*\,2} + \left(\frac{-2ab - 4c^2}{a^2}\right) L_{TB}^{*} + \frac{b^2}{a^2} = 0$$

where,

$$a = 1 - \frac{v_{SG}}{v_{TB}} = 0.2864$$

$$b = \frac{v_{SG} - v_{GLS}\left(2 - H_{LLS}\right)}{v_{TB}} L_{LS} = -1.8511$$

$$c = \frac{v_{TB} - v_{LLS}}{\sqrt{2g}} H_{LLS} = 0.297$$

The quadratic equation becomes

$$L_{TB}^{*\,2} + 8.625\, L_{TB}^{*} + 41.77 = 0$$

Since the above quadratic equation does not have a real root, compute the pressure drop with the developed flow assumption.

Pressure drop estimation:

$$\rho_{LS} = \rho_L H_{LLS} + \rho_G (1 - H_{LLS}) = 43.3 \text{ lbm / ft}^3$$

$$\mu_{LS} = \mu_L H_{LLS} + \mu_G H_{GLS} = 2.524e-4 \text{ lbm / ft.s}$$

$$N_{Re} = \frac{\rho_{LS} v_m D}{\mu_{LS}} = 357193.3$$

$$f_{LS} = \left[-2\log\left\{ \frac{\varepsilon/D}{3.7} - \left(\frac{5.02}{N_{Re}} \log\left(\frac{\varepsilon/D}{3.7} + \frac{13}{N_{Re}} \right) \right) \right\} \right]^{-2} = 0.02$$

$$\left(\frac{dP}{dz}\right)_E = \frac{\left[(1-\beta)\rho_{LS} + \beta\rho_G\right]g}{4633.06} = 0.0945 \text{ psia / ft./slug unit}$$

$$(\Delta P)_E = \left(\frac{dP}{dz}\right)_E (\text{length of slug unit}) = 2.266 \text{ psia / slug unit}$$

$$\left(\frac{dP}{dz}\right)_f = \frac{f_{LS}\rho_{LS}v_m^2}{2D(4633\,06)}(1-\beta) = 0.0183 \text{ psia / ft./slug unit}$$

$$(\Delta P)_f = \left(\frac{dP}{dz}\right)_f (\text{length of liquid slug}) = 0.0913 \text{ psia / slug unit}$$

The total pressure drop was found to be,

$$(\Delta P)_T = \left[(\Delta P)_E + (\Delta P)_f\right](\text{no. of slug units}) = 49.15 \text{ psia}$$

The pressure drop computed by the FORTRN code was found to be 48.1 psia.

APPENDIX E

Example Calculation of Pressure Drop: Annular Flow

In Appendix E, a second well has been analyzed. The well analyzed in Appendix E was found to be in the annular flow regime based on the Barnea transition criteria. The well data is presented below:

Well head temperature (T_w)	: 110 °F
Bottomhole temperature (T_{BH})	: 209 °F
Well head pressure (P_w)	: 2450 psia
Bottomhole pressure (P_{BH})	: 3211 psia
Well Depth	: 8051 ft.
Pipe Diameter	: 1.995 in
Gas production	: 2179 MSCFD
Water production	: 78 B/D

Estimate temperature and pressure:

$$\frac{dT}{dz} = \frac{T_{BH} - T_w}{WD} = \frac{209 - 110}{8051} = 0.0123^\circ F / ft.$$

$$T_1 = T_w + \left(\frac{dT}{dz}\right) WD$$

$$= 110 + 0.0123(500) = 116.15^\circ F$$

$$T_a = \frac{T_w + T_1}{2} = 573.08\ R$$

$$\frac{dP}{dz} = \frac{P_{BH} - P_w}{WD} = \frac{3211 - 2450}{8051} = 0.095\ psia / ft.$$

$$P_1 = P_w + \left(\frac{dP}{dz}\right) WD = 2497.26\ psia$$

Gas Viscosity (μ_g):

Gas density (ρ_g) : 9.2 lbm/ft^3 = 0.147 gm/cc

Molecular weight (M) : 18.9 lbm/lb mole

Temperature (T) : 573.08 R

$$K = \frac{[7.77 + 0.0063M]T^{1.5}}{122.4 + 12.9M + T} = 115.24$$

$$X = 2.57 + \frac{1914.5}{T} + 0.0095M = 6.09$$

$$Y = 1.11 + 0.04X = 1.35$$

$$\mu_g = K\exp\left(X\rho^Y\right) = 1.22e-5 \text{ lbm / ft.s}$$

Water Viscosity (μ_l):

Temperature (T) : 573.08 K

a = -52.843 b = 3703.6 c = 5.866 d = 5.879e-29 e = 10

$$\mu_l = \exp\left(a + \frac{b}{T} + c\ln T + dT^e\right) = 4.11e-4 \text{ lbm / ft.s}$$

Surface Tension (σ_L):

Temperature (T) : 318.19 K

Critical Temperature (T_c) : 647.13 K

a = 0.18546 b = 2.717 c = -3.554 d = 2.047

$$T_r = \frac{T}{T_c} = 0.49$$

$$\sigma_L = a\left[1 - T_r\right]^{b+cT_r+dT_r^2} = 0.151 \text{ lbm / s}^2$$

Flow Regime Analysis:

Check for existence of annular flow.

Condition I : $$v_{SG} \geq 3.1\left[\frac{g\sigma_L(\rho_L - \rho_G)}{\rho_g^2}\right]^{0.25}$$

Condition II : $$\left(H_{I.F} + \lambda_{I.C}\frac{A_c}{A_p}\right) \leq 0.12$$

Check for condition I:

Liquid Density (ρ_L) : 61.7 lbm/ft^3

Gas Density (ρ_G) : 9.2 lbm/ft^3

Gravity (g) : 32 ft/s^2

Surface Tension (σ_L) : 0.151 lbm/s^2

Convert standard volume to actual volume.

$V_{std} = q_{G\text{-}std} = 2179000$ ft^3/day

$T_{std} = 298$ K $\qquad T_{ac} = 318.19$ K

$P_{std} = 1$ atm $\qquad P_{ac} = 169.9$ atm

$$q_{g-ac} = V_{ac} = \frac{P_{std}V_{std}}{T_{std}}\frac{T_{ac}}{P_{ac}} = 13694.12 \text{ ft}^3/\text{day} = 0.158 \text{ ft}^3/\text{s}$$

$$v_{SG} = \frac{q_{g-ac}}{A_p} = 7.28 \text{ ft./s}$$

The computer code does flash calculations to estimate the amount of gas flow. Hence the superficial gas velocity estimated by the computer code will vary from the above calculated value, though marginally. The superficial gas velocity, computed by the code as 6.65 ft./s, will be taken for subsequent calculations to avoid accumulating the effect of this error.

$$3.1\left[\frac{g\sigma_L(\rho_L-\rho_G)}{\rho_g^2}\right]^{0.25} = 4.08 < v_{SG}$$

Condition I is satisfied.

Check for condition II.

Holdup fraction (λ_{LC}) estimation:

Superficial liquid velocity (v_{LS}): 0.236 ft/s

$$v_{crit} = 10000\frac{v_{SG}\mu_G}{\sigma_L}\left(\frac{\rho_G}{\rho_L}\right)^{0.5} = 2.075$$

$$F_E = 1-\exp\left[-0.125\left(v_{crit}-1.5\right)\right] = 0.069$$

$$\lambda_{LC} = \frac{F_E v_{LS}}{v_{SG}+F_E v_{LS}} = 0.00244$$

Estimation of Lockhart-Martinelli parameters:

$$X_M = \sqrt{\frac{B\left(\frac{dP}{dz}\right)_{SL}}{\left(\frac{dP}{dz}\right)_{SC}}}$$

Estimate $\left(\frac{dP}{dz}\right)_{SL}$:

$$N_{ReSL} = \frac{\rho_L v_{SL} D}{\mu_L} = 5870$$

$$\frac{\varepsilon}{D} = 0.0009$$

$$f_{SL} = \left[-2\log\left\{ \frac{\varepsilon/D}{3.7} - \left(\frac{5.02}{N_{ReSL}} \log\left(\frac{\varepsilon/D}{3.7} + \frac{13}{N_{ReSL}} \right) \right) \right\} \right]^{-2} = 0.037$$

$$\left(\frac{dP}{dz} \right)_{SL} = \frac{f_{SL} \rho_L v_{SL}^2}{2D} = 0.38$$

Estimate $\left(\frac{dP}{dz} \right)_{SC}$:

$$v_{SC} = F_E v_{SL} + v_{SG} = 6.666 \text{ ft/s}$$

$$\mu_C = \mu_L \lambda_{LC} + \mu_G (1 - \lambda_{LC}) = 1.317e-5 \text{ lbm/ft.s}$$

$$\rho_C = \rho_L \lambda_{LC} + \rho_G (1 - \lambda_{LC}) = 9.328 \text{ lbm/ft}^3$$

$$N_{ReSC} = \frac{\rho_C v_{SC} d}{\mu_C} = 784927.83$$

$$f_{SC} = \left[-2\log\left\{ \frac{\varepsilon/D}{3.7} - \left(\frac{5.02}{N_{ReSC}} \log\left(\frac{\varepsilon/D}{3.7} + \frac{13}{N_{ReSC}} \right) \right) \right\} \right]^{-2} = 0.0196$$

$$\left(\frac{dP}{dL} \right)_{SC} = \frac{f_{SC} \rho_C v_{SC}^2}{2D} = 24.39$$

Estimate f_F:

Mass flow rate of liquid (M_{TL}) : 0.317 lbm/s

$$N_{Re\,Film} = \frac{4(1 - F_E) M_{TL}}{\mu_L \pi D} = 5502$$

$$N_{ReG} = \frac{\rho_G D v_{SG}}{\mu_G} = 833702.87$$

$$F = \frac{\left\{\left[0.707\sqrt{N_{ReFilm}}\right]^{2.5} + \left[0.0379\left(N_{ReG}\right)^{0.9}\right]^{2.5}\right\}^{0.4}}{\left(N_{ReG}\right)^{0.9}\left(\frac{\mu_G}{\mu_L}\right)\left(\frac{\rho_L}{\rho_G}\right)^{0.5}} = 0.0059$$

$$\underline{\delta} = \frac{\varepsilon}{D} = \frac{6.59F}{(1+1400F)^{0.5}} = 0.013$$

$$d_{HF} = 4\underline{\delta}(1-\underline{\delta})D = 0.0084$$

$$v_F = \frac{v_{SL}(1-F_E)}{4\underline{\delta}(1-\underline{\delta})} = 4.347$$

$$N_{ReF} = \frac{\rho_L v_F d_{HF}}{\mu_L} = 5483.8$$

$$f_F = \left[-2\log\left\{\frac{\varepsilon/D}{3.7} - \left(\frac{5.02}{N_{ReF}}\log\left(\frac{\varepsilon/D}{3.7} + \frac{13}{N_{ReF}}\right)\right)\right\}\right]^{-2} = 0.0286$$

$$B = (1-F_E)^2\frac{f_F}{f_{SL}} = 0.77$$

$$X_M = \sqrt{\frac{B\left(\frac{dP}{dz}\right)_{SL}}{\left(\frac{dP}{dz}\right)_{SC}}} = 0.1024$$

$$Y_M = \frac{gSin\theta(\rho_L - \rho_C)}{\left(\frac{dP}{dz}\right)_{SC}} = 68.71$$

Estimate minimum dimension-less film thickness required for stability of liquid film by solving the following equation by the "bisection method".

$$Y_M = \frac{2 - 1.5H_{LF}}{H_{LF}^3\left(1 - 1.5H_{LF}\right)} X_M^2$$

where, $H_{LF} = 4\underline{\delta}_{min}\left(1 - \underline{\delta}_{min}\right)$

The minimum dimension-less film thickness ($\underline{\delta}_{min}$) was found to be 0.02.

$$H_{LF} = 4\underline{\delta}_{min}\left(1 - \underline{\delta}_{min}\right) = 0.0784$$

$$A_C = \frac{\pi\left(D - 2D\underline{\delta}_{min}\right)^2}{4} = 0.0208$$

$$\left(H_{I.F} + \lambda_{I.C}\frac{A_c}{A_p}\right) = 0.081 < 0.12$$

Condition II is satisfied. Therefore, the flow is in the annular regime.

Pressure drop estimation using Yao and Sylvester (1987) model:

$\rho_m = \rho_c = 9.328$ lbm/ft^3

$\mu_m = \mu_c = 1.317\text{e-}5$ lbm/ft.s

$F_E = 0.069$

$M_{TL} = 0.317$ lbm/s

$M_G = 1.329$ lbm/s

$A_P = 0.0217$ ft^2

$$V_m = \frac{F_E M_{TL} + M_G}{\rho_m A_P} = 6.672 \text{ ft / s}$$

Estimate friction factor:

$$Re_m = \frac{D\rho_m V_m}{\mu_m} = 785642$$

$$f_t = \left[-2\log\left\{ \frac{\varepsilon/D}{3.7} - \left(\frac{5.02}{Re_m} \log\left(\frac{\varepsilon/D}{3.7} + \frac{13}{Re_m} \right) \right) \right\} \right]^{-2} = 0.0416$$

$$\left(\frac{dP}{dz}\right)_E = \rho_m g = 298.5 \text{ lbm} / \text{ft}^2\text{s}^2$$

$$\left(\frac{dP}{dz}\right)_f = \frac{\rho_m f_t V_m^2}{2D} = 51.9 \text{ lbm} / \text{ft}^2\text{s}^2$$

The pressure drop due to acceleration can be neglected when the calculations are done manually since constant flow rates are assumed throughout the well string. It was found that the acceleration component of the pressure drop, computed by the computer code, was extremely small. Therefore neglecting the acceleration component is a good assumption. The overall pressure drop was found to be:

$$(\Delta P)_T = \left\{ \frac{\left(\frac{dP}{dz}\right)_E + \left(\frac{dP}{dz}\right)_f}{4633.06} \right\} 500 = 37.8 \text{ psia}$$

The pressure drop computed by the FORTRAN code was found to be 38.6 psia.

<u>Pressure drop estimation using Ansari et. al (1994) model</u>:

$$\left(\frac{dP}{dz}\right)_{SC} = 24.39 \text{ lbm} / \text{ft}^2\text{s}^2$$

$$\rho_c = 9.328 \text{ lbm} / \text{ft}^3$$

$$\theta = 90^\circ$$

The total pressure drop in the annular regime is given by

$$\left(\frac{dP}{dz}\right)_T = \frac{Z}{(1-2\underline{\delta})^5}\left(\frac{dP}{dz}\right)_{SC} + \rho_C g \, Sin\theta$$

where,

$$Z = 1 + 300\underline{\delta}, \qquad F_E > 0.9$$

$$Z = 1 + 24\left(\frac{\rho_L}{\rho_g}\right)^{1/3}\underline{\delta}, \qquad F_E \le 0.9$$

The superficial pressure gradient in the core, $\left(\frac{dP}{dz}\right)_{SC}$, has already been evaluated in the flow regime analysis section while calculating the Lockhart-Martinelli parameters. The only unknown in the pressure drop equation is the dimension-less film thickness. The dimension-less film thickness is estimated as the root of the following equation:

$$Y_M - \frac{Z}{4\underline{\delta}(1-\underline{\delta})\left[1-4\underline{\delta}(1-\underline{\delta})\right]^{2.5}} + \frac{X_M^2}{\left[4\underline{\delta}(1-\underline{\delta})\right]^3} = 0$$

$$X_M = 0.1024$$

$$Y_M = 68.71$$

$$Z = 1 + 45.26\,\underline{\delta}$$

Since the above equation is a monotonic function increasing with increasing $\underline{\delta}$, for $0<\underline{\delta}<0.5$, the equation will have only one root for the values of dimension-less film thickness considered. Bisection method gives a dimension-less thickness of 0.14.

$$\left(\frac{dP}{dz}\right)_T = \frac{Z}{(1-2\underline{\delta})^5}\left(\frac{dP}{dz}\right)_{SC} + \rho_C g \, Sin\theta = 1223.61 \text{ lbm / ft}^2\text{s}^2$$

$$(\Delta P)_T = \frac{\left(\frac{dP}{dz}\right)_T}{4633.06}(\text{length of well string}) = 132.05 \text{ psia}$$

The pressure drop computed by the FORTRAN code was found to be 132 psia.

VITA

Venkataraghavan Raman

Candidate for the Degree of

Master of Science

Thesis: DOWNHOLE PRESSURE DROP MODELING

Major Field: Chemical Engineering

Biographical:

Personal Data: Born in Madras, INDIA, on February 15, 1973, the son of Lakshmi and Raman.

Education: Graduated from Padma Seshadri Junior College, Madras, INDIA in May 1990; received Bachelor of Technology degree in Chemical Engineering from Indian Institute of Technology, Madras, INDIA in May 1994. Completed the requirements for the Master of Science degree with a major in Chemical Engineering at Oklahoma State University in December 1996.

Experience. Employed by Oklahoma State University, School of Chemical Engineering as a graduate research assistant; Oklahoma State University, School of Chemical Engineering, 1994 to present.

Professional Memberships: AIChE, Omega Chi Epsilon